APPENDIX A

COMPUTER FILE LISTING

File	Description
Palisades_CL.DB	Base model geometry for crack tip insertion [3]
CL_axial.INP	Input file to modify base mesh for axial crack tip insertion
BCNODES.INP	Input file for nodal component definitions
FM_CL_AXL*.INP	Geometry input files to create circumferential flaw at specified depth. * = 05, 30, 50, 75, and 95
FM_CL_AXL*_COORD.INP	Input files to determine circumferential crack face element centroid coordinates. * = 05, 30, 50, 75, and 95
FM_CL_AXL*_GETSTR.INP	Input files to extract circumferential crack face stresses from residual stress analysis. * = 05, 30, 50, 75, and 95
FM_CL_AXL*_IMPORT.INP	Input files to transfer stresses into circumferential crack face pressure (plus operating pressure on crack face and applied pipe moment). * = 05, 30, 50, 75, and 95
Axial*_Nodes.INP	Crack tip definition file for axial cracks
FM_PALISADES_CL_C#.INP	Geometry input files to create circumferential flaw at specified depth. # = 05, 30, 50, 75, and 95
FM_PALISADES_CL_C#_COORD.INP	Input files to determine circumferential crack face element centroid coordinates. # = 05, 30, 50, 75, and 95
FM_PALISADES_CL_C#_GETSTR.INP	Input files to extract circumferential crack face stresses from residual stress analysis. # = 05, 30, 50, 75, and 95
FM_PALISADES_CL_C#_IMPORT.INP	Input files to transfer stresses into circumferential crack face pressure (plus operating pressure on crack face and applied pipe moment). # = 05, 30, 50, 75, and 95
NodesC#.INP	Crack tip definition file for circumferential cracks
STR_FieldOper_STR_C##1.txt	Extracted circumferential crack face stresses from residual stress analysis. ## = 05, 30, 50, 75, and 95
STR_FieldOper_Axl**1.txt	Extracted axial crack face stresses from residual stress analysis. ** = 00, and 90
FM_CL_AXL**_IMPORT_K.CSV	Formatted K result outputs for axial crack. ** = 00, and 90
FM_PALISADES_CL_C##_IMPORT_K.CSV	Formatted K result outputs for circumferential crack. ## = 05, 30, 50, 75, and 95
CircFlaw_$$$$.pcf	**pc-CRACK** PWSCC growth input file for circ flaw. $$$$ = 0025 and 01, 0025 = 0.025" and 01 = 0.1" initial flaw size
AxialFlaw_0_$$$$.pcf	**pc-CRACK** PWSCC growth input file for axial flaw on 0° plane. $$$$ = 0025 and 01
AxialFlaw_90_$$$$.pcf	**pc-CRACK** PWSCC growth input file for axial flaw on 90° plane. $$$$ = 0025 and 01
CircFlaw_$$$$.rpt	**pc-CRACK** PWSCC growth output file for circ flaw. $$$$ = 0025 and 01
AxialFlaw_0_$$$$.rpt	**pc-CRACK** PWSCC growth output file for axial flaw on 0° plane. $$$$ = 0025 and 01
AxialFlaw_90_$$$$.rpt	**pc-CRACK** PWSCC growth output file for axial flaw on 90° plane. $$$$ = 0025 and 01

Structural Integrity Associates, Inc.®	File No.: 1400669.310
CALCULATION PACKAGE	**Project No.: 1400669** Quality Program Type: ☒ Nuclear ☐ Commercial

PROJECT NAME:
Palisades Flaw Readiness Program for 1R24 NDE Inspection

CONTRACT NO.:
10426669

CLIENT:	**PLANT:**
Entergy Nuclear Operations, Inc.	Palisades Nuclear Plant

CALCULATION TITLE:
Finite Element Model for Hot Leg Drain Nozzle

Document Revision	Affected Pages	Revision Description	Project Manager Approval Signature & Date	Preparer(s) & Checker(s) Signatures & Date
0	1 - 20 A-1 - A-2 Computer Files	Initial Issue	Norman Eng Norman Eng NE 03/09/2015	Preparer: Minji Fong Minji Fong MF 03/09/2015 Checkers: Charles Fourcade CJF 03/09/2015 Gole Mukhim GSM 03/09/2015

Table of Contents

List of Tables

List of Figures

1.0 OBJECTIVE

The objective of this calculation package is to document the development of a finite element model (FEM) for the reactor hot leg drain nozzle at the Palisades Nuclear Plant, which will be used to perform residual and operational-based fracture mechanics analyses to support a subsequent fracture mechanics evaluation as part of a flaw readiness program.

2.0 TECHNICAL APPROACH

One three-dimensional (3-D) finite element model is developed using the ANSYS finite element analysis software package [1]. The area of interest is the nozzle-to-pipe weld. The model uses elastic-plastic material properties intended for weld residual stress analysis, and elastic material properties for linear elastic analyses.

3.0 ASSUMPTIONS / DESIGN INPUTS

The dimensions and material types to develop the finite element model are provided in References 2 and 3 and summarized in Figure 1. The material properties are obtained from References 4 and 5. A number of assumptions were made during development of the finite element model, which are listed as follows:

- The drain nozzle is modeled as a straight pipe without the nozzle transition since the area of interest is the nozzle-to-hot leg piping weld which is away from the nozzle-to-safe end transition.
- The axial length of the modeled portion of the hot leg piping is arbitrarily set at 36 inches, which is sufficiently long enough to negate possible end effects in the region of interest.
- The ID patch weld is added after removal of the backing ring according to the weld procedure mentioned in the drawing [2]. The same material of the nozzle-to-pipe weld is used for the ID patch weld.

4.0 FINITE ELEMENT MODEL

The model includes a local portion of the hot leg pipe and cladding, the drain nozzle, and the nozzle-to-pipe weld, including the ID patch weld, as shown in Figure 2. As shown in the figure, a single 90° quadrant of the drain nozzle penetration is modeled due to geometric symmetry. The included portion of the hot leg piping measures 36 inches longitudinally and 180 degree circumferentially. The mesh of the finite element model is shown in Figure 3.

4.1 Element Type and Mesh

The 8-node solid element (SOLID185) in ANSYS [1] is used for the model. SOLID185 elements support material plasticity which is suitable for residual stress and elastic plastic fracture mechanics (EPFM) analyses. The model contains adequate mesh refinement within the weld region to predict the residual stresses from welding.

4.2 Materials

The material designation for the modeled components is listed in Table 1. The temperature dependent nonlinear material property values are provided in a separate calculation package [5], which are based on the 2001 Edition of the ASME Code with Addenda through 2003 [4]. The material properties are listed in Table 2 through Table 9.

4.2.1 Creep Properties

Since post weld heat treatment (PWHT) will be considered in the subsequent residual stress calculation, creep properties are required. In general, creep becomes significant at temperatures above 800°F; thus, creep behavior under 800°F will not be considered in this analysis.

There are two main categories of creep: primary and secondary. The primary creep addresses the creep characteristics for a short duration at the early stages of the creep regime, while the secondary creep accounts for the creep behavior for a long duration – usually more than 10,000 hours. Based on this definition, the PWHT falls within the primary creep characteristics. However, primary creep rates for materials are difficult to obtain, so the conservative secondary creep rates are used since primary creep rate is typically an order of magnitude higher than that for secondary creep.

In general, the primary creep rate for the materials is governed by the equation:

$$\frac{d\varepsilon}{dt} = A\sigma^n$$

The creep data for the SA-516 Grade 70 hot leg material is based on carbon steel material [6]. The creep data for the Alloy 82/182 and ER308L weld metals are not available, so the creep properties for their base metals are used instead. The creep data for Type 304 (for ER308L) is provided in the same

reference document as the carbon steel [6], while the creep data for the Alloy 600 (for Alloy 82/182) is provided in a separate reference document [7]. All the creep strengths, σ, are provided at two creep rates [6, 7] for each temperature point.

When creep strength is provided at two creep rates at the same temperature point, as listed in Table 10, then A and n can be calculated as follows, where subscripts 1 and 2 refer to the creep data sets 1 and 2:

$$\frac{d\varepsilon}{dt} = \dot{\varepsilon} = A\sigma^n$$

$$\dot{\varepsilon}_1 = A\sigma_1^{\,n};\quad \dot{\varepsilon}_2 = A\sigma_2^{\,n}$$

$$\frac{\dot{\varepsilon}_1}{\dot{\varepsilon}_2} = \left(\frac{\sigma_1}{\sigma_2}\right)^n$$

$$\ln\left(\frac{\dot{\varepsilon}_1}{\dot{\varepsilon}_2}\right) = n\ln\left(\frac{\sigma_1}{\sigma_2}\right)$$

$$n = \frac{\ln\left(\dfrac{\dot{\varepsilon}_1}{\dot{\varepsilon}_2}\right)}{\ln\left(\dfrac{\sigma_1}{\sigma_2}\right)}$$

$$A = \frac{\dot{\varepsilon}_1}{\sigma_1^{\,n}}$$

4.3 Loads and Boundary Conditions

No loads or boundary conditions of any kind are included in the finite element model in this calculation. Specific loads and boundary conditions, appropriate to the specific analyses, will be applied in the subsequent residual and thermal/mechanical stress calculation packages.

5.0 CONCLUSIONS

A finite element model of the hot leg drain nozzle is developed. The model will be used in subsequent weld residual stress analyses and fracture mechanics analyses. The necessary ANSYS input file names are listed in Appendix A.

6.0 REFERENCES

1. ANSYS Mechanical APDL and PrepPost, Release 14.5 (w/ Service Pack 1), ANSYS, Inc., September 2012.
2. Drawing No. VEN-M1-D, Sheet 108, Rev. 10, "Nozzle Details," SI File No. 1400669.202.
3. Drawing No. VEN-M1-D, Sheet 106, Rev. 10, "Piping Assembly & Details," SI File No. 1400669.202.
4. ASME Boiler and Pressure Vessel Code, Section II, Part D – Properties, 2001 Edition with Addenda through 2003.
5. SI Calculation No. 0800777.307, Rev.5, "Material Properties for Residual Stress Analyses, Including MISO Properties Up To Material Flow Stress."
6. "Steels for Elevated Temperature Service," United States Steel Co., 1949.
7. Publication SMC-027, "Inconel Alloy 600," Special Metals Corp., 2004, SI File No. 0800777.211.
8. Palisades Design Input Record, "Palisades Alloy 600 Flaw Evaluation DIR 3-4-15 Rev 1.pdf," SI File No. 1400669.201.

Table 1: Component Materials

Component	Material	References
Hot Leg Piping	SA-516 Grade 70	[8]
Pipe Cladding	ER308L (1)	[3]
Drain Nozzle	SB-166 (N06600, Alloy 600) (2)	[2]
Drain Nozzle-to-Pipe Weld	Alloy 182	[8]
ID Patch Weld	Alloy 182	[8]

Notes:
1. The material properties are based on equivalent Type 304 base material.
2. Alloy SB-166 is assumed to have the same material properties as Alloy 600.

Table 2: Elastic Properties for SA-516 Grade 70 (≤ 4" Thick)

Temperature (°F)	Young's Modulus ($x10^3$ ksi)	Mean Thermal Expansion ($x10^{-6}$ in/in/°F)	Thermal Conductivity (2) (Btu/min-in-°F)	Specific Heat (2) (Btu/lb-°F)
70	29.5	6.4	0.0488	0.103
500	27.3	7.3	0.0410	0.128
700	25.5	7.6	0.0369	0.138
1100	18.0	8.2	0.0290	0.171
1500	5.0	8.6	0.0218	0.198
2500	0.1	9.5	0.0014	0.204
2500.1	–	0.0	–	–

Notes:
1. All values per [5].
2. Density (ρ) = 0.283 lb/in^3 [5], assumed temperature independent.
3. Poisson's Ratio (υ) = 0.3 [5], assumed temperature independent.

Table 3: Stress-Strain Curves for SA-516 Grade 70 (≤ 4" Thick)

Temperature (°F)	Strain (in/in)	Stress (ksi)
70	0.00128814	38.000
	0.00187809	42.000
	0.00257329	46.000
	0.00381110	50.000
	0.00600383	54.000
500	0.00113553	31.000
	0.00142679	35.875
	0.00183954	40.750
	0.00261139	45.625
	0.00415246	50.500
700	0.00106667	27.200
	0.00132412	32.550
	0.00166876	37.900
	0.00228121	43.250
	0.00354341	48.600
1100	0.00116667	21.000
	0.05116163	22.125
	0.05915444	23.250
	0.06794123	24.375
	0.07755935	25.500
1500	0.00300000	15.000
	0.16717493	15.125
	0.16992011	15.250
	0.17268761	15.375
	0.17547742	15.500
2500[2]	0.01000000	1.000
	0.10961239	1.125
	0.12781277	1.250
	0.14689940	1.375
	0.16683167	1.500

Notes:
1. All values per [5].
2. Values at 2500°F assumed arbitrarily small values for convergence stability.

Table 4: Elastic Properties for ER308L

Temperature (°F)	Young's Modulus ($x10^3$ ksi)	Mean Thermal Expansion ($x10^{-6}$ in/in/°F)	Thermal Conductivity (2) (Btu/min-in-°F)	Specific Heat (2) (Btu/lb-°F)
70	28.3	8.5	0.0119	0.116
500	25.8	9.7	0.0151	0.131
700	24.8	10.0	0.0164	0.135
1100	22.1	10.5	0.0189	0.140
1500	18.1	10.8	0.0213	0.145
2500	0.1	11.5	0.0292	0.159
2500.1	–	0.0	–	–

Notes:
1. All values per [5].
2. Density (ρ) = 0.283 lb/in^3 [5], assumed temperature independent.
3. Poisson's Ratio (υ) = 0.3 [5], assumed temperature independent.

Table 5: Stress-Strain Curves for ER308L

Temperature (°F)	Strain (in/in)	Stress (ksi)
70	0.00203180	57.500
	0.02471351	61.563
	0.03107296	65.625
	0.03861377	69.688
	0.04747167	73.750
500	0.00140089	36.143
	0.00714793	40.250
	0.01065407	44.357
	0.01558289	48.464
	0.02233857	52.571
700	0.00132488	32.857
	0.00477547	37.125
	0.00743595	41.393
	0.01143777	45.661
	0.01727192	49.929
1100	0.00121913	26.943
	0.00264833	30.138
	0.00404100	33.332
	0.00634529	36.527
	0.01005286	39.721
1500	0.00117995	21.357
	0.05352064	21.563
	0.05610492	21.768
	0.05878975	21.973
	0.06157807	22.179
2500[2]	0.01000000	1.000
	0.10961239	1.125
	0.12781277	1.250
	0.14689940	1.375
	0.16683167	1.500

Notes:
1. All values per [5].
2. Values at 2500°F assumed arbitrarily small values for convergence stability.

Table 6: Elastic Properties for Alloy 600

Temperature (°F)	Young's Modulus ($x10^3$ ksi)	Mean Thermal Expansion ($x10^{-6}$ in/in/°F)	Thermal Conductivity (2) (Btu/min-in-°F)	Specific Heat (2) (Btu/lb-°F)
70	31.0	6.8	0.0119	0.108
500	29.0	7.6	0.0147	0.120
700	28.2	7.9	0.0161	0.125
1100	25.9	8.4	0.0192	0.139
1500	23.1	9.0	0.0222	0.148
2500	0.1	10.0	0.0306	0.177
2500.1	–	0.0	–	–

Notes:
1. All values per [5].
2. Density (ρ) = 0.300 lb/in^3 [5], assumed temperature independent.
3. Poisson's Ratio (υ) = 0.29 [5], assumed temperature independent.

Table 7: Stress-Strain Curves for Alloy 600

Temperature (°F)	Strain (in/in)	Stress (ksi)
70	0.00157419	48.800
	0.01658847	55.300
	0.02343324	61.800
	0.03212188	68.300
	0.04291703	74.800
500	0.00152069	44.100
	0.01539220	50.338
	0.02210610	56.575
	0.03072476	62.813
	0.04153277	69.050
700	0.00152128	42.900
	0.01634485	49.000
	0.02334760	55.100
	0.03227153	61.200
	0.04338643	67.300
1100	0.00155985	40.400
	0.02275193	44.475
	0.03004563	48.550
	0.03888203	52.625
	0.04943592	56.700
1500	0.00092641	21.400
	0.08827666	22.475
	0.09785101	23.550
	0.10796967	24.625
	0.11863796	25.700
2500[2]	0.01000000	1.000
	0.10961239	1.125
	0.12781277	1.250
	0.14689940	1.375
	0.16683167	1.500

Notes:
1. All values per [5].
2. Values at 2500°F assumed arbitrarily small values for convergence stability.

Table 8: Elastic Properties for Alloy 182

Temperature (°F)	Young's Modulus ($x10^3$ ksi)	Mean Thermal Expansion ($x10^{-6}$ in/in/°F)	Thermal Conductivity (2) (Btu/min-in-°F)	Specific Heat (2) (Btu/lb-°F)
70	31.0	6.8	0.0119	0.108
500	29.0	7.6	0.0147	0.120
700	28.2	7.9	0.0161	0.125
1100	25.9	8.4	0.0192	0.139
1500	23.1	9.0	0.0222	0.148
2500	0.1	10.0	0.0306	0.177
2500.1	–	0.0	–	–

Notes:
1. All values per [5].
2. Density (ρ) = 0.300 lb/in^3 [5], assumed temperature independent.
3. Poisson's Ratio (υ) = 0.29 [5], assumed temperature independent.

Table 9: Stress-Strain Curves for Alloy 182

Temperature (°F)	Strain (in/in)	Stress (ksi)
70	0.00179032	55.500
	0.03456710	60.113
	0.04292837	64.725
	0.05257245	69.338
	0.06359421	73.950
500	0.00164483	47.700
	0.02976152	52.313
	0.03809895	56.925
	0.04790379	61.538
	0.05929946	66.150
700	0.00159574	45.000
	0.02849157	49.538
	0.03680454	54.075
	0.04663682	58.613
	0.05812078	63.150
1100	0.00159073	41.200
	0.03568855	44.488
	0.04402702	47.775
	0.05360088	51.063
	0.06449835	54.350
1500	0.00106494	24.600
	0.11812735	25.325
	0.12540227	26.050
	0.13290814	26.775
	0.14064577	27.500
2500[(2)]	0.01000000	1.000
	0.10961239	1.125
	0.12781277	1.250
	0.14689940	1.375
	0.16683167	1.500

Notes:
1. All values per [5].
2. Values at 2500°F assumed arbitrarily small values for convergence stability.

Table 10: Creep Properties

Material	Temperature (°F)	Creep Strength (ksi)		*A* (ksi/hr)	*n*
		σ_1 (0.0001%/hr)	σ_2 (0.00001%/hr)		
SA-516 Gr. 70 (Based on carbon steel) Per [6]	800	19.0	12.4	1.26E-13	5.40
	900	9.0	6.7	3.59E-14	7.80
	1000	3.5	2.8	2.43E-12	10.32
	1100	1.4	0.8	2.50E-07	4.11
ER308L (Based on Type 304) Per [6]	800	33.4	25.0	7.73E-19	7.95
	900	24.0	17.6	5.67E-17	7.42
	1000	17.6	11.5	1.82E-13	5.41
	1100	11.5	7.1	8.62E-12	4.77
Alloy 600 Alloy 182 (Based on Alloy 600) Per [7]	800	40.0	30.0	1.50E-19	8.00
	900	28.0	18.0	2.87E-14	5.21
	1000	12.5	6.1	3.02E-10	3.21
	1100	6.8	3.4	1.72E-09	3.32

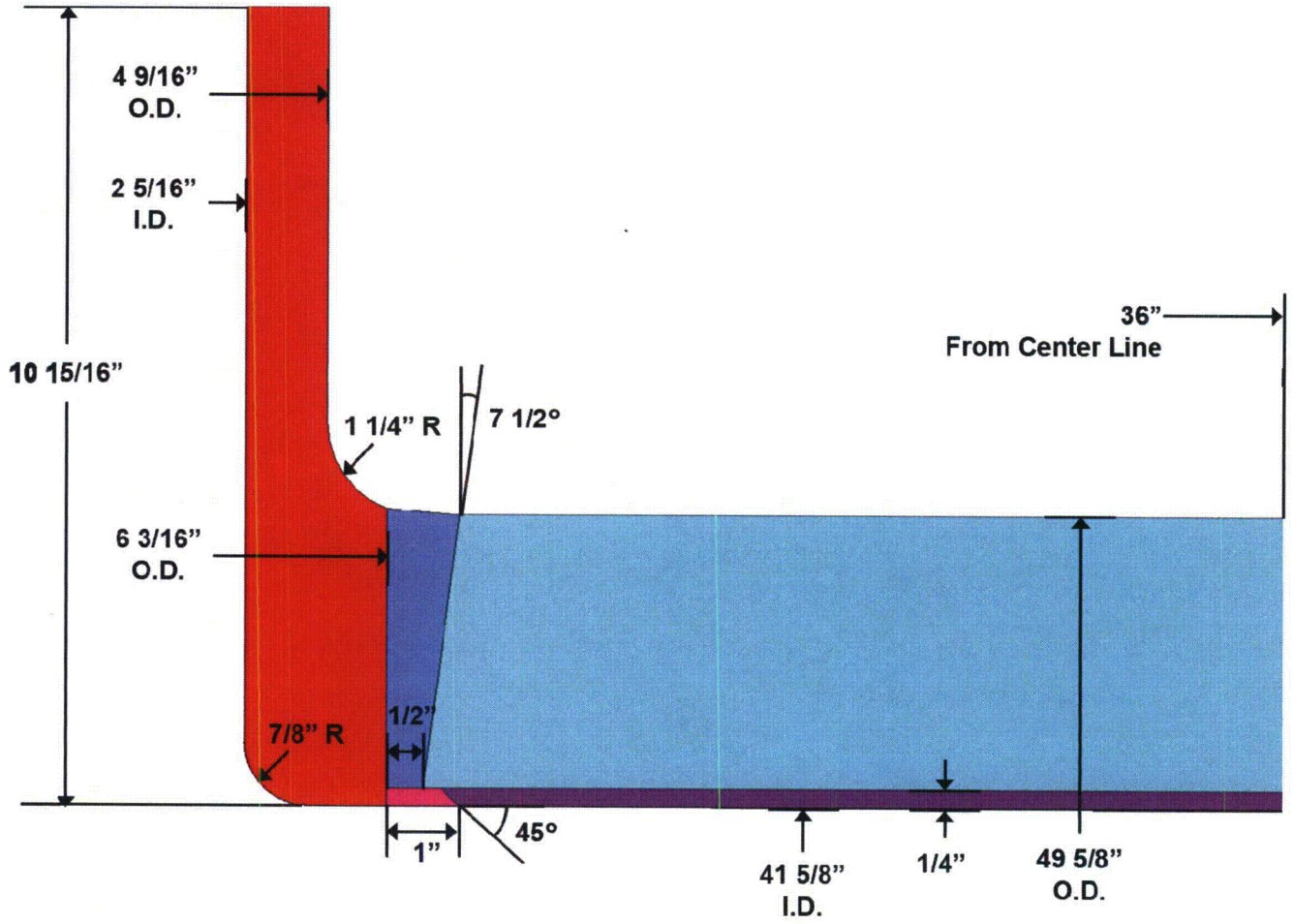

Figure 1. Finite Element Model Dimensions
Note: Dimensions obtained from [2, 3].

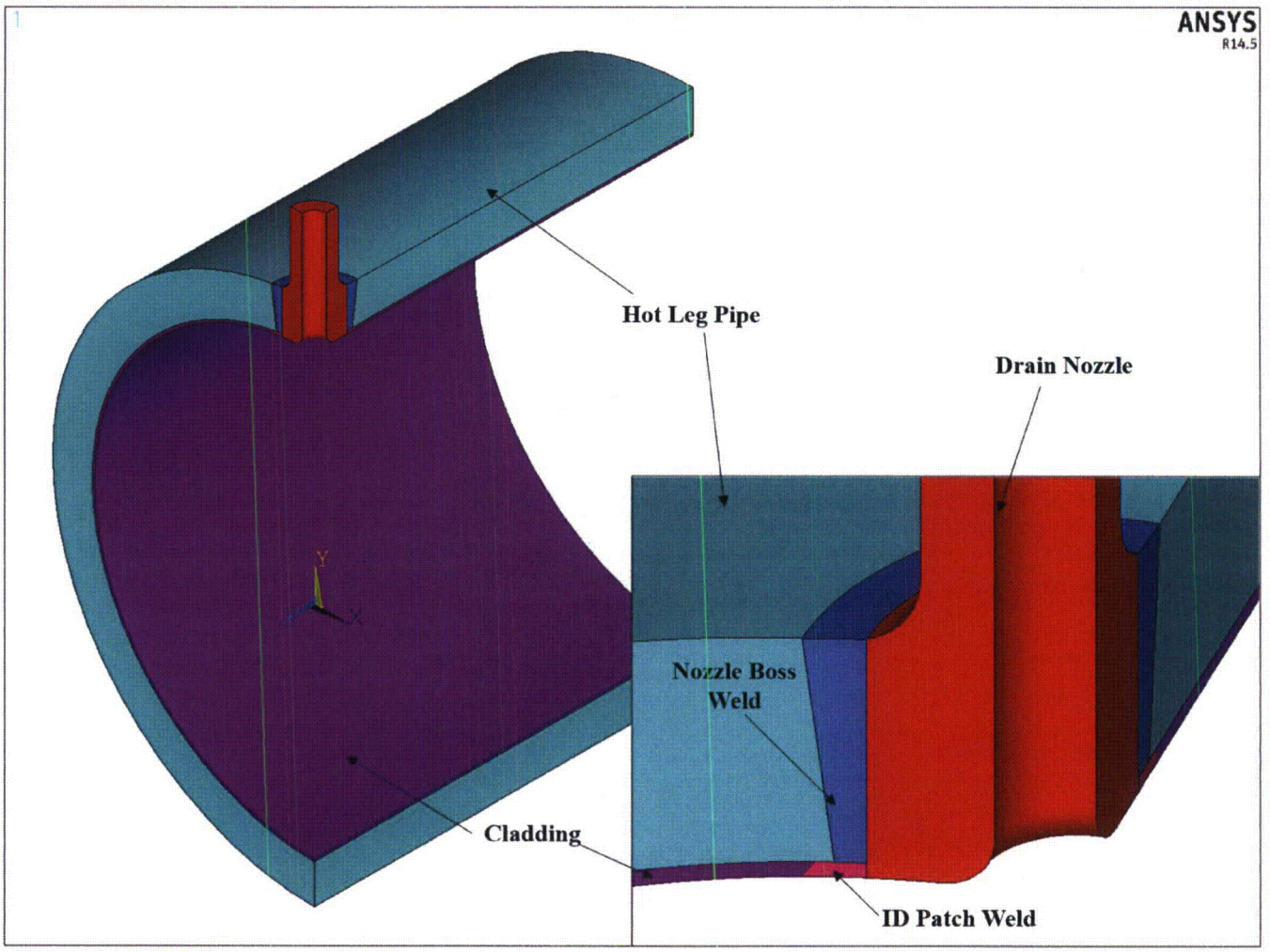

Figure 2. Components Included in the Finite Element Model

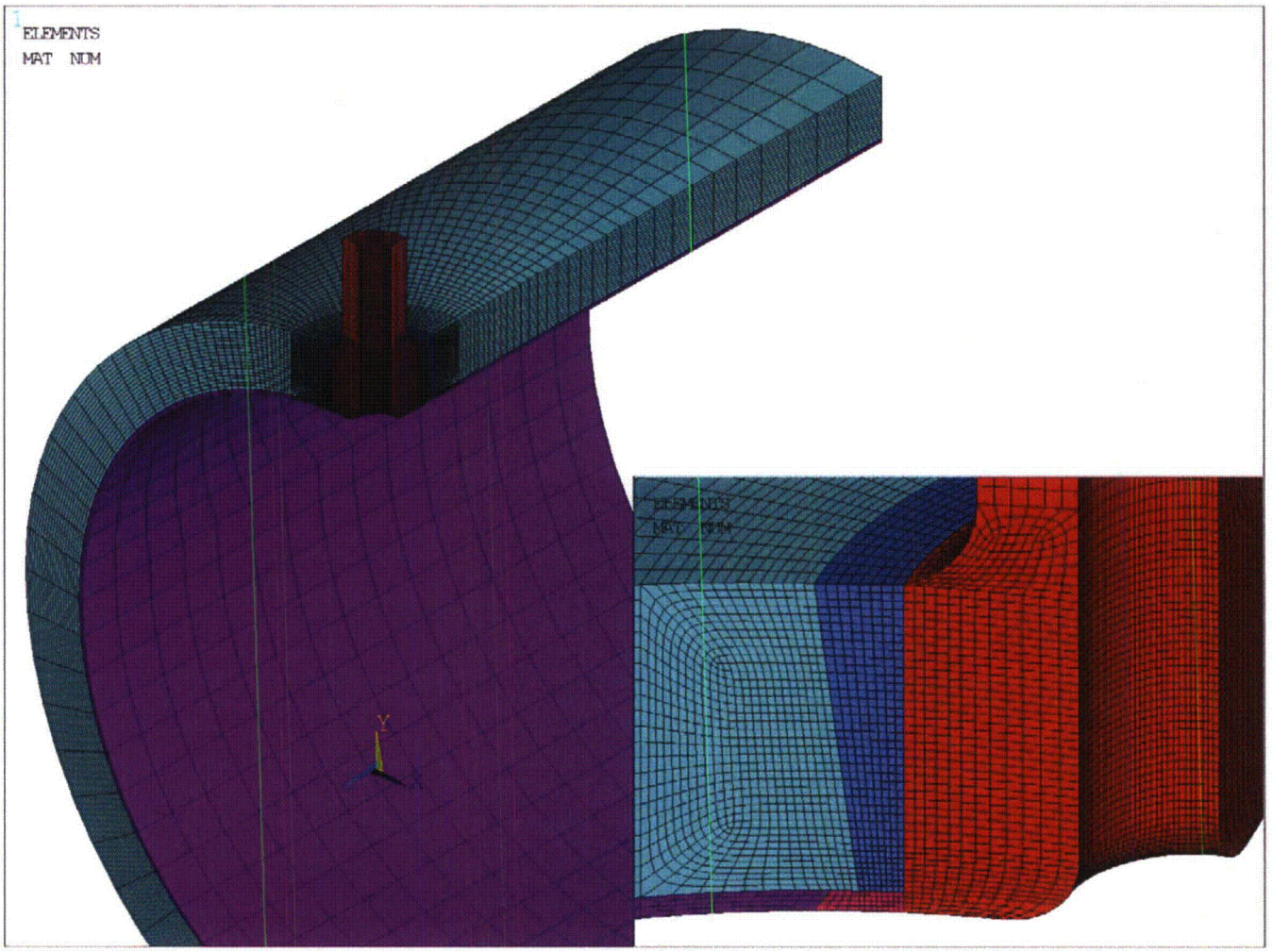

Figure 3. Isometric View of the Finite Element Model
(Nozzle weld detail shown in bottom right corner)

APPENDIX A

COMPUTER FILES LISTING

File Name	Description
Palisades_HL_Drain.INP	Input file to create base model geometry
MProp_MISO.INP	Elastic-plastic Material properties inputs

Structural Integrity Associates, Inc.®

CALCULATION PACKAGE

File No.: 1400669.320

Project No.: 1400669

Quality Program: ☒ Nuclear ☐ Commercial

PROJECT NAME:
Palisades Flaw Readiness Program for 1R24 NDE Inspections

CONTRACT NO.:
10426669

CLIENT:	**PLANT:**
Entergy Nuclear Operations, Inc.	Palisades Nuclear Plant

CALCULATION TITLE:
Finite Element Model Development for the Cold Leg Drain, Spray, and Charging Nozzles

Document Revision	Affected Pages	Revision Description	Project Manager Approval Signature & Date	Preparer(s) & Checker(s) Signatures & Date
0	1 - 20 A-1 - A-2 Computer Files	Initial Issue	Norman Eng NE 4/3/15	Preparer: Wilson Wong WW 4/3/15 Checker: Charles Fourcade CJF 4/3/15 Gole Mukhim GSM 4/3/15

Table of Contents

List of Tables

List of Figures

1.0 OBJECTIVE

The objective of this calculation package is to document the development of a bounding finite element model for the reactor cold leg spray, drain, and charging nozzles at the Palisades Nuclear Plant, which will be used to perform residual and operational-based fracture mechanics analyses to support a subsequent fracture mechanics evaluation as part of a flaw readiness program.

2.0 TECHNICAL APPROACH

One bounding three-dimensional (3-D) finite element model is developed using the ANSYS finite element analysis software package [1] to represent a group of cold leg nozzles. All three nozzles are of similar size near the forging boss area (within 1/16 inch) [2, 3, and 4]. Therefore, the largest inside diameter (ID) and smallest outside diameter (OD) of the three nozzles is chosen for the bounding model. The spray and drain nozzles have identical nozzle and boss OD dimensions of 4-9/16 inch and 6-3/16 inch, respectively, which are slightly smaller than the charging nozzle OD dimensions of 4-5/8 inch and 6-1/4 inch. For the nozzle ID, the charging nozzle is bored out to 2-5/8 inch in the first 1.5 inch to accommodate a thermal sleeve. For conservatism, it is assumed that the entire nozzle ID is 2-5/8 inch.

The area of interest is the nozzle-to-pipe weld. The model uses elastic-plastic material properties intended for weld residual stress analysis, and elastic material properties for linear elastic analyses.

3.0 ASSUMPTIONS / DESIGN INPUTS

The dimensions and material types to develop the finite element model are provided in References 2, 3, and 4 and summarized in Figure 1. The material properties are obtained from References 5 and 6. A number of assumptions were made during development of the finite element model, which are listed as follows:

- Since the area of interest is the nozzle to cold leg weld, dimensional differences between nozzles on the attached piping side are considered insignificant.
- The largest inside diameter (ID) and smallest outside diameter (OD) of the three nozzles will be chosen for the bounding model. This is conservative for pressure and mechanical loads.
- The axial length of the modeled portion of the cold leg piping is arbitrarily set at 36 inches, which is sufficiently long to negate possible end effects in the region of interest.
- The ID patch weld is added after removal of the backing ring according to the weld procedure mentioned in the drawings [2, 3]. The same material of the nozzle-to-pipe weld is used for the ID patch weld.

4.0 FINITE ELEMENT MODEL

The model includes a local portion of the cold leg pipe and cladding, the nozzle, and the nozzle-to-pipe weld, including the ID patch weld, as shown in Figure 2. As shown in the figure, a single 90° quadrant of the nozzle penetration is modeled due to geometric symmetry. The included portion of the cold leg piping measures 36 inches longitudinally and 180 degrees circumferentially. The mesh of the finite element model is shown in Figure 3.

4.1 Element Type and Mesh

The 8-node solid element (SOLID185) in ANSYS [1] is used for the model. SOLID185 elements support material plasticity which is suitable for residual stress and elastic plastic fracture mechanics (EPFM) analyses. The model contains adequate mesh refinement within the weld region to predict the residual stresses from welding.

4.2 Materials

The material designation for the modeled components is listed in Table 1. The temperature dependent nonlinear material property values are provided in a separate calculation package [6], which are based on the 2001 Edition of the ASME Code with Addenda through 2003 [5]. The material properties are listed in Table 2 through Table 9.

4.2.1 Creep Properties

Since post weld heat treatment (PWHT) will be considered in the subsequent residual stress calculation, creep properties are required. In general, creep becomes significant at temperatures above 800°F; thus, creep behavior under 800°F will not be considered in this analysis.

There are two main categories of creep: primary and secondary. The primary creep addresses the creep characteristics for a short duration at the early stages of the creep regime, while the secondary creep accounts for the creep behavior for a long duration – usually more than 10,000 hours. Based on this definition, the PWHT falls within the primary creep characteristics. However, primary creep rates for materials are difficult to obtain, so the conservative secondary creep rates are used since primary creep rate is typically an order of magnitude higher than that for secondary creep.

In general, the primary creep rate for the materials is governed by the equation:

$$\frac{d\varepsilon}{dt} = A\sigma^n$$

The creep data for the SA-516 Grade 70 cold leg material is based on carbon steel material [7]. The creep data for the Alloy 82/182 and ER308L weld metals are not available, so the creep properties for their base metals are used instead. The creep data for Type 304 (for ER308L) is provided in the same reference document as the carbon steel [7], while the creep data for the Alloy 600 (for Alloy 82/182) is provided in a separate reference document [8]. All the creep strengths, σ, are provided at two creep rates [7, 8] for each temperature point.

When creep strength is provided at two creep rates at the same temperature point, as listed in Table 10, then A and n can be calculated as follows, where subscripts 1 and 2 refer to the creep data sets 1 and 2:

$$\frac{d\varepsilon}{dt} = \dot{\varepsilon} = A\sigma^n$$

$$\dot{\varepsilon}_1 = A\sigma_1^n; \quad \dot{\varepsilon}_2 = A\sigma_2^n$$

$$\frac{\dot{\varepsilon}_1}{\dot{\varepsilon}_2} = \left(\frac{\sigma_1}{\sigma_2}\right)^n$$

$$\ln\left(\frac{\dot{\varepsilon}_1}{\dot{\varepsilon}_2}\right) = n\ln\left(\frac{\sigma_1}{\sigma_2}\right)$$

$$n = \frac{\ln\left(\frac{\dot{\varepsilon}_1}{\dot{\varepsilon}_2}\right)}{\ln\left(\frac{\sigma_1}{\sigma_2}\right)}$$

$$A = \frac{\dot{\varepsilon}_1}{\sigma_1^n}$$

4.3 Loads and Boundary Conditions

No loads or boundary conditions of any kind are included in the finite element model in this calculation. Specific loads and boundary conditions, appropriate to the specific analyses, will be applied in the subsequent residual and thermal/mechanical stress calculation packages.

5.0 CONCLUSIONS

A bounding finite element model for the cold leg spray, drain, and charging nozzles is developed. The model will be used in subsequent weld residual stress analyses and fracture mechanics analyses. The necessary ANSYS input file names are listed in Appendix A.

6.0 REFERENCES

1. ANSYS Mechanical APDL and PrepPost, Release 14.5 (w/ Service Pack 1), ANSYS, Inc., September 2012.
2. Combustion Engineering Drawing E232-675-4, "Nozzle Details," SI File No. 1400669.202.
3. Combustion Engineering Drawing E232-676-7, "Nozzle Details," SI File No. 1400669.202.
4. Combustion Engineering Drawing E232-673-7, "Piping Assembly & Details," SI File No. 1400669.202.
5. ASME Boiler and Pressure Vessel Code, Section II, Part D – Properties, 2001 Edition with Addenda through 2003.
6. SI Calculation No. 0800777.307, Rev. 5, "Material Properties for Residual Stress Analyses, Including MISO Properties Up To Material Flow Stress."
7. "Steels for Elevated Temperature Service," United States Steel Co., 1949.
8. Publication SMC-027, "Inconel Alloy 600," Special Metals Corp., 2004, SI File 0800777.211.
9. Palisades Design Input Record, "Palisades Alloy 600 Flaw Eval DIR 3-4-15 Rev 1.pdf," SI File No. 1400669.201.

Table 1: Component Materials

Component	Material	References
Cold Leg Piping	SA-516 Grade 70	[9]
Pipe Cladding	ER308L [1]	[4]
Bounding Nozzle	SB-166 (N06600, Alloy 600)[2]	[2, 3]
Weld	Alloy 182	[9]
ID Patch Weld	Alloy 182	[9]

Notes:
1. The material properties are based on equivalent Type 304 base material.
2. Alloy SB-166 is assumed to have the same material properties as Alloy 600.

Table 2: Elastic Properties for SA-516 Grade 70 (≤ 4" Thick)

Temperature (°F)	Elastic Modulus ($x10^3$ ksi)	Mean Thermal Expansion ($x10^{-6}$ in/in/°F)	Thermal Conductivity[2] (Btu/min-in-°F)	Specific Heat[2] (Btu/lb-°F)
70	29.5	6.4	0.0488	0.103
500	27.3	7.3	0.0410	0.128
700	25.5	7.6	0.0369	0.138
1100	18.0	8.2	0.0290	0.171
1500	5.0	8.6	0.0218	0.198
2500	0.1	9.5	0.0014	0.204
2500.1	--	0	--	--

Notes:
1. All values per [6].
2. Density (ρ) = 0.283 lb/in^3 [6], assumed temperature independent.
3. Poisson's Ratio (ν) = 0.3 [6], assumed temperature independent.

Table 3: Stress-Strain Curves for SA-516 Grade 70 (≤ 4" Thick)

Temperature (°F)	Strain (in/in)	Stress (ksi)
70	0.00128814	38.000
	0.00187809	42.000
	0.00257329	46.000
	0.00381110	50.000
	0.00600383	54.000
500	0.00113553	31.000
	0.00142679	35.875
	0.00183954	40.750
	0.00261139	45.625
	0.00415246	50.500
700	0.00106667	27.200
	0.00132412	32.550
	0.00166876	37.900
	0.00228121	43.250
	0.00354341	48.600
1100	0.00116667	21.000
	0.05116163	22.125
	0.05915444	23.250
	0.06794123	24.375
	0.07755935	25.500
1500	0.00300000	15.000
	0.16717493	15.125
	0.16992011	15.250
	0.17268761	15.375
	0.17547742	15.500
2500[2]	0.01000000	1.000
	0.10961239	1.125
	0.12781277	1.250
	0.14689940	1.375
	0.16683167	1.500

Notes:
1. All values per [6].
2. Values at 2500°F assumed arbitrarily small values for convergence stability.

Table 4: Elastic Properties for ER308L

Temperature (°F)	Elastic Modulus ($x10^3$ ksi)	Mean Thermal Expansion ($x10^{-6}$ in/in/°F)	Thermal Conductivity[2] (Btu/min-in-°F)	Specific Heat[2] (Btu/lb-°F)
70	28.3	8.5	0.0119	0.116
500	25.8	9.7	0.0151	0.131
700	24.8	10.0	0.0164	0.135
1100	22.1	10.5	0.0189	0.140
1500	18.1	10.8	0.0212	0.145
2500	0.1	11.5	0.0292	0.159
2500.1	--	0	--	--

Notes:
1. All values per [6].
2. Density (ρ) = 0.283 lb/in^3 [6], assumed temperature independent.
3. Poisson's Ratio (ν) = 0.3 [6], assumed temperature independent.

Table 5: Stress-Strain Curves for ER308L

Temperature (°F)	Strain (in/in)	Stress (ksi)
70	0.00203180	57.500
	0.02471351	61.563
	0.03107296	65.625
	0.03861377	69.688
	0.04747167	73.750
500	0.00140089	36.143
	0.00714793	40.250
	0.01065407	44.357
	0.01558289	48.464
	0.02233857	52.571
700	0.00132488	32.857
	0.00477547	37.125
	0.00743595	41.393
	0.01143777	45.661
	0.01727192	49.929
1100	0.00121913	26.943
	0.00264833	30.138
	0.00404100	33.332
	0.00634529	36.527
	0.01005286	39.721
1500	0.00117995	21.357
	0.05352064	21.563
	0.05610492	21.768
	0.05878975	21.973
	0.06157807	22.179
2500 [2]	0.01000000	1.000
	0.10961239	1.125
	0.12781277	1.250
	0.14689940	1.375
	0.16683167	1.500

Notes:
1. All values per [6].
2. Values at 2500°F assumed arbitrarily small values for convergence stability.

Table 6: Elastic Properties for Alloy 600

Temperature (°F)	Elastic Modulus ($x10^3$ ksi)	Mean Thermal Expansion ($x10^{-6}$ in/in/°F)	Thermal Conductivity[2] (Btu/min-in-°F)	Specific Heat[2] (Btu/lb-°F)
70	31.0	6.8	0.0119	0.108
500	29.0	7.6	0.0147	0.120
700	28.2	7.9	0.0161	0.125
1100	25.9	8.4	0.0192	0.139
1500	23.1	9.0	0.0222	0.148
2500	0.1	10.0	0.0306	0.177
2500.1	--	0	--	--

Notes:
1. All values per [6].
2. Density (ρ) = 0.300 lb/in^3 [6], assumed temperature independent.
3. Poisson's Ratio (ν) = 0.29 [6], assumed temperature independent.

Table 7: Stress-Strain Curves for Alloy 600

Temperature (°F)	Strain (in/in)	Stress (ksi)
70	0.00157419	48.800
	0.01658847	55.300
	0.02343324	61.800
	0.03212188	68.300
	0.04291703	74.800
500	0.00152069	44.100
	0.01539220	50.338
	0.02210610	56.575
	0.03072476	62.813
	0.04153277	69.050
700	0.00152128	42.900
	0.01634485	49.000
	0.02334760	55.100
	0.03227153	61.200
	0.04338643	67.300
1100	0.00155985	40.400
	0.02275193	44.475
	0.03004563	48.550
	0.03888203	52.625
	0.04943592	56.700
1500	0.00092641	21.400
	0.08827666	22.475
	0.09785101	23.550
	0.10796967	24.625
	0.11863796	25.700
2500 [2]	0.01000000	1.000
	0.10961239	1.125
	0.12781277	1.250
	0.14689940	1.375
	0.16683167	1.500

Notes:
1. All values per [6].
2. Values at 2500°F assumed arbitrarily small values for convergence stability.

Table 8: Elastic Properties for Alloy 82/182

Temperature (°F)	Elastic Modulus ($x10^3$ ksi)	Mean Thermal Expansion ($x10^{-6}$ in/in/°F)	Thermal Conductivity (2) (Btu/min-in-°F)	Specific Heat (2) (Btu/lb-°F)
70	31.0	6.8	0.0119	0.108
500	29.0	7.6	0.0147	0.120
700	28.2	7.9	0.0161	0.125
1100	25.9	8.4	0.0192	0.139
1500	23.1	9.0	0.0222	0.148
2500	0.1	10.0	0.0306	0.177
2500.1	–	0.0	–	–

Notes:

1. All values per [6].
2. Density (ρ) = 0.300 lb/in^3 [6], assumed temperature independent.
3. Poisson's Ratio (ν) = 0.29 [6], assumed temperature independent.

Table 9: Stress-Strain Curves for Alloy 82/182

Temperature (°F)	Strain (in/in)	Stress (ksi)
70	0.00179032	55.500
	0.03456710	60.113
	0.04292837	64.725
	0.05257245	69.338
	0.06359421	73.950
500	0.00164483	47.700
	0.02976152	52.313
	0.03809895	56.925
	0.04790379	61.538
	0.05929946	66.150
700	0.00159574	45.000
	0.02849157	49.538
	0.03680454	54.075
	0.04663682	58.613
	0.05812078	63.150
1100	0.00159073	41.200
	0.03568855	44.488
	0.04402702	47.775
	0.05360088	51.063
	0.06449835	54.350
1500	0.00106494	24.600
	0.11812735	25.325
	0.12540227	26.050
	0.13290814	26.775
	0.14064577	27.500
2500[(2)]	0.01000000	1.000
	0.10961239	1.125
	0.12781277	1.250
	0.14689940	1.375
	0.16683167	1.500

Notes:
1. All values per [6].
2. Values at 2500°F assumed arbitrarily small values for convergence stability.

Table 10: Creep Properties

Material	Temperature (°F)	Creep Strength (ksi)		*A* (ksi/hr)	*n*
		σ_1 (0.0001%/hr)	σ_2 (0.00001%/hr)		
SA-516 Gr. 70 (Based on carbon steel per [7])	800	19.0	12.4	1.26E-13	5.40
	900	9.0	6.7	3.59E-14	7.80
	1000	3.5	2.8	2.43E-12	10.32
	1100	1.4	0.8	2.50E-07	4.11
ER308L (Based on Type 304 per [7])	800	33.4	25.0	7.73E-19	7.95
	900	24.0	17.6	5.67E-17	7.42
	1000	17.6	11.5	1.82E-13	5.41
	1100	11.5	7.1	8.62E-12	4.77
Alloy 600 Alloy 82/182 (Based on Alloy 600 per [8])	800	40.0	30.0	1.50E-19	8.00
	900	28.0	18.0	2.87E-14	5.21
	1000	12.5	6.1	3.02E-10	3.21
	1100	6.8	3.4	1.72E-09	3.32

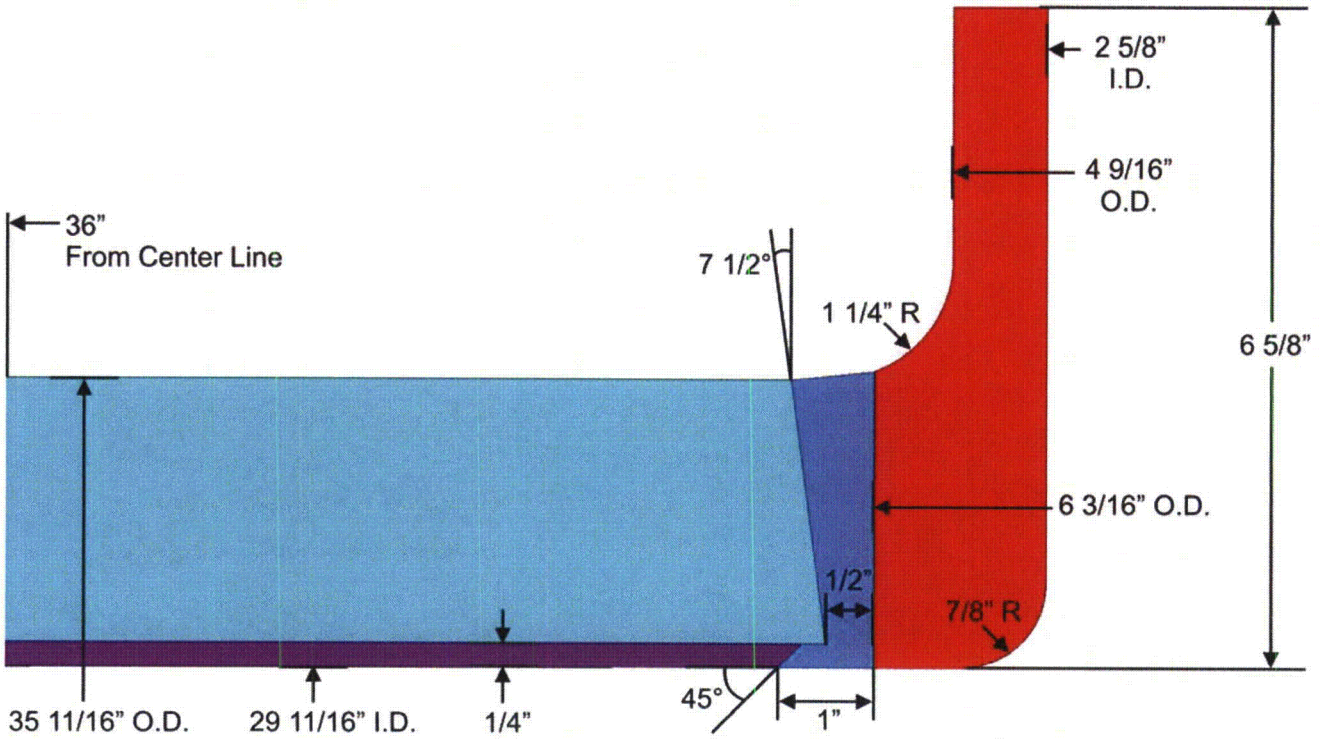

Figure 1. Finite Element Model Dimensions

Note: Dimensions obtained from [2, 3, and 4].

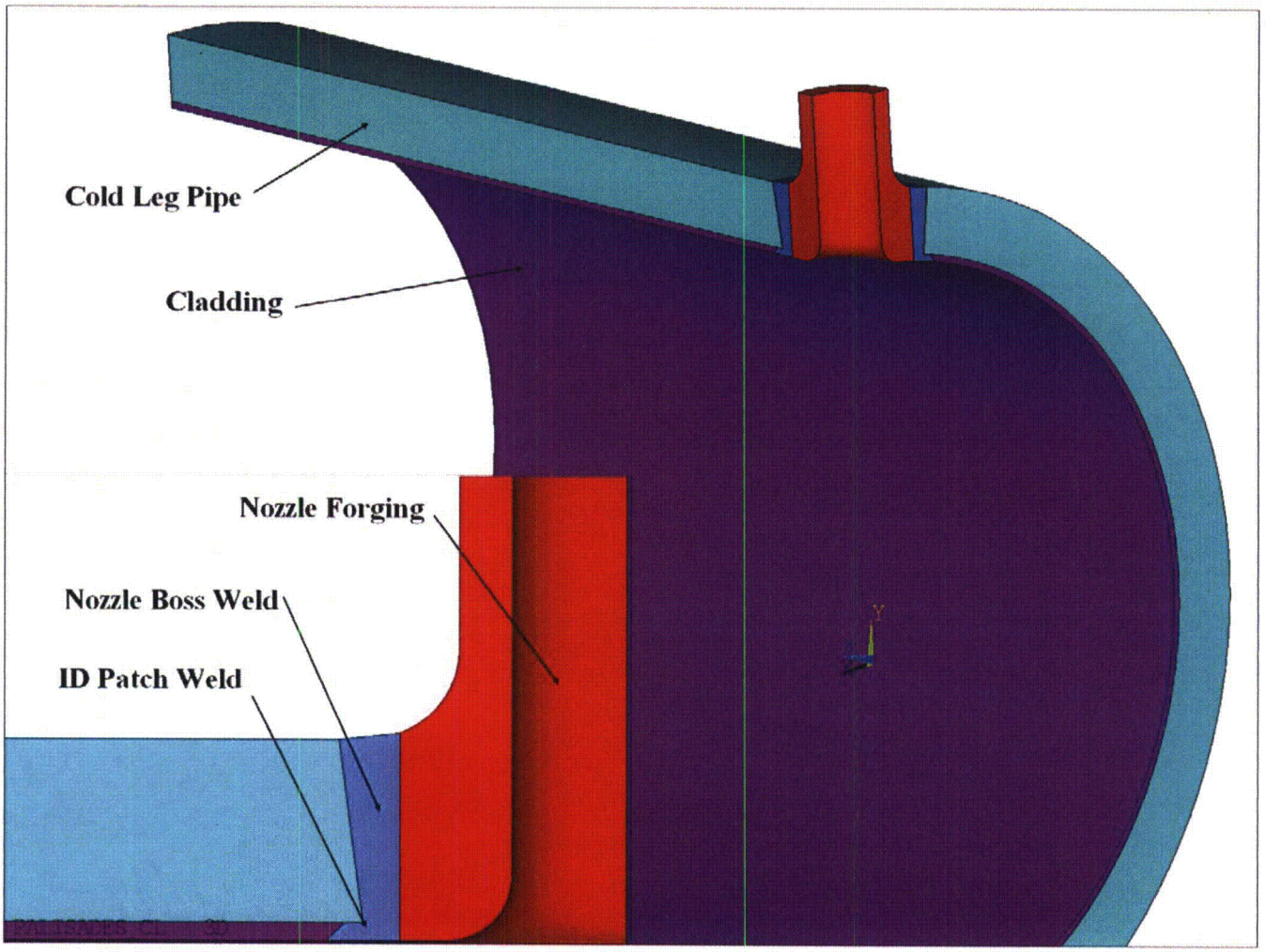

Figure 2. Components Included in the Finite Element Model

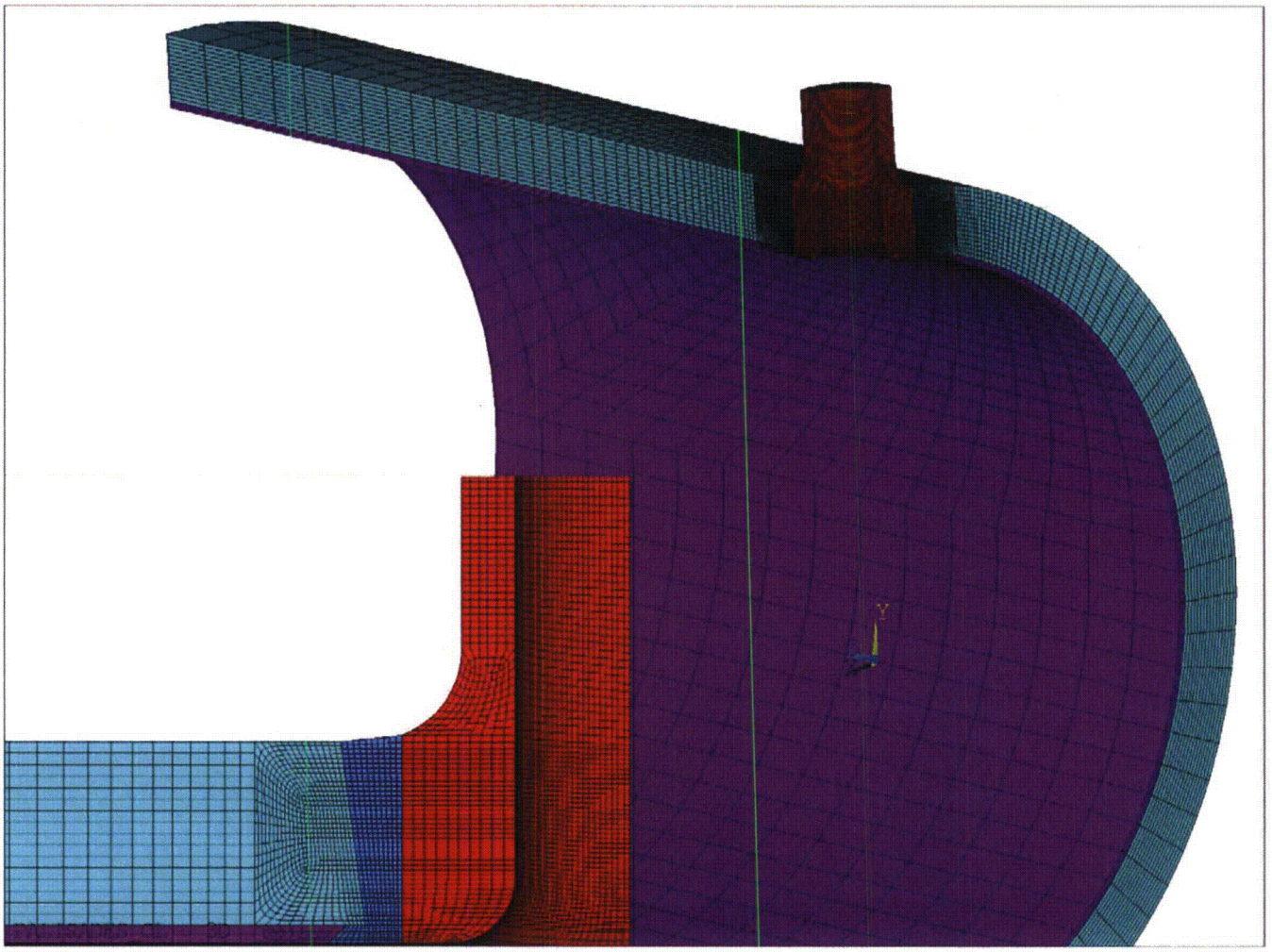

Figure 3. Isometric View of the Finite Element Model

(Nozzle detail shown in bottom left corner)

APPENDIX A

COMPUTER FILES LISTING

File Name	Description
Palisades_CL.INP	Input file to create base model geometry
MProp_Miso.INP	Elastic plastic material properties inputs
MatProp.xls	Excel spreadsheet containing calculations of elastic-plastic material properties for residual stress analysis

Structural Integrity Associates, Inc.®

CALCULATION PACKAGE

File No.: 1400669.312

Project No.: 1400669

Quality Program Type: ☒ Nuclear ☐ Commercial

PROJECT NAME:
Palisades Flaw Readiness Program for 1R24 NDE Inspection

CONTRACT NO.:
10426669

CLIENT:	**PLANT:**
Entergy Nuclear Operations, Inc.	Palisades Nuclear Plant

CALCULATION TITLE:
Hot Leg Drain Nozzle Weld Residual Stress Analysis

Document Revision	Affected Pages	Revision Description	Project Manager Approval Signature & Date	Preparer(s) & Checker(s) Signatures & Date
0	1 - 38 A-1 - A-2 Computer Files	Initial Issue	Norman Eng NE 5/5/2015	Preparer: Minji Fong MF 5/5/2015 Checkers: Charles Fourcade CJF 5/5/2015 Gole Mukhim GSM 5/5/2015

Table of Contents

List of Tables

List of Figures

1.0 OBJECTIVE

The objective of this calculation package is to document the weld residual stress analysis for the hot leg drain nozzle at the Palisades Nuclear Plant (Palisades). The weld residual stress analysis is based on the latest methodology and process developed by Structural Integrity Associates (SI).

2.0 TECHNICAL APPROACH

The finite element model is obtained from a previous finite element model (FEM) calculation package [1] and the weld residual stress analysis uses the latest weld residual stress analysis methodology developed by SI, using the ANSYS finite element analysis (FEA) program [3].

The residual stress analysis consists of a thermal pass followed by a stress pass, where the temperature distribution time history from the thermal pass is used as temperature input into the stress pass to determine stresses. Stress results from the weld residual stress analysis are obtained and saved for future use to evaluate flaws which will be performed in a separate calculation package.

The finite element model includes all components in the post-nozzle installation stage because new elements cannot be added during an ANSYS analysis run. Since all the weld elements need to be included in the initial model, the element "birth and death" technique in ANSYS is used to initially deactivate the weld elements, with elements corresponding to the active weld segment reactivated at the melting temperature, thus simulating the weld metal deposition.

2.1 Material Properties

The weld residual stress analysis performed in this calculation uses the material properties specifically developed in a separate calculation package for weld residual stress analyses [2]. Per the material designation used in the FEM calculation [1], the following materials are used:

- SA-516 Grade 70: Hot leg base metal
- ER308L: Hot leg cladding (typical weld metal for Type 304)
- Alloy 182: Boss weld and ID patch weld
- Alloy 600 (SB-166): Drain nozzle

The material properties are reproduced in Table 1 through Table 8.

2.2 Finite Element Model for Weld Residual Stress Analysis

The finite element model for the analysis was developed in a previous FEM calculation [1], which was created using the ANSYS finite element analysis software package [3]. The base finite element model for the weld residual stress analysis is meshed with 8-node solid elements (SOLID185) in ANSYS. This finite element model is shown in Figure 1.

2.3 Welding Simulation

The FEA for predicting the weld residual stresses is performed as a continuous analysis so that the load history from the cladding is carried over the nozzle-to-pipe weld and ID patch weld. Specifically, the residual stresses and strains at the end of one weld pass are used as initial conditions at the start of the next weld pass.

The procedures for this complex multi-step simulation are encoded in ANSYS Parametric Design Language (APDL) macros which utilize elastic-plastic material behavior and elements with large deformation capability to predict the residual stresses due to the various welding processes.

2.4 Heat Inputs

The deposition of the weld metal is simulated by imposing a heat generation function on the elements of the FEM representing the active weld, which is applied as a volumetric body heat generation rate. The amount of equivalent heat input energy, Q (in terms of kJ/inch), is determined from the welding parameters.

Since the welding parameters for the welds are not available, a typical heat input of 28 kJ/inch, with an overall heat efficiency of 0.8, is assumed for all the welds. The heat efficiency represents a "composite" value reflecting the concepts of arc efficiency, melting efficiency, etc., and is an optimum value to produce reasonable heat penetration in the analysis.

The APDL macros automatically calculate the appropriate time intervals for the thermal pass to ensure that sufficient heat penetration is achieved, the required interpass temperature between weld passes is met, and a reasonable overall temperature distribution within the finite element model is achieved. The resulting temperature time history is then imported into the stress pass in order to calculate the residual stresses due to the thermal cycling of the weld elements using nonlinear, elastic-plastic load/unload stress reversal relations.

The following summarizes the welding parameters used in the analysis:

- Interpass temperature = 350°F [4]
- Melting temperature = 2500°F (See Section 3.0)
- Reference temperature = 70°F (See Section 3.0)

- Heat input for all welds = 28 kJ/in (See Section 3.0)
- Heat efficiency for all welds = 0.8 (See Section 3.0)
- Inside/Outside heat transfer coefficient = 5 Btu/hr-ft^2-°F (See Section 3.0)
- Inside/Outside temperature = 70°F (See Section 3.0)

2.5 Creep Properties

Strain relaxation due to creep at high temperature is considered in the post-weld heat treatment (PWHT) step of the analysis. In general, creep becomes significant at temperature above 800°F; thus, creep behavior under 800°F will not be considered in this analysis. The creep properties listed in Table 9 are determined in the previous FEM calculation [1].

2.6 Mechanical Boundary Conditions

The mechanical boundary conditions for the stress analysis are symmetric boundary conditions at the symmetry planes of the model, axial displacement restraint at the end of the nozzle, and axial displacement coupling at the end of the hot leg piping, as shown in Figure 2.

3.0 ASSUMPTIONS

The following assumptions are used in the analyses:

- The hot leg cladding material is assumed to be ER308L, which is a typical weld metal for Type 304 stainless steel cladding.
- The metal melting temperature is assumed to be 2500°F, which is the temperature point where the strength of the material is set to near zero [1].
- The analysis is performed with a reference temperature of 70°F.
- The exposed surface of the model is subject to a typical ambient air cooling convection film coefficient of 5 Btu/hr-ft^2-°F at a bulk temperature of 70°F. The exposed surfaces are defined as the exterior surfaces of the model, excluding the symmetry planes and the far ends of the modeled piping and nozzle.
- Since the welding parameters for the welds are not available, a typical heat input of 28 kJ/in, with an overall heat efficiency of 0.8, is assumed for all of the welds.
- The focus of this analysis is the residual stresses in the drain nozzle boss weld region, while the interaction between the clad buildup and the hot leg base metal has secondary effects on the region of interest. Therefore, the clad is assumed to be fully deposited in a single one-layer pass.

- The boss weld is represented by a 40-bead process, as shown in Figure 3, with each bead represented by a one pass "bead ring" nugget. This approach is a common and acceptable industry practice when information regarding the bead start/stop position and sequencing are unknown.
- Similarly, the ID patch weld is represented by a 6-bead process, as shown in Figure 4, with each bead represented by a one pass "bead ring" nugget.
- For model simplification, the penetration hole is present during the deposition of the clad material. This is acceptable since any localized stress with or without the hole would have negligible impact on the final results.
- For convenience, the modeled ID patch weld has the same geometry as the backing ring for the boss weld.
- Additional assumptions on PWHT are discussed in Section 4.4.

4.0 WELD RESIDUAL STRESS ANALYSIS

The weld residual stress analysis consists of a thermal analysis to determine the temperature distribution followed by a stress analysis to determine the resulting stresses. The analytical sequence described below is used in the finite element analysis, followed by detailed discussions of the steps in Sections 4.1 through 4.6:

1. Deposit cladding on hot leg pipe inside (ID) surface.
2. Install drain nozzle, backing ring, and deposit boss weld.
3. Remove backing ring and deposit ID patch weld.
4. Post-weld heat treatment, including creep effects based upon experimental data per Table 9.
5. Subject the configuration to hydrostatic test.
6. Impose five cycles of "shake down" with normal operating temperature and pressure to stabilize the residual stress fluctuations due to stress redistribution caused by normal operating loads.

4.1 Hot Leg Cladding

The clad material is typically welded onto the inside surface of the hot leg pipe, and the nominal thickness of the clad is thicker than the typical thickness for a single weld layer used in the process. However, the focus of this analysis is on the as-welded residual stresses, while the interaction between the clad buildup and the base material during the many actual weld passes is not of interest. Therefore, the clad is assumed to be fully deposited in a single pass.

At this step, only the hot leg pipe base metal elements and clad material elements are active; all other components are deactivated during the analysis. At the end of the cladding application, the entire model is cooled to 70°F before application of the boss weld.

4.2 Boss Weld

The boss weld connects the drain nozzle boss to the hot leg piping. As shown in Figure 3, the weld is composed of 40 nuggets deposited in 20 weld layers. In the absence of detailed weld fabrication information, a weld sequence is assumed based on standard welding practice at the time of fabrication. In particular, for every layer, the first nugget is deposited on the hot leg side, the second nugget on the nozzle side.

At this step, the drain nozzle elements and backing ring elements are reactivated, and the boss weld nuggets are reactivated sequentially to simulate the welding process. The preheat temperature of the boss weld is 250°F [4]. At the end of the boss weld, the entire model is cooled to 70°F before the application of the ID patch weld.

4.3 ID Patch Weld

The final weld step is to add the ID patch weld, which replaces the backing ring. As seen in Figure 4, the ID patch weld is composed of 6 nuggets deposited in 2 layers.

At this step, the backing ring is first deactivated to allow the residual stresses to redistribute, and the ID patch weld nuggets are reactivated sequentially to simulate the welding process. The preheat temperature of the ID patch weld is 250°F [4]. At the end of the ID patch weld, the entire model is cooled to 70°F before the post-weld heat treatment (PWHT).

4.4 Post-weld Heat Treatment

PWHT is assumed to be performed as per the following procedure outlined in Article N-532 of the ASME Code, Section III [7] and the welding procedure [4] for welding on material group P-1:

1. Heat welded piping component to 1150°F [4] at a heating rate of 400°F per hour divided by the maximum metal thickness (100°F per hour for 4 inch thick hot leg) [7, Article N-532.3 (2)].
2. Hold at temperature for approximately 4 hours (1hr/in of weld thickness) [7, Table N-532].
3. Allow to cool to 600°F at a cooling rate of 500°F per hour divided by the maximum metal thickness (125°F per hour for 4 inch thick hot leg) at temperature above 600°F [7, Article N-532.3 (5)].
4. Air-cool from 600°F to ambient [7, Article N-532.3 (5)].
5. A steady state load step is imposed at the end of the PWHT process.

During the PWHT, creep behavior is activated for time steps with the maximum temperature above 800°F. At the end of the PWHT, the entire model is cooled to 70°F before the application of the hydrostatic test.

4.5 Hydrostatic Test

A hydrostatic test pressure of 3110 psig (3125 psia) and a temperature of 400°F [8, page 9] are applied after the welding. The pressure is applied on the ID surfaces of the hot leg pipe and drain nozzle. End-cap loads, $P_{end\text{-}cap\text{-}hl}$ is applied at the free end of the hot leg piping. This is calculated based on the following expression:

$$P_{end-cap-hl} = \frac{P \times r_{inside-hl}^2}{r_{outside-hl}^2 - r_{inside-hl}^2}$$

where,

P	= Hydrostatic test pressure (ksi)
$P_{end\text{-}cap\text{-}hl}$	= End cap pressure on hot leg pipe end (ksi)
$r_{inside\text{-}hl}$	= Inside radius of hot leg pipe (in)
$r_{outside\text{-}hl}$	= Outside radius of hot leg pipe (in)

The applied pressure loads on the model are shown in Figure 5.

4.6 Five Normal Operating Cycles (NOC)

After the hydrostatic test, the assembled configuration is put into service and subjected to five cycles of shake down to stabilize the as-welded residual stresses. This step involves ramping the model from zero-load to steady-state conditions at normal operating temperature and pressure then back to steady-state at 70°F and no pressure five times.

The applied operating pressure is 2085 psig (2100 psia) and temperature is 583°F [9]. The temperature is assumed to be uniform throughout the components and operating pressure is applied as an internal pressure on the ID surface, with corresponding end cap pressures calculated using the equation in the previous section. The term "P" is replaced by the operating pressure in the expression.

5.0 RESULTS OF WELD RESIDUAL STRESS ANALYSIS

The ANSYS input files and computer output files for the analyses are listed in Appendix A.

5.1 Welding Temperature Contours

The maximum temperature prediction contours for each weld are created using the macro **MapTemp.mac**. This type of contour plot is also called a "fusion boundary" plot because it provides an overview of the maximum temperature on each node throughout the thermal transient for each welding process. The plots are useful in visualizing the melting of weld metal and the extent of heat penetration.

The predicted fusion boundary contours for the cladding, the nozzle-to-pipe weld, and ID patch weld applications are shown in Figure 6, Figure 7, and Figure 8, respectively. The purple color in the plots represents elements at melting temperature (>2500°F); the plots show complete melting of the weld metal for each weld and slight melting of the base metal along the weld interface.

5.2 PWHT Temperature Results

Figure 9 plots the inside surface temperature curve for the PWHT process. It shows the linear 100°F/hr heating rate, 4 hours (240 minutes) hold time at 1150°F, 125°F/hr cooling rate at temperature above 600°F, and the air cooling to room temperature of 70°F.

5.3 Residual Stress Results

Figure 10 plots the von Mises residual stresses after welding is complete, but before PWHT. It shows extensive residual stresses of greater than 66.3 ksi in the weld material. However, as shown in Figure 11, after the PWHT the residual stresses in the weld have relaxed significantly, to below 49.2 ksi, but the residual stresses in the cladding remain essentially unchanged.

To further investigate the effects of the PWHT, before and after PWHT residual stresses are extracted along the two through-wall paths shown in Figure 12. The through-wall residual stresses are compared in Figure 13, and it shows that there is little to no stress reduction in the clad material, while there is significant stress reduction in the pipe base metal.

The PWHT results from the FEA trend comparably well with the data in EPRI report TR-105697 [10], which contains a comparable through-wall clad residual stress distribution based on experimental measurements, as shown in Figure 14. The experimental measurements were for a low alloy steel vessel with a Type 304 stainless steel clad. The data shows tensile stress through the clad thickness and the base metal near the clad interface, but the stress drops rapidly to compressive values at farther distances from the clad.

Figure 15 depicts the predicted von Mises residual stresses after the hydrostatic test. It shows an insignificant reduction in maximum stress when compared to the post-PWHT step: 73.749 ksi (Figure 15) versus 73.750 ksi (Figure 11), while the overall stress contour remains essentially the same.

Figure 16 and Figure 17 depict the combined weld residual plus operating radial and hoop stresses at the fifth stabilization NOC cycle, respectively. The stress results at this step are used in the fracture mechanics evaluations.

6.0 CONCLUSIONS

Finite element residual stress analysis has been performed on the hot leg drain nozzle boss weld at Palisades. Stresses at normal operating conditions combined with residual stresses have been obtained and saved for future use. The stress results will be used in a separate calculation to determine crack growth.

7.0 REFERENCES

1. SI Calculation No. 1400669.310, Rev. 0, "Finite Element Model for Hot Leg Drain Nozzle."
2. SI Calculation No. 0800777.307, Rev.5, "Material Properties for Residual Stress Analyses, Including MISO Properties Up To Material Flow Stress."
3. ANSYS Mechanical APDL and PrepPost, Release 14.5 (w/ Service Pack 1), ANSYS, Inc., September 2012.
4. Combustion Engineering Welding Procedure No. MA-41, Rev.0, SI File No. 1400669.204.
5. "Steels for Elevated Temperature Service," United States Steel Co., 1949.
6. Publication SMC-027, "Inconel Alloy 600," Special Metals Corp., 2004, SI File No. 0800777.211.
7. ASME Boiler and Pressure Vessel Code, Section III, 1965 Edition with Addenda through Winter 1966.
8. Combustion Engineering Specification No. 0070P-006, Rev.2, "Engineering Specification for Primary Coolant Pipe and Fittings," SI File No. 1300086.203.
9. Palisades Design Input Record, "Palisades Alloy 600 Flaw Eval DIR 3-4-15 Rev1.pdf," SI File No. 1400669.201.
10. EPRI Report No. TR-105697, "BWR Reactor Pressure Vessel Shell Weld Inspection Recommendations (BWRVIP-05)," September 1995.

Table 1: Elastic Properties for SA-516 Grade 70 (≤ 4" Thick)

Temperature (°F)	Young's Modulus ($x10^3$ ksi)	Mean Thermal Expansion ($x10^{-6}$ in/in/°F)	Thermal Conductivity (2) (Btu/min-in-°F)	Specific Heat (2) (Btu/lb-°F)
70	29.5	6.4	0.0488	0.103
500	27.3	7.3	0.0410	0.128
700	25.5	7.6	0.0369	0.138
1100	18.0	8.2	0.0290	0.171
1500	5.0	8.6	0.0218	0.198
2500	0.1	9.5	0.0014	0.204
2500.1	–	0.0	–	–

Notes:
1. All values per [2].
2. Density (ρ) = 0.283 lb/in^3 [2], assumed temperature independent.
3. Poisson's Ratio (υ) = 0.3 [2], assumed temperature independent.

Table 2: Elastic Properties for ER308L

Temperature (°F)	Young's Modulus ($x10^3$ ksi)	Mean Thermal Expansion ($x10^{-6}$ in/in/°F)	Thermal Conductivity (2) (Btu/min-in-°F)	Specific Heat (2) (Btu/lb-°F)
70	28.3	8.5	0.0119	0.116
500	25.8	9.7	0.0151	0.131
700	24.8	10.0	0.0164	0.135
1100	22.1	10.5	0.0189	0.140
1500	18.1	10.8	0.0213	0.145
2500	0.1	11.5	0.0292	0.159
2500.1	–	0.0	–	–

Notes:
1. All values per [2].
2. Density (ρ) = 0.283 lb/in^3 [2], assumed temperature independent.
3. Poisson's Ratio (υ) = 0.3 [2], assumed temperature independent.

Table 3: Elastic Properties for Alloy 600

Temperature (°F)	Young's Modulus ($x10^3$ ksi)	Mean Thermal Expansion ($x10^{-6}$ in/in/°F)	Thermal Conductivity (2) (Btu/min-in-°F)	Specific Heat (2) (Btu/lb-°F)
70	31.0	6.8	0.0119	0.108
500	29.0	7.6	0.0147	0.120
700	28.2	7.9	0.0161	0.125
1100	25.9	8.4	0.0192	0.139
1500	23.1	9.0	0.0222	0.148
2500	0.1	10.0	0.0306	0.177
2500.1	–	0.0	–	–

Notes:
1. All values per [2].
2. Density (ρ) = 0.300 lb/in^3 [2], assumed temperature independent.
3. Poisson's Ratio (υ) = 0.29 [2], assumed temperature independent.

Table 4: Elastic Properties for Alloy 182

Temperature (°F)	Young's Modulus ($x10^3$ ksi)	Mean Thermal Expansion ($x10^{-6}$ in/in/°F)	Thermal Conductivity (2) (Btu/min-in-°F)	Specific Heat (2) (Btu/lb-°F)
70	31.0	6.8	0.0119	0.108
500	29.0	7.6	0.0147	0.120
700	28.2	7.9	0.0161	0.125
1100	25.9	8.4	0.0192	0.139
1500	23.1	9.0	0.0222	0.148
2500	0.1	10.0	0.0306	0.177
2500.1	–	0.0	–	–

Notes:
1. All values per [2].
2. Density (ρ) = 0.300 lb/in^3 [2], assumed temperature independent.
3. Poisson's Ratio (υ) = 0.29 [2], assumed temperature independent.

Table 5: Stress-Strain Curves for SA-516 Grade 70 (≤ 4" Thick)

Temperature (°F)	Strain (in/in)	Stress (ksi)
70	0.00128814	38.000
	0.00187809	42.000
	0.00257329	46.000
	0.00381110	50.000
	0.00600383	54.000
500	0.00113553	31.000
	0.00142679	35.875
	0.00183954	40.750
	0.00261139	45.625
	0.00415246	50.500
700	0.00106667	27.200
	0.00132412	32.550
	0.00166876	37.900
	0.00228121	43.250
	0.00354341	48.600
1100	0.00116667	21.000
	0.05116163	22.125
	0.05915444	23.250
	0.06794123	24.375
	0.07755935	25.500
1500	0.00300000	15.000
	0.16717493	15.125
	0.16992011	15.250
	0.17268761	15.375
	0.17547742	15.500
2500[2]	0.01000000	1.000
	0.10961239	1.125
	0.12781277	1.250
	0.14689940	1.375
	0.16683167	1.500

Notes:
1. All values per [2].
2. Values at 2500°F assumed arbitrarily small values for convergence stability.

Table 6: Stress-Strain Curves for ER308L

Temperature (°F)	Strain (in/in)	Stress (ksi)
70	0.00203180	57.500
	0.02471351	61.563
	0.03107296	65.625
	0.03861377	69.688
	0.04747167	73.750
500	0.00140089	36.143
	0.00714793	40.250
	0.01065407	44.357
	0.01558289	48.464
	0.02233857	52.571
700	0.00132488	32.857
	0.00477547	37.125
	0.00743595	41.393
	0.01143777	45.661
	0.01727192	49.929
1100	0.00121913	26.943
	0.00264833	30.138
	0.00404100	33.332
	0.00634529	36.527
	0.01005286	39.721
1500	0.00117995	21.357
	0.05352064	21.563
	0.05610492	21.768
	0.05878975	21.973
	0.06157807	22.179
2500[(2)]	0.01000000	1.000
	0.10961239	1.125
	0.12781277	1.250
	0.14689940	1.375
	0.16683167	1.500

Notes:
1. All values per [2].
2. Values at 2500°F assumed arbitrarily small values for convergence stability.

Table 7: Stress-Strain Curves for Alloy 600

Temperature (°F)	Strain (in/in)	Stress (ksi)
70	0.00157419	48.800
	0.01658847	55.300
	0.02343324	61.800
	0.03212188	68.300
	0.04291703	74.800
500	0.00152069	44.100
	0.01539220	50.338
	0.02210610	56.575
	0.03072476	62.813
	0.04153277	69.050
700	0.00152128	42.900
	0.01634485	49.000
	0.02334760	55.100
	0.03227153	61.200
	0.04338643	67.300
1100	0.00155985	40.400
	0.02275193	44.475
	0.03004563	48.550
	0.03888203	52.625
	0.04943592	56.700
1500	0.00092641	21.400
	0.08827666	22.475
	0.09785101	23.550
	0.10796967	24.625
	0.11863796	25.700
2500[(2)]	0.01000000	1.000
	0.10961239	1.125
	0.12781277	1.250
	0.14689940	1.375
	0.16683167	1.500

Notes:
1. All values per [2].
2. Values at 2500°F assumed arbitrarily small values for convergence stability.

Table 8: Stress-Strain Curves for Alloy 182

Temperature (°F)	Strain (in/in)	Stress (ksi)
70	0.00179032	55.500
	0.03456710	60.113
	0.04292837	64.725
	0.05257245	69.338
	0.06359421	73.950
500	0.00164483	47.700
	0.02976152	52.313
	0.03809895	56.925
	0.04790379	61.538
	0.05929946	66.150
700	0.00159574	45.000
	0.02849157	49.538
	0.03680454	54.075
	0.04663682	58.613
	0.05812078	63.150
1100	0.00159073	41.200
	0.03568855	44.488
	0.04402702	47.775
	0.05360088	51.063
	0.06449835	54.350
1500	0.00106494	24.600
	0.11812735	25.325
	0.12540227	26.050
	0.13290814	26.775
	0.14064577	27.500
2500[2]	0.01000000	1.000
	0.10961239	1.125
	0.12781277	1.250
	0.14689940	1.375
	0.16683167	1.500

Notes:
1. All values per [2].
2. Values at 2500°F assumed arbitrarily small values for convergence stability.

Table 9: Creep Properties

Material	Temperature (°F)	Creep Strength (ksi)		*A* (ksi/hr)	*n*
		σ_1 (0.0001%/hr)	σ_2 (0.00001%/hr)		
SA-516 Gr. 70 (Based on carbon steel) Per [5]	800	19.0	12.4	1.26E-13	5.40
	900	9.0	6.7	3.59E-14	7.80
	1000	3.5	2.8	2.43E-12	10.32
	1100	1.4	0.8	2.50E-07	4.11
ER308L (Based on Type 304) Per [5]	800	33.4	25.0	7.73E-19	7.95
	900	24.0	17.6	5.67E-17	7.42
	1000	17.6	11.5	1.82E-13	5.41
	1100	11.5	7.1	8.62E-12	4.77
Alloy 600 Alloy 182 (Based on Alloy 600) Per [6]	800	40.0	30.0	1.50E-19	8.00
	900	28.0	18.0	2.87E-14	5.21
	1000	12.5	6.1	3.02E-10	3.21
	1100	6.8	3.4	1.72E-09	3.32

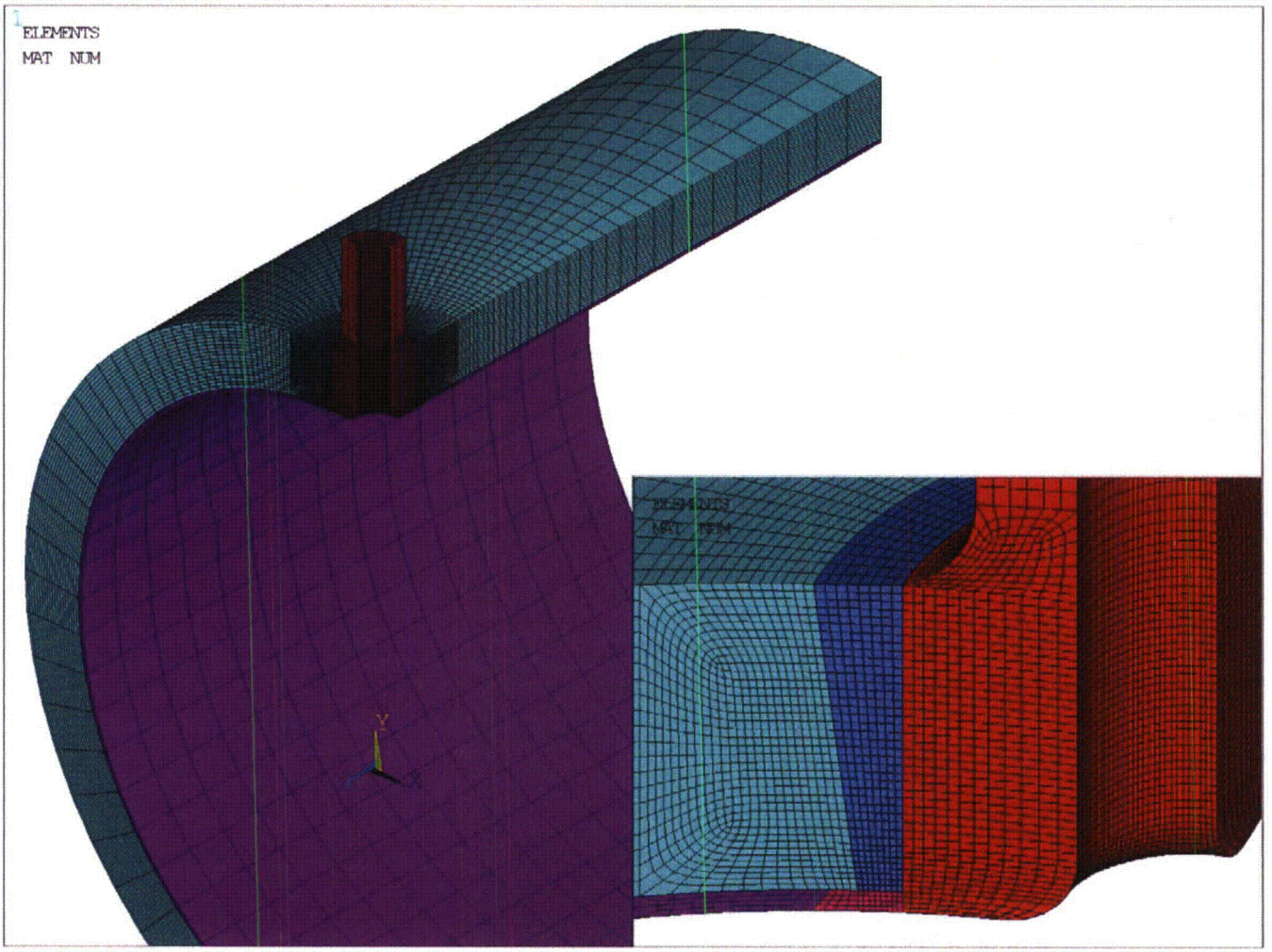

Figure 1. Finite Element Model for Residual Stress Analysis

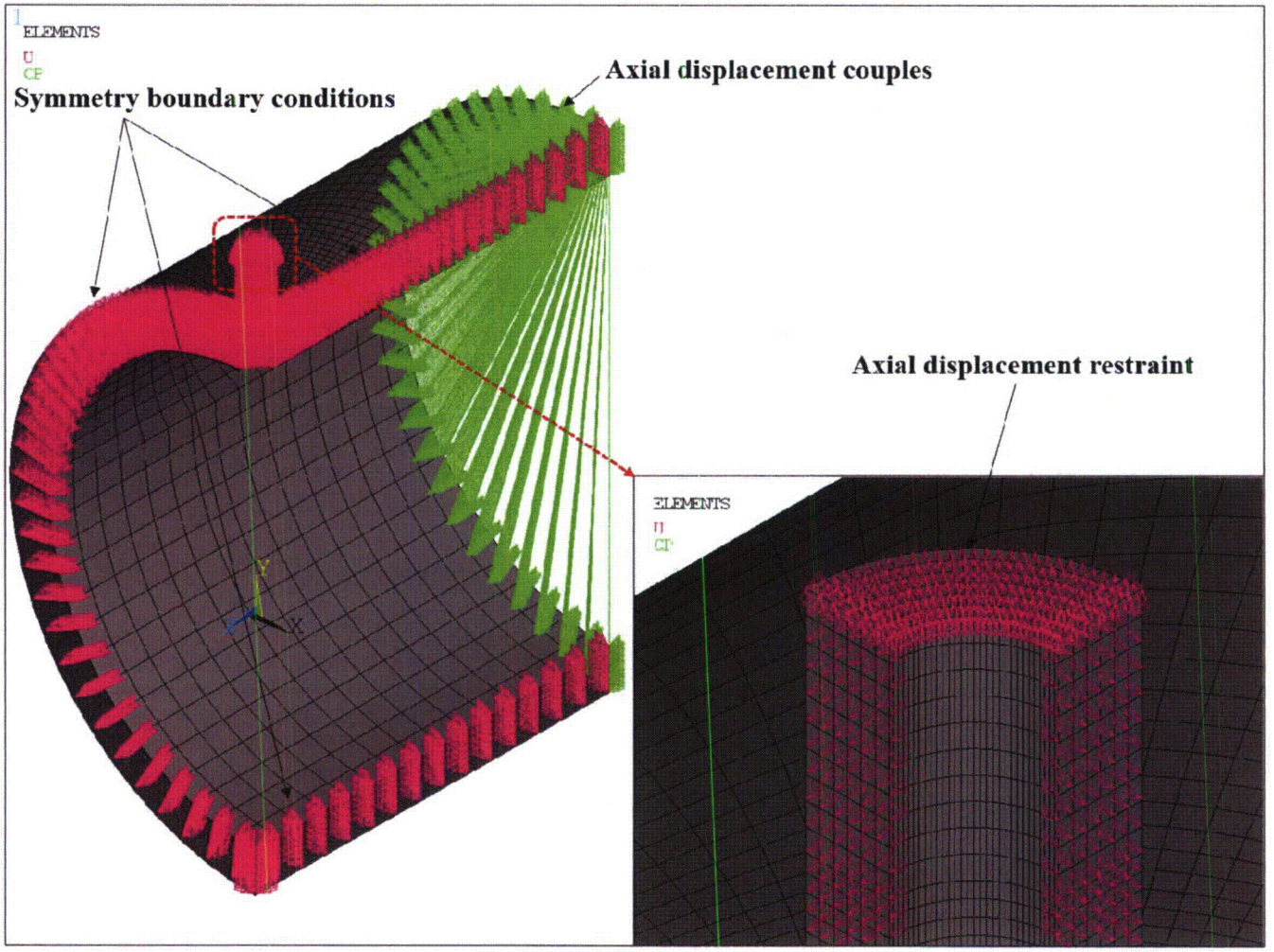

Figure 2. Applied Mechanical Boundary Conditions

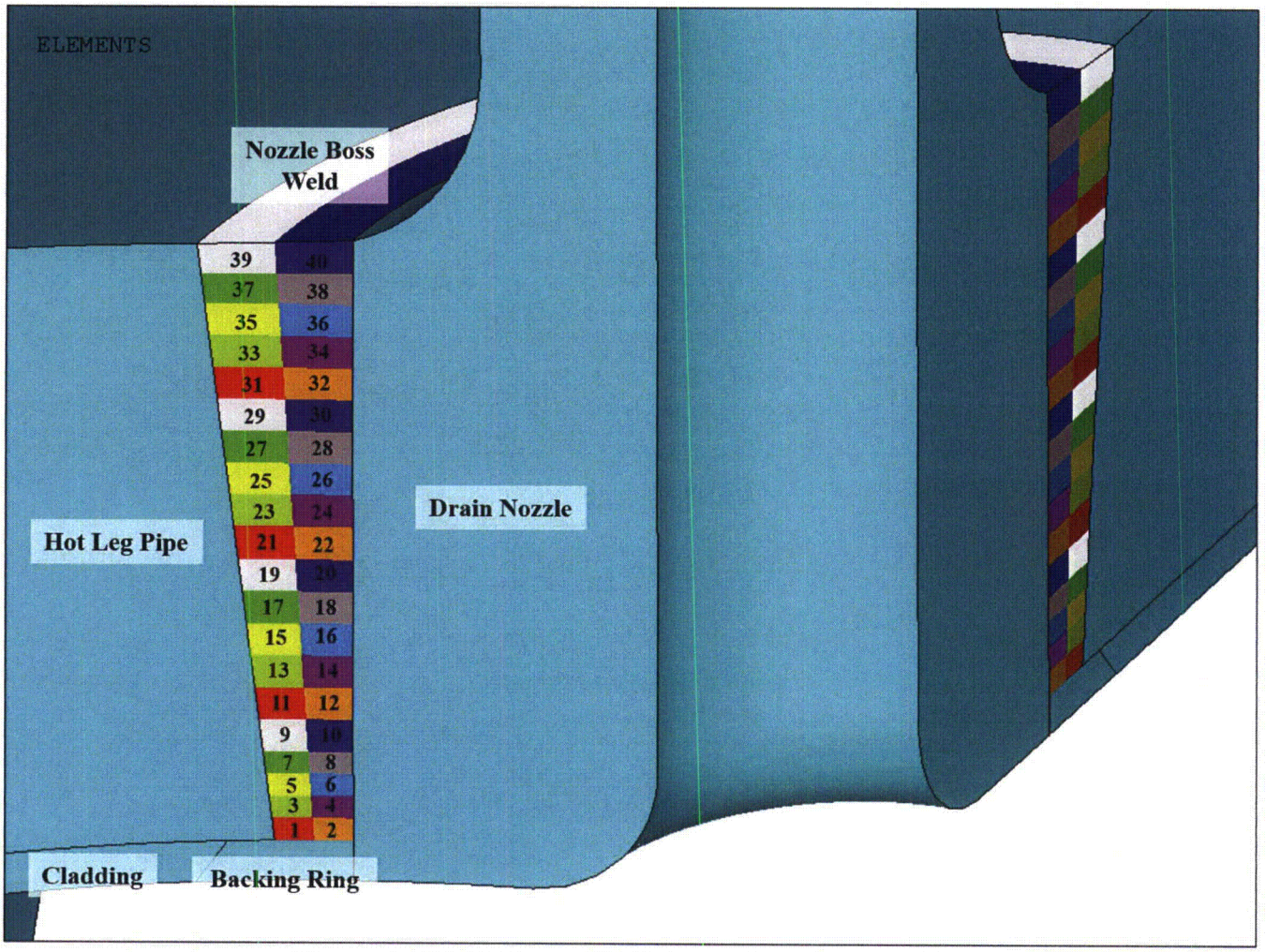

Figure 3. Weld Nugget Definitions for the Boss Weld

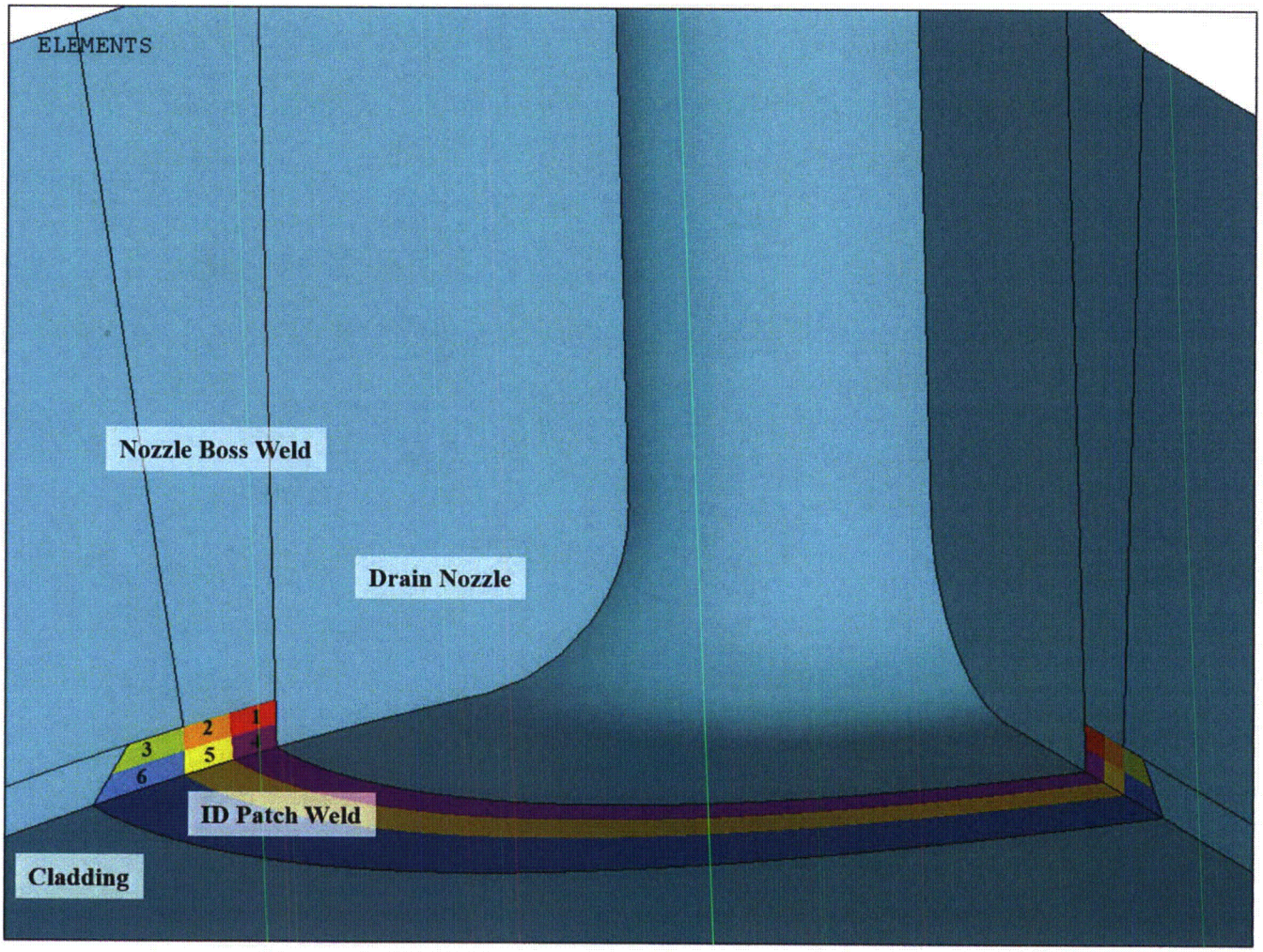

Figure 4. Weld Nugget Definitions for the ID Patch Weld

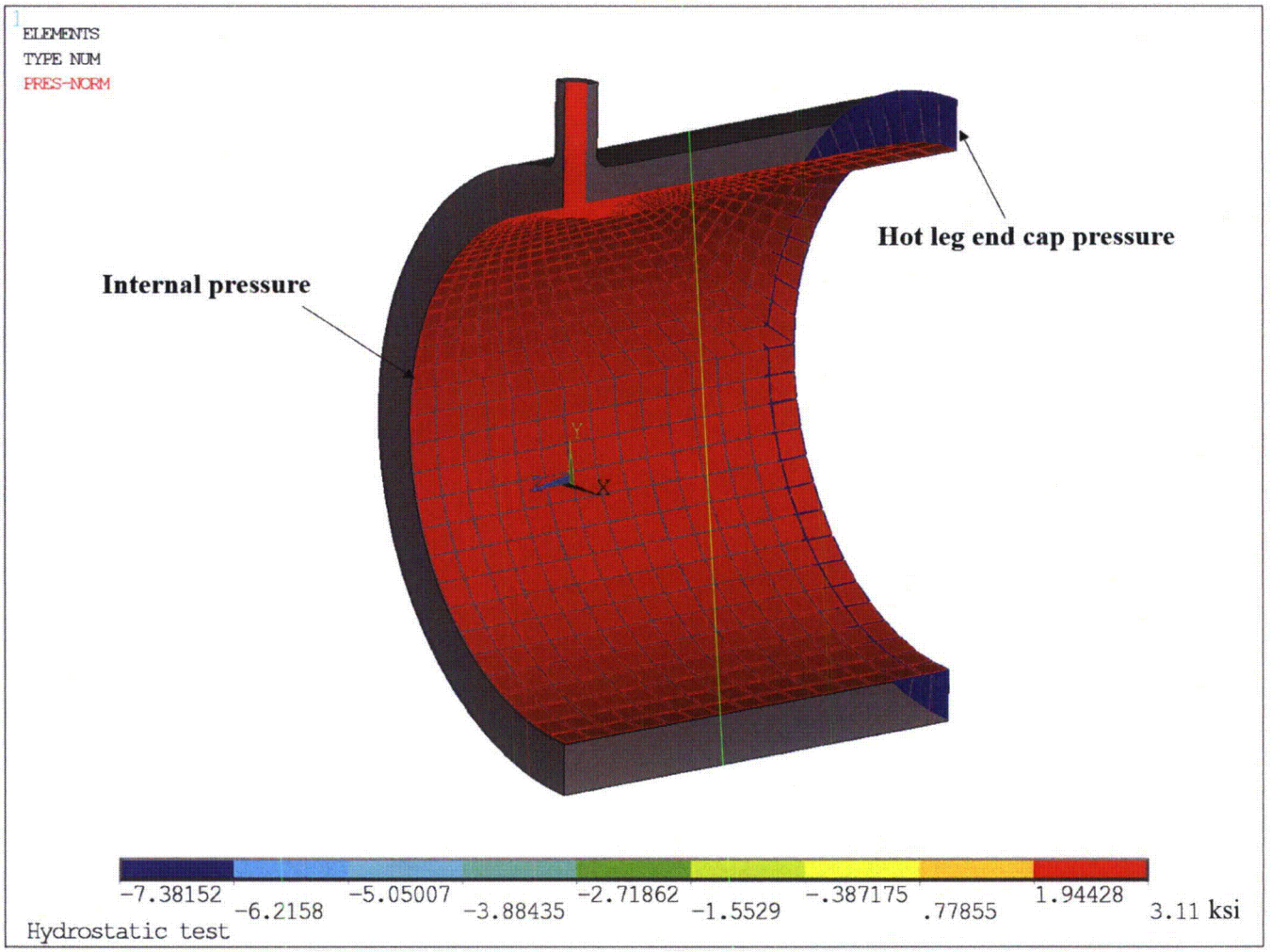

Figure 5. Applied Hydrostatic Test Pressure and Corresponding End Cap Pressure Loads

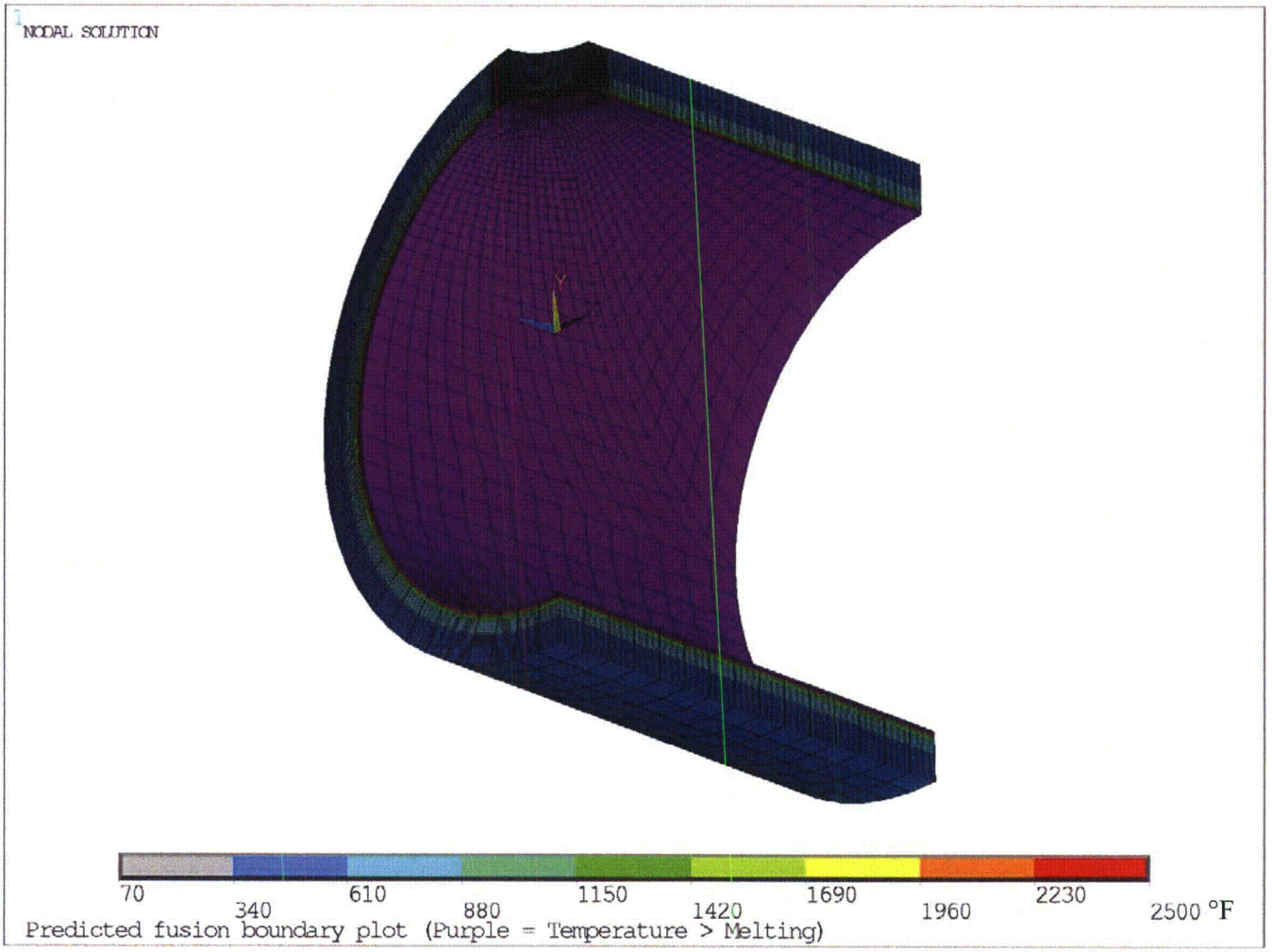

Figure 6. Predicted Fusion Boundary Plot for Cladding
(Note: Purple = Temperature > Melting temperature of 2500°F)

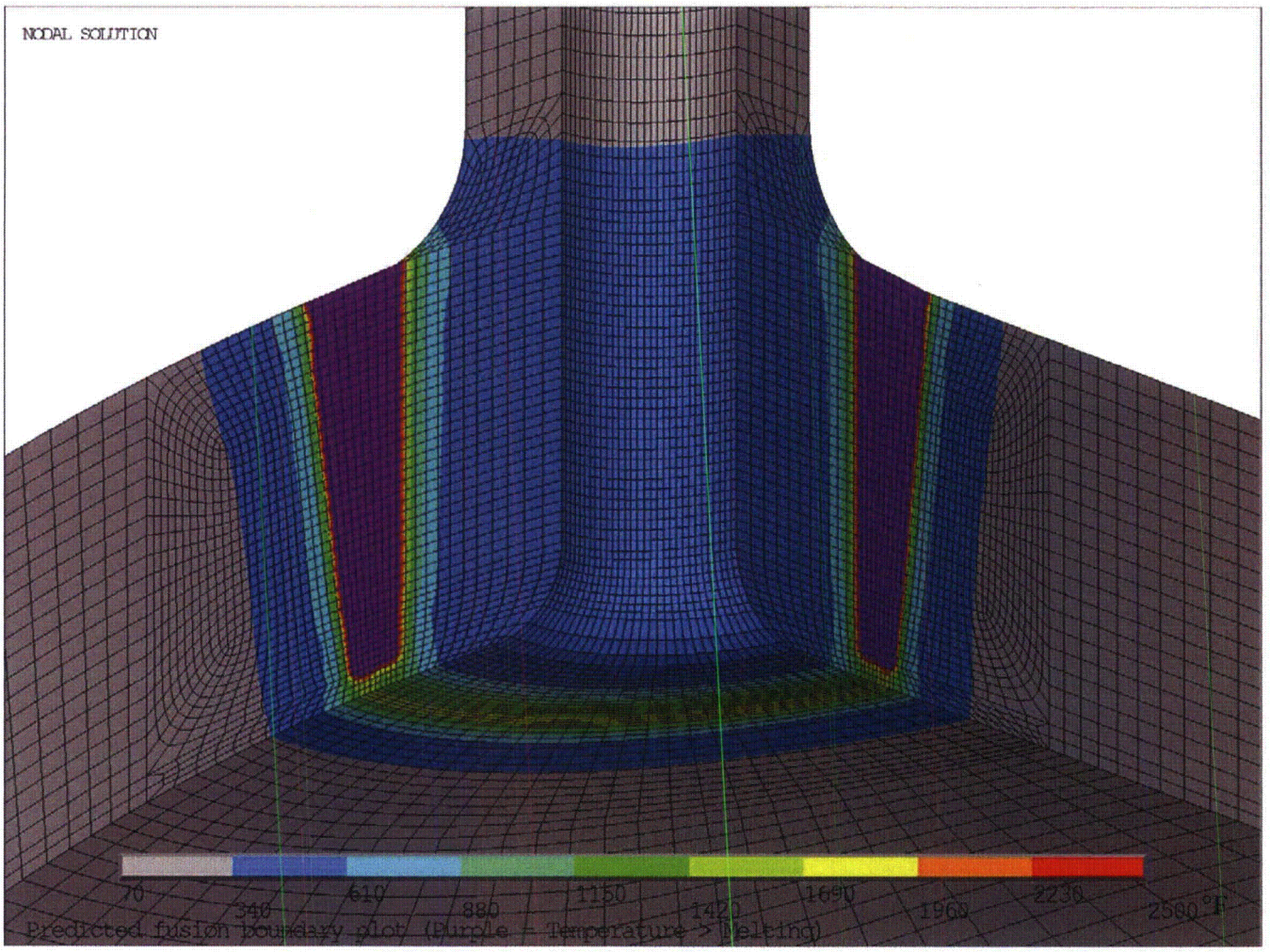

Figure 7. Predicted Fusion Boundary Plot for Boss Weld
(Note: Purple = Temperature > Melting temperature of 2500°F)

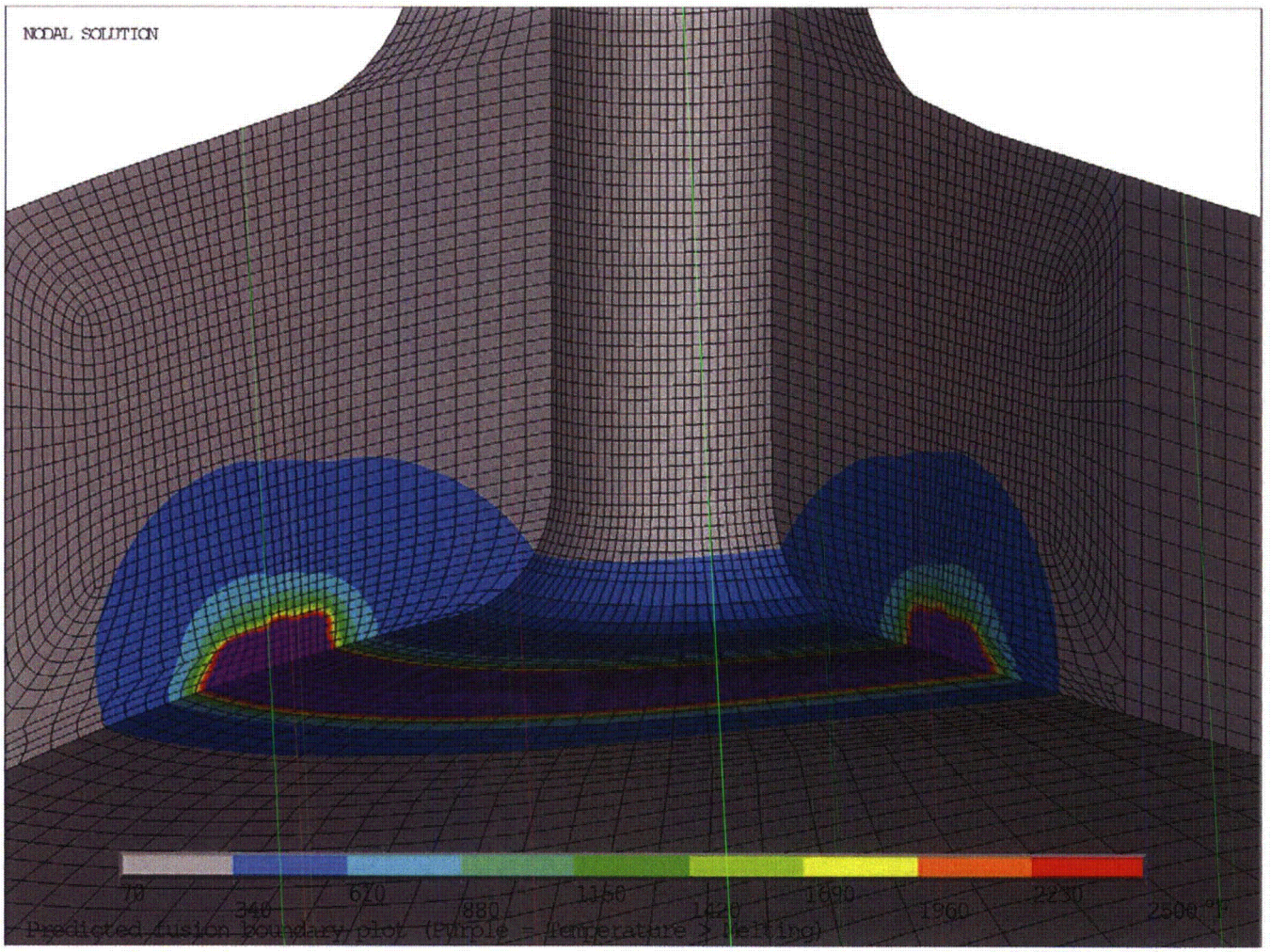

Figure 8. Predicted Fusion Boundary Plot for ID Patch Weld
(Note: Purple = Temperature > Melting temperature of 2500°F)

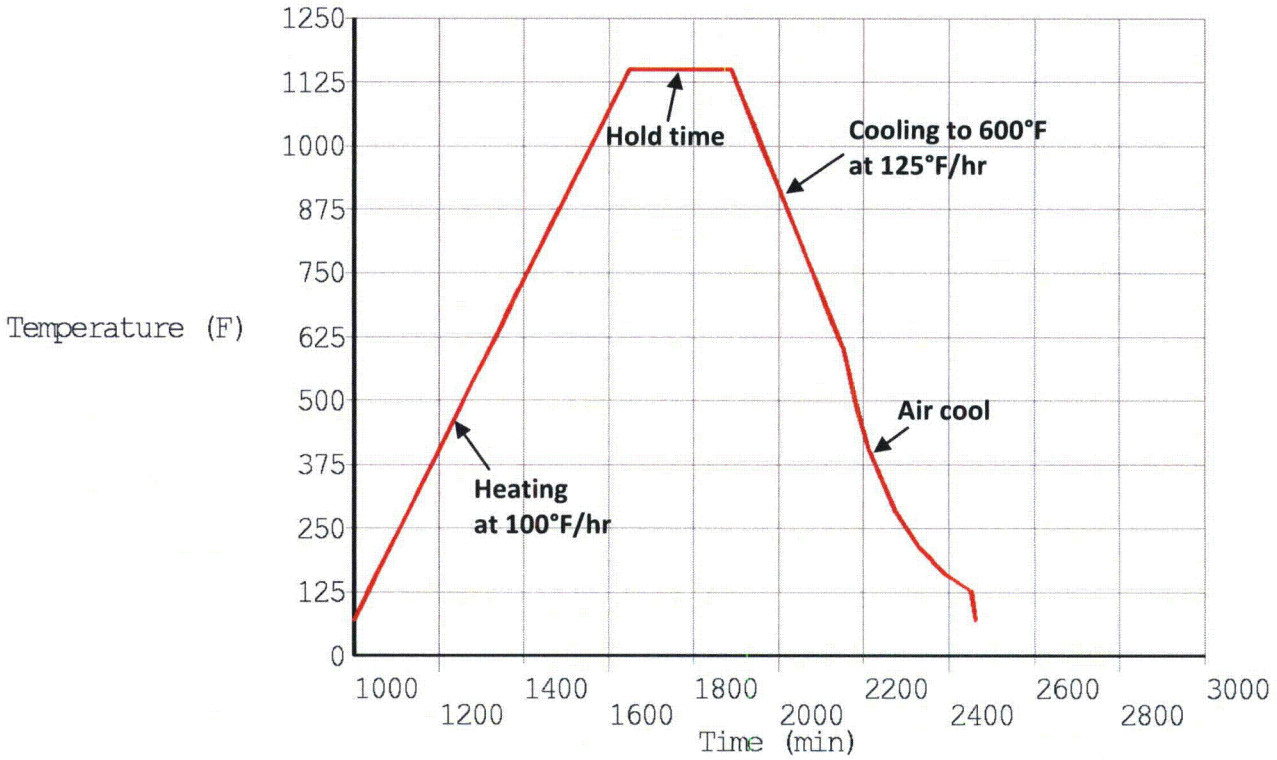

Figure 9. Time vs. Temperature Curve for PWHT

Note:

1. PWHT temperature history is for a typical ID node on the model.

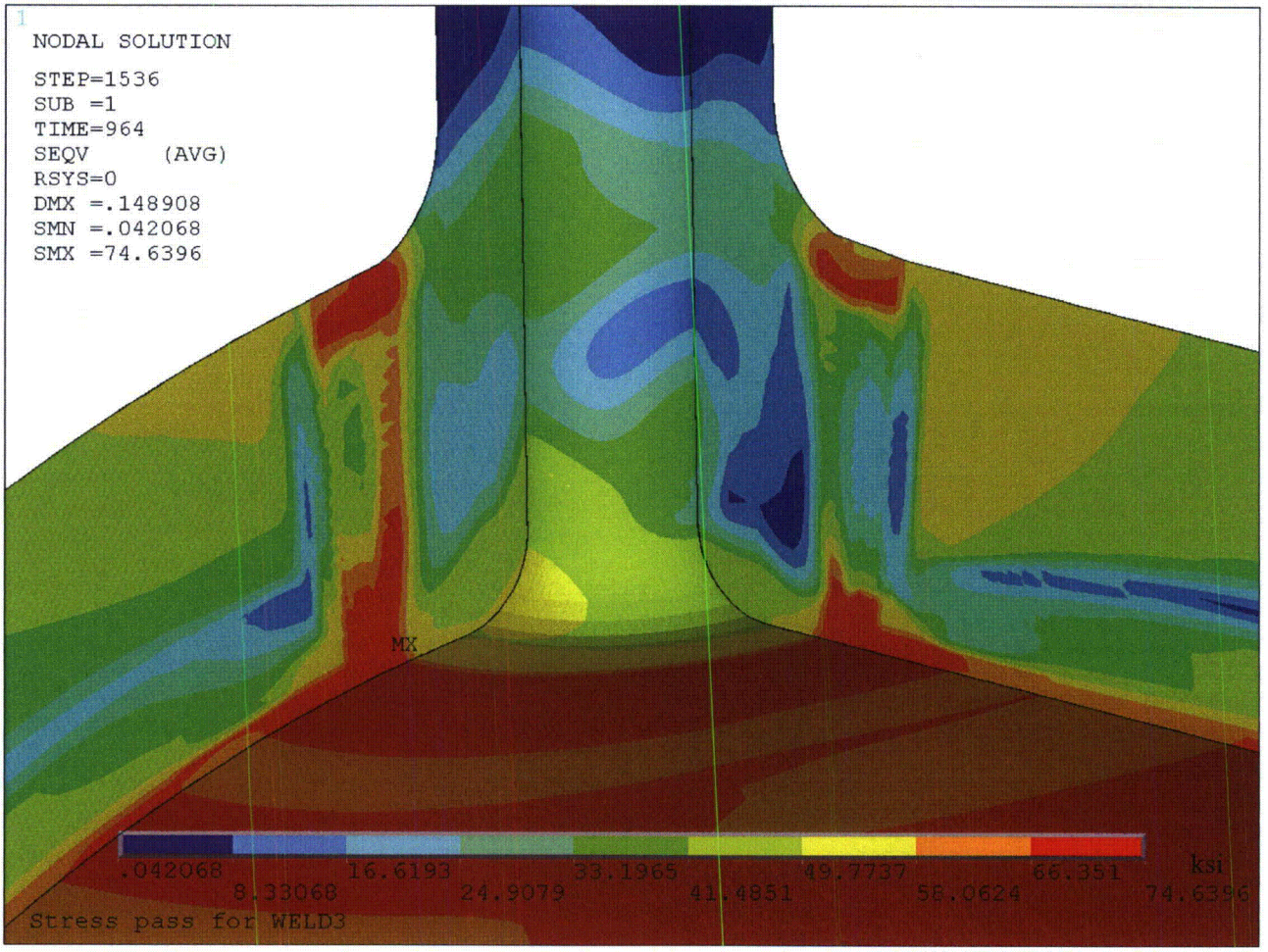

Figure 10. Predicted von Mises Residual Stress at 70°F after ID Patch Weld

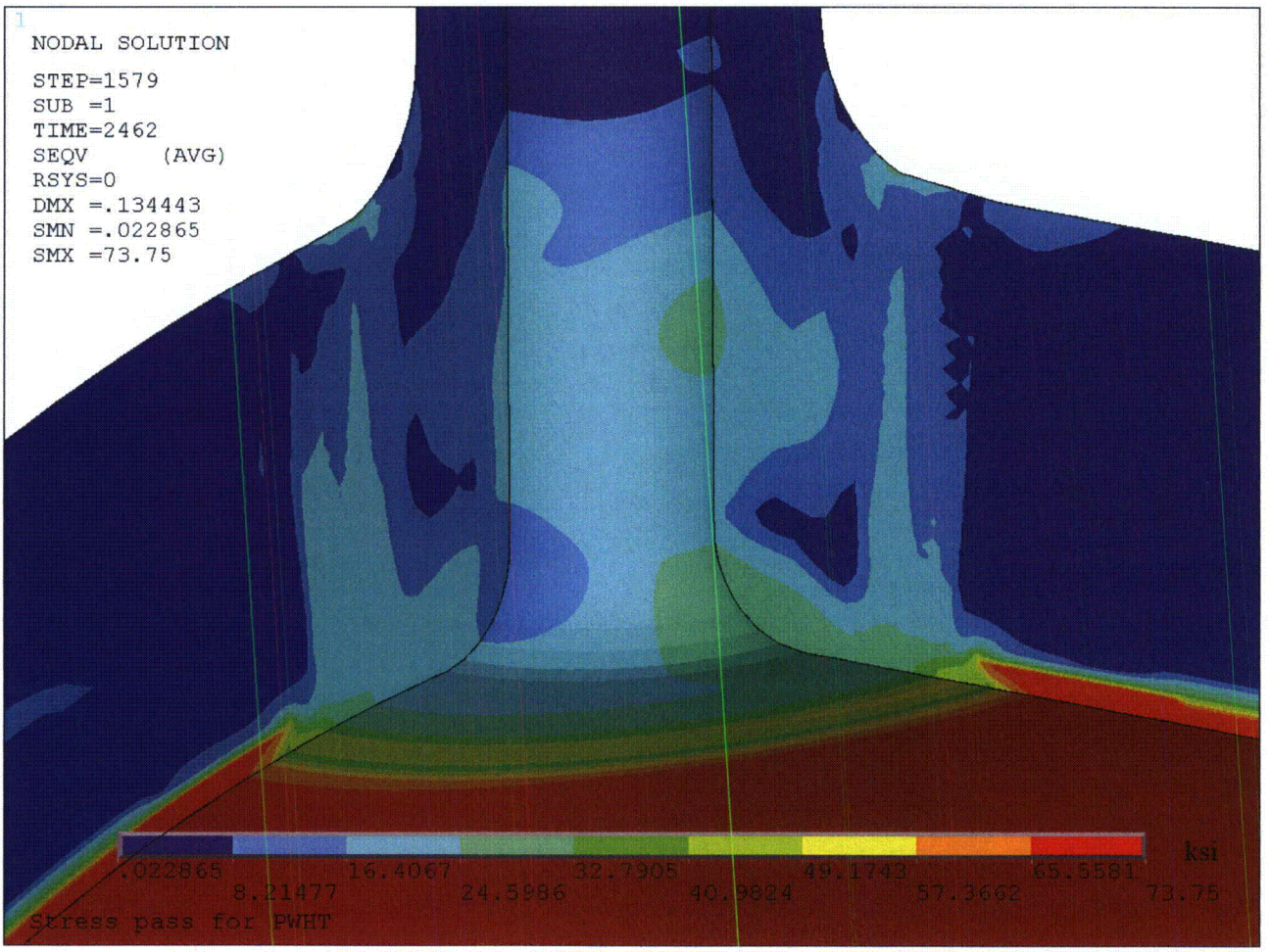

Figure 11. Predicted von Mises Residual Stress at 70°F after PWHT

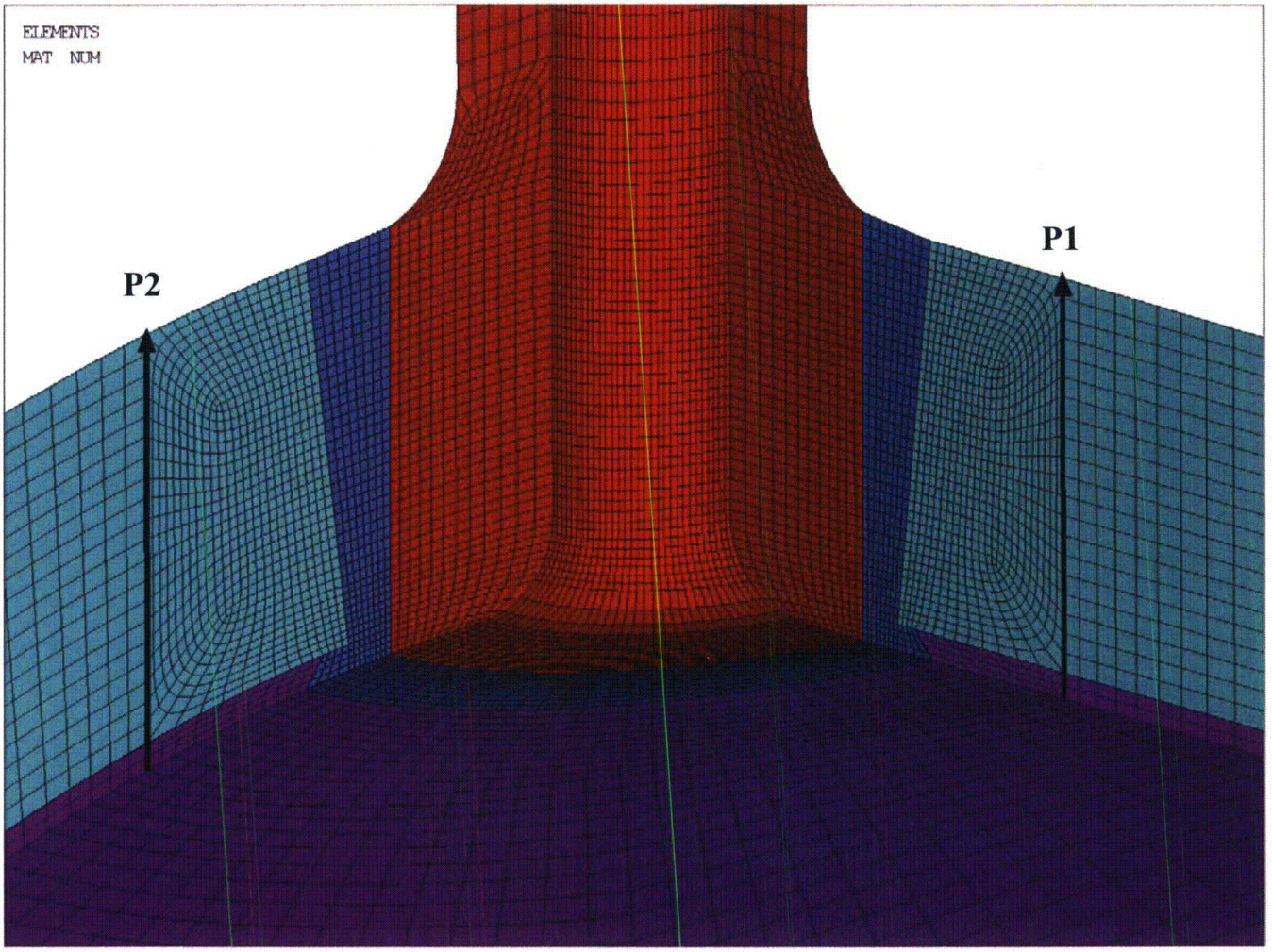

Figure 12. Paths for Stress Extraction

Notes:

1. In the hot leg coordinates, hoop residual stresses along path P1 and axial residual stresses along path P2 are extracted for comparison of before and after PWHT.
2. The before and after PWHT through-wall residual stresses are compared in Figure 13.

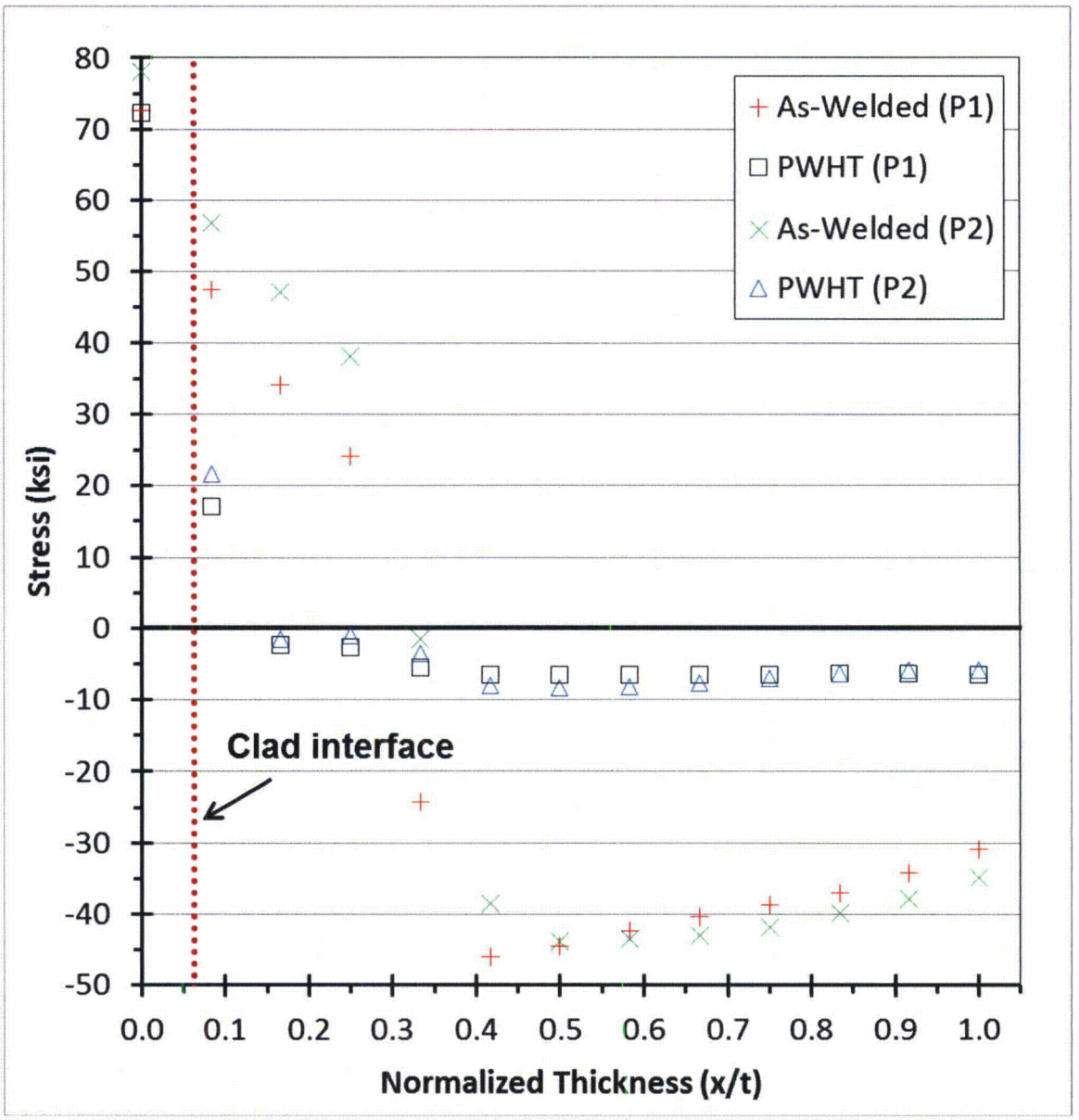

Figure 13. Residual Stress Comparison at 70°F Before and After PWHT

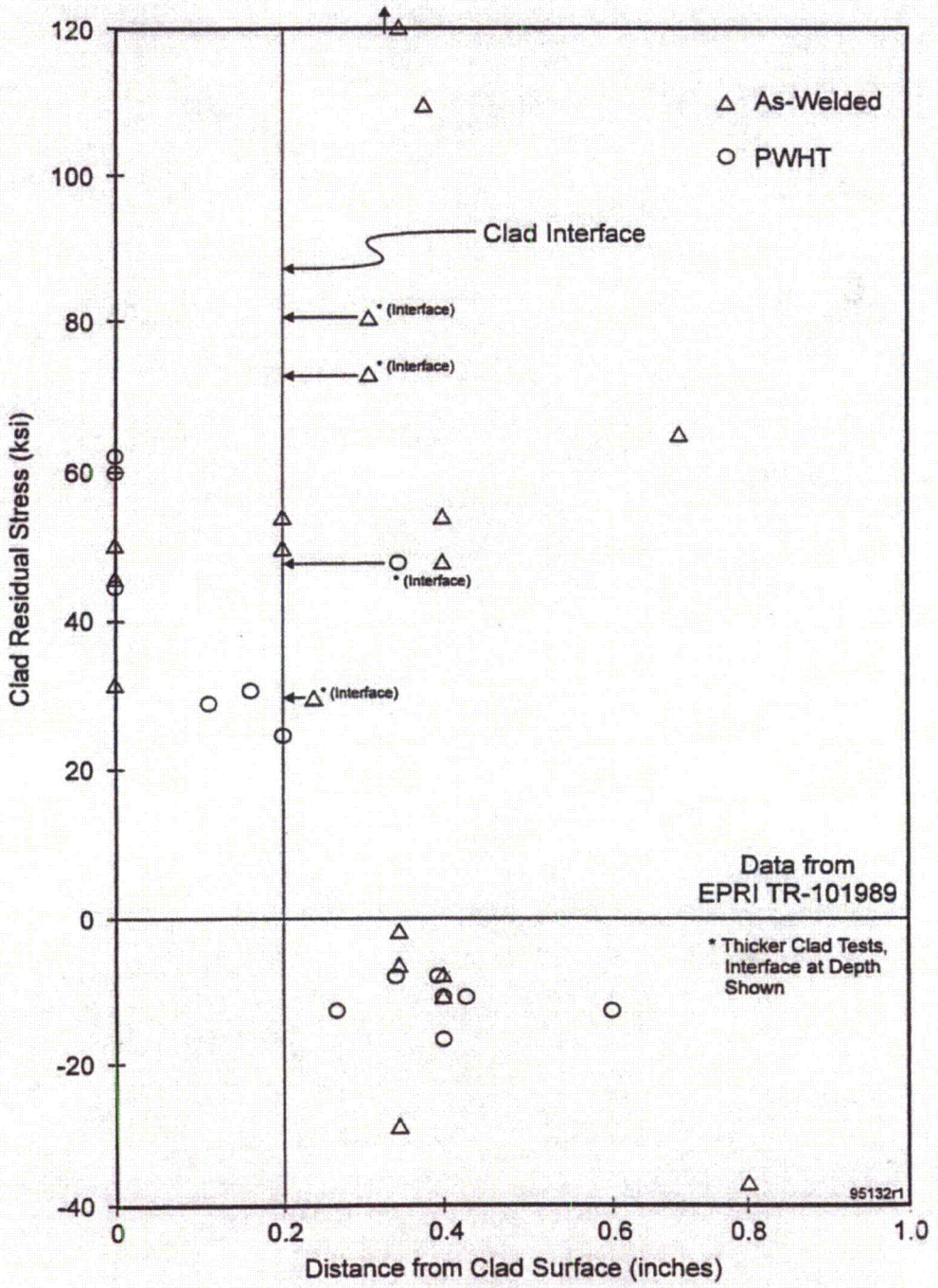

Figure 14. Measured Through-Wall Residual Stresses for PWHT

Notes:

1. Figure is obtained from EPRI report TR-105697 [10].
2. Measurements show little to no stress reduction in the cladding after PWHT.
3. Measurements show significant stress reduction in the base metal after PWHT.

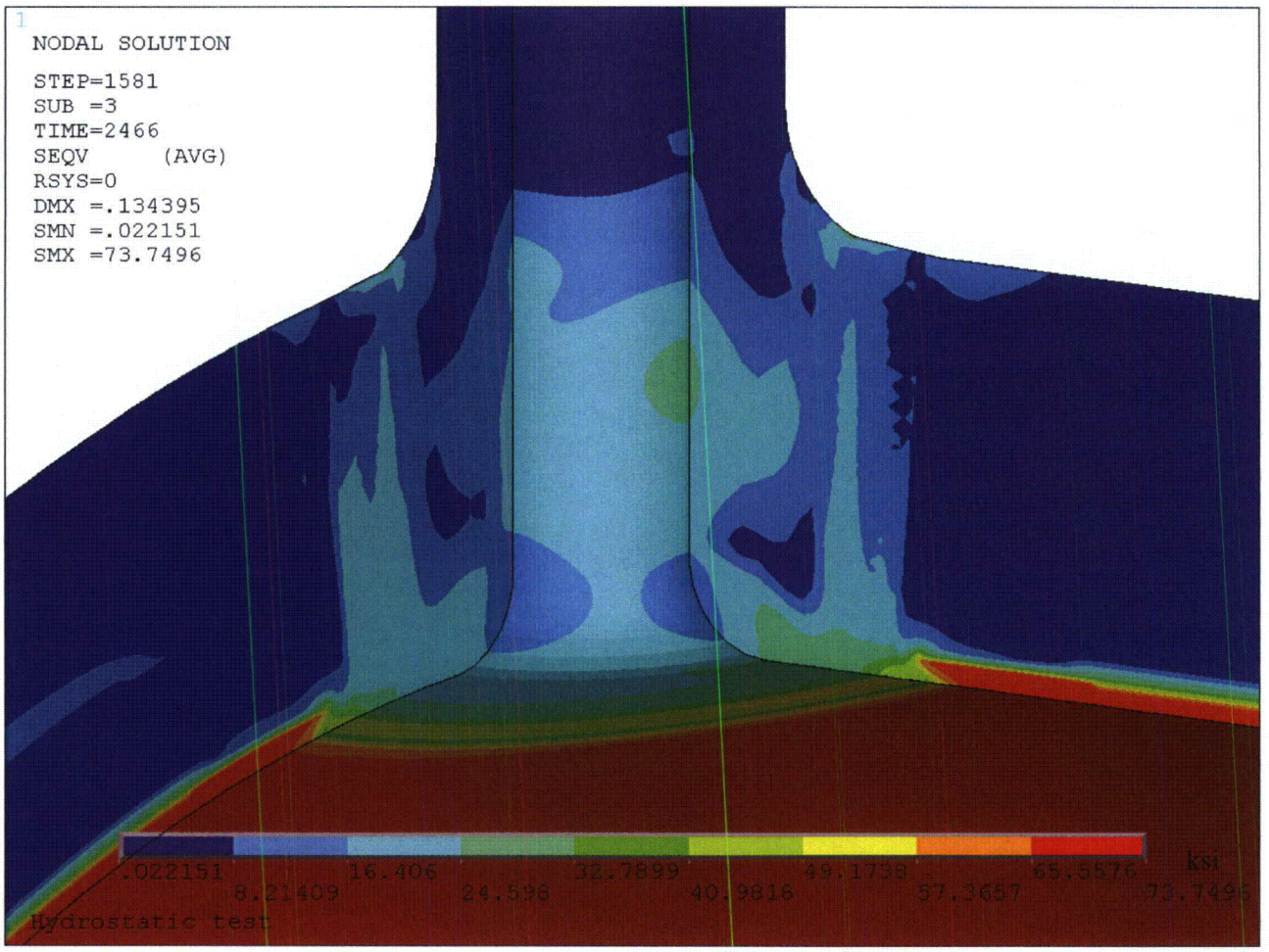

Figure 15. Predicted von Mises Residual Stress at 70°F after Hydrostatic Test

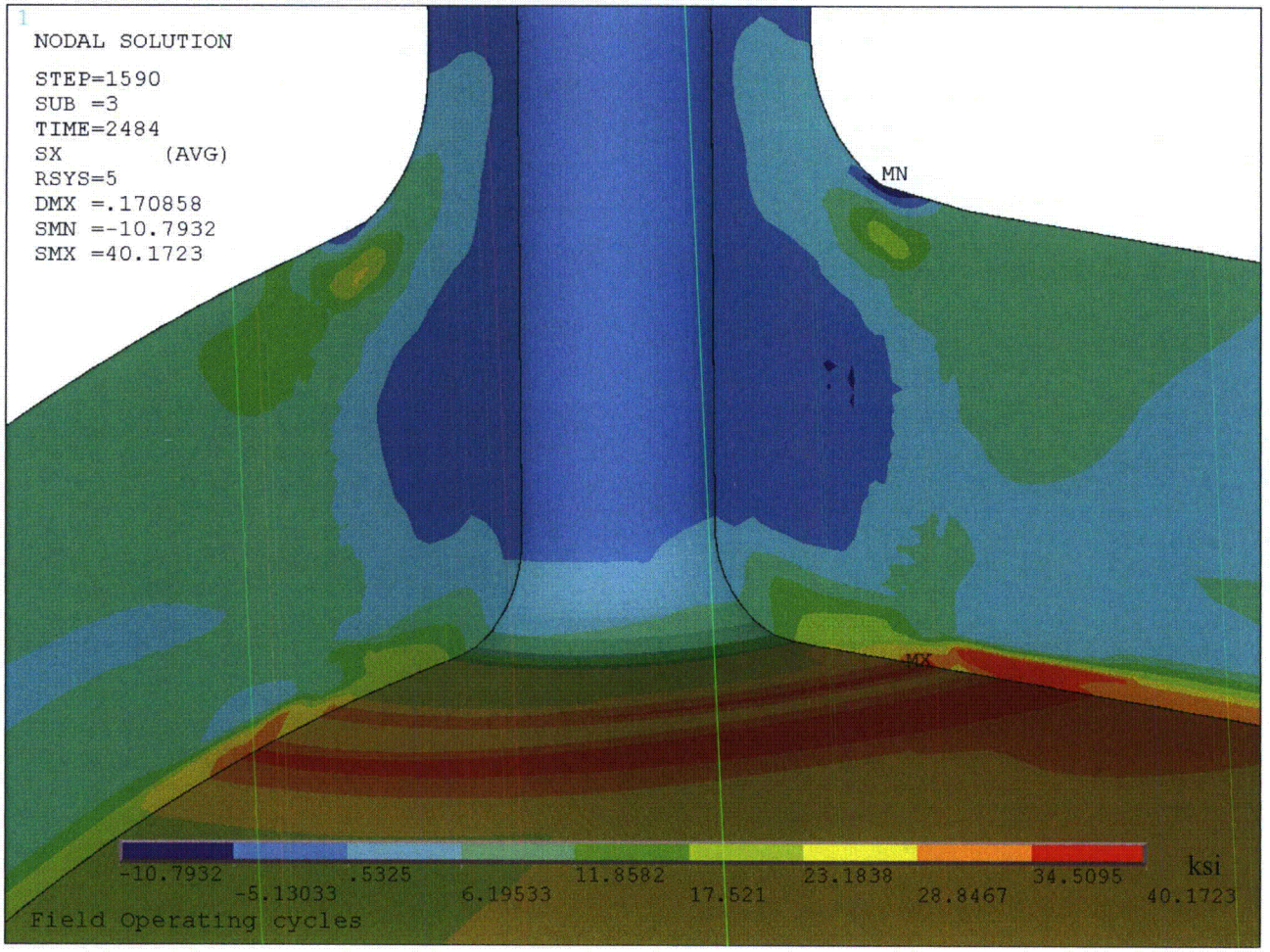

Figure 16. Predicted Radial Residual Stress + Operating Conditions (5th NOC Cycle)

Note: Radial stresses shown in the nozzle axis radial direction.

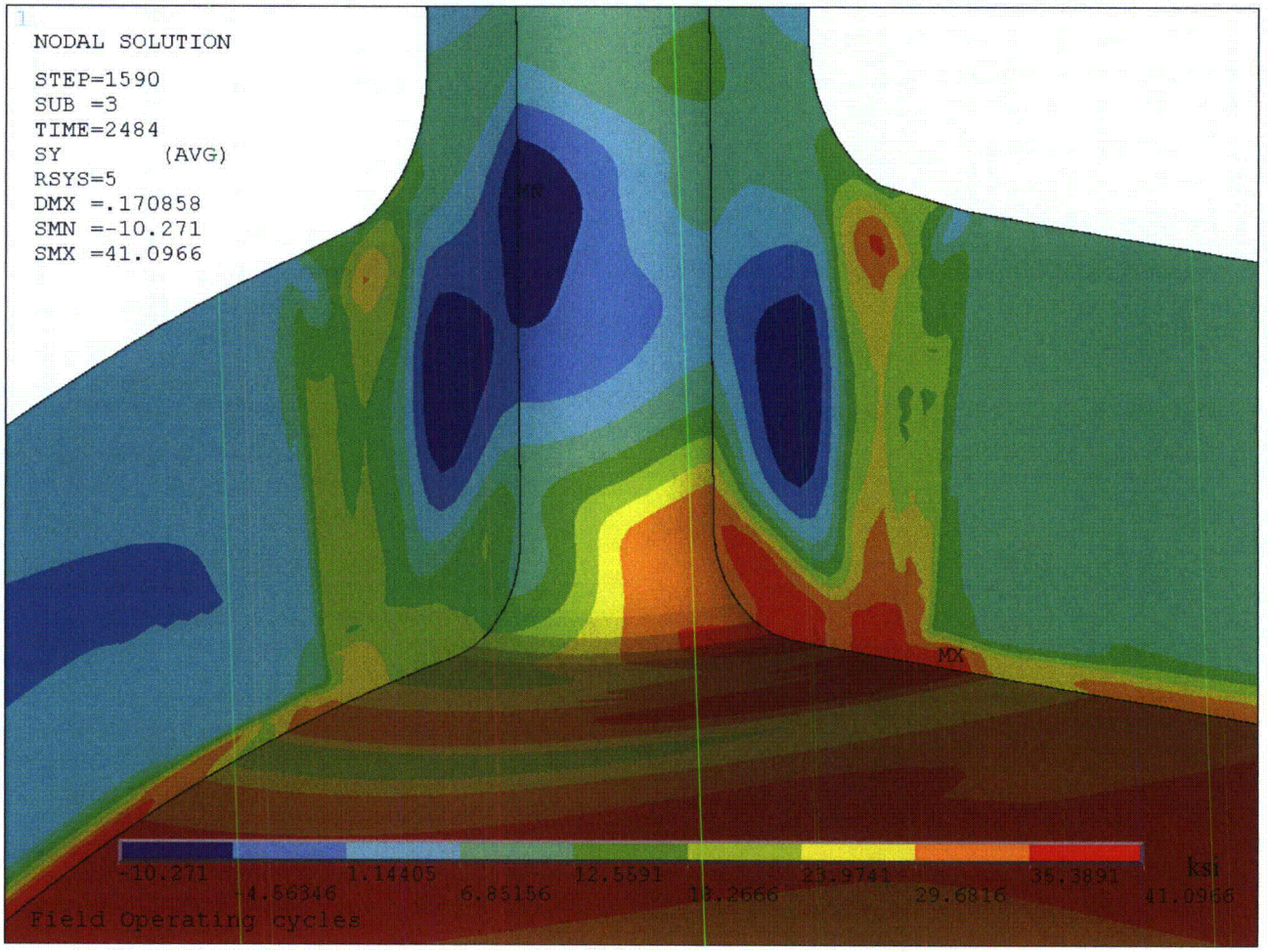

Figure 17. Predicted Hoop Residual Stress + Operating Conditions (5th NOC Cycle)

Note: Hoop stresses shown in the nozzle axis circumferential direction.

APPENDIX A

COMPUTER FILES LISTING

File Name	Description
Palisades_HL_Drain.INP	Input file to create base geometry model [1]
MProp_MISO.INP	Elastic-plastic Material properties inputs [1]
Autonugsel.mac	Macro that groups elements into nuggets
BCNUGGET3D.INP	Weld pass and model boundary definition file
THERMAL3D.INP	Input file to perform the thermal pass of welding simulation
THM_PWHT.INP	Input file to perform the thermal pass of PWHT
STRESS3D.INP	Input file to perform the stress pass of welding simulation
CBC.INP	Input file to apply mechanical boundary conditions
THM_PWHT_mntr.inp	Processed thermal pass load steps for PWHT
INSERT3D.INP	Input file to perform the stress pass of hydrostatic test
WELD#_mntr.inp	Processed thermal pass load steps for stress pass # = 1-3
*.mac	WRS analysis macro files required for analysis
THERMAL3D.TXT	Parameter input file for thermal pass of welding simulation
STRESS3D.TXT	Parameter input file for stress pass
GenStress.mac	Macro to extract PWHT stress results
GETPATH.TXT	Through-wall stress path definition to extract PWHT stress results

Structural Integrity Associates, Inc.®	File No.: 1400669.322
CALCULATION PACKAGE	**Project No.: 1400669** Quality Program: ☒ Nuclear ☐ Commercial

PROJECT NAME:
Palisades Flaw Readiness Program for 1R24 NDE Inspection

CONTRACT NO.:
10426669

CLIENT:	**PLANT:**
Entergy Nuclear Operations, Inc.	Palisades Nuclear Plant

CALCULATION TITLE:
Cold Leg Bounding Nozzle Weld Residual Stress Analysis

Document Revision	Affected Pages	Revision Description	Project Manager Approval Signature & Date	Preparer(s) & Checker(s) Signatures & Date
0	1 - 38 A-1 - A-2 Computer Files	Initial Issue	Norman Eng NE 5/5/2015	Preparer: Wilson Wong WW 5/5/2015 Checkers: Minji Fong MF 5/5/2015 Gole Mukhim GSM 5/5/2015

Table of Contents

List of Tables

List of Figures

1.0 OBJECTIVE

The objective of this calculation package is to document the weld residual stress analysis for the bounding cold leg nozzle at the Palisades Nuclear Plant (Palisades). The bounding nozzle bounds the spray, drain, and charging nozzles discussed in a separate calculation package [1]. The weld residual stress analysis is based on the latest methodology and process developed by Structural Integrity Associates (SI).

2.0 TECHNICAL APPROACH

The finite element model is obtained from a previous finite element model (FEM) calculation package [1] and the weld residual stress analysis uses the latest weld residual stress analysis methodology developed by SI, using the ANSYS finite element analysis (FEA) program [3].

The residual stress analysis consists of a thermal pass followed by a stress pass where the temperature distribution time history from the thermal pass is used as temperature input into the stress pass to determine stresses. Stress results from the weld residual stress analysis are obtained and saved for future use to evaluate flaws which will be performed in a separate calculation package.

The finite element model includes all components in the post-nozzle installation stage because new elements cannot be added during an ANSYS analysis. Since all the weld elements need to be included in the initial model, the element "birth and death" technique in ANSYS is used to initially deactivate the weld elements, with elements corresponding to the active weld segment reactivated at the melting temperature, thus simulating the weld metal deposition.

2.1 Material Properties

The weld residual stress analysis performed in this calculation uses the material properties specifically developed in a separate calculation package for weld residual stress analyses [2]. Per the material designation used in the FEM calculation [1], the following materials are used:

- SA-516 Grade 70: Cold leg base metal
- ER308L: Cold leg cladding (typical weld metal for Type 304)
- Alloy 82/182: Boss weld and ID patch weld
- Alloy 600 (SB-166): Nozzle

The material properties are reproduced in Table 1 through Table 8.

2.2 Finite Element Model for Weld Residual Stress Analysis

The finite element model for the analysis was developed in a previous FEM calculation [1], which was created using the ANSYS finite element analysis software package [3]. The base finite element model

for the weld residual stress analysis is meshed with 8-node solid elements (SOLID185) in ANSYS. This finite element model is shown in Figure 1.

2.3 Welding Simulation

The FEA for predicting the weld residual stresses is performed as a continuous analysis so that the load history from the cladding is carried over to the nozzle-to-pipe weld and the ID patch weld. Specifically, the residual stresses and strains at the end of a weld pass are used as initial conditions at the start of the next weld pass.

The procedures for this complex multi-step simulation are encoded in ANSYS Parametric Design Language (APDL) macros which utilize elastic-plastic material behavior and elements with large deformation capability to predict the residual stresses due to the various welding processes.

2.4 Heat Inputs

The deposition of the weld metal is simulated by imposing a heat generation function on the elements of the FEM representing the active weld, which is applied as a volumetric body heat generation rate. The amount of equivalent heat input energy, Q (in terms of kJ/inch), is determined from the welding parameters.

Since the welding parameters for the welds are not available, a typical heat input of 28 kJ/inch, with an overall heat efficiency of 0.8, is assumed for all the welds. The heat efficiency represents a "composite" value reflecting the concepts of arc efficiency, melting efficiency, etc., and is an optimum value to produce reasonable heat penetration in the analysis.

The APDL macros automatically calculate the appropriate time intervals for the thermal pass to ensure that sufficient heat penetration is achieved, the required interpass temperature between weld passes is met, and a reasonable overall temperature distribution within the finite element model is achieved. The resulting temperature time history is then imported into the stress pass in order to calculate the residual stresses due to the thermal cycling of the weld elements using nonlinear, elastic-plastic load/unload stress reversal relations.

The following summarizes the welding parameters used in the analysis:

- Interpass temperature = 350°F [4]
- Melting temperature = 2500°F (See Section 3.0)
- Reference temperature = 70°F (See Section 3.0)
- Heat input for all welds = 28 kJ/in (See Section 3.0)
- Heat efficiency for all welds = 0.8 (See Section 3.0)
- Inside/Outside heat transfer coefficient = 5 Btu/hr-ft^2-°F (See Section 3.0)
- Inside/Outside temperature = 70°F (See Section 3.0)

2.5 Creep Properties

Strain relaxation due to creep at high temperature is considered in the post-weld heat treatment (PWHT) step of the analysis. In general, creep becomes significant at temperatures above 800°F; thus, creep behavior under 800°F will not be considered in this analysis. The creep properties listed in Table 9 are determined in the previous FEM calculation [1].

2.6 Mechanical Boundary Conditions

The mechanical boundary conditions for the stress analysis are symmetric boundary conditions at the symmetry planes of the model, axial displacement restraint at the end of the nozzle, and axial displacement coupling at the end of the cold leg piping, as shown in Figure 2.

3.0 ASSUMPTIONS

The following assumptions are used in the analyses:

- The cold leg cladding material is assumed to be ER308L, which is a typical weld metal for Type 304 stainless steel cladding.
- The metal melting temperature is assumed to be 2500°F, which is the temperature point where the strength of the material is set to near zero [2].
- The analysis is performed with a reference temperature of 70°F.
- The exposed surface of the model is subject to a typical ambient air cooling convection film coefficient of 5 Btu/hr-ft^2-°F at a bulk temperature of 70°F. The exposed surfaces are defined as the exterior surfaces of the model excluding the symmetry planes and the far ends of the modeled piping and nozzle.
- Since the welding parameters for the welds are not available, a typical heat input of 28 kJ/in, with an overall heat efficiency of 0.8, is assumed for all of the welds.
- The focus of this analysis is the residual stresses in the nozzle boss weld region, while the interaction between the clad buildup and the cold leg base metal has secondary effects on the region of interest. Therefore, the clad is assumed to be fully deposited in a single one-layer pass.
- The boss weld is represented by a 40-bead process, as shown in Figure 3, with each bead represented by a one pass "bead ring" nugget. This approach is a common and acceptable industry practice when information regarding the bead start/stop position and sequencing are unknown.
- Similarly, the ID patch weld is represented by a 6-bead process, as shown in Figure 4, with each bead represented by a one pass "bead ring" nugget.
- For model simplification, the penetration hole is present during the deposition of the clad material. This is acceptable since any localized stress with or without the hole would have negligible impact on the final results.

- For convenience, the modeled ID patch weld has the same geometry as the backing ring for the boss weld.
- Additional assumptions on PWHT are discussed in Section 4.4.

4.0 WELD RESIDUAL STRESS ANALYSIS

The weld residual stress analysis consists of a thermal analysis to determine the temperature distribution followed by a stress analysis to determine the resulting stresses. The analytical sequence described below is used in the finite element analysis, followed by detailed discussions of the steps in Sections 4.1 through 4.6:

1. Deposit cladding on cold leg pipe inside (ID) surface.
2. Install nozzle, backing ring, and deposit boss weld.
3. Remove backing ring and deposit ID patch weld.
4. Post-weld heat treatment, including creep effects based upon experimental data per Table 9.
5. Subject the configuration to a hydrostatic test.
6. Impose five cycles of "shake down" with normal operating temperature and pressure to stabilize the residual stress fluctuations due to stress redistribution caused by normal operating loads.

4.1 Cold leg Cladding

The clad material is typically welded onto the inside surface of the cold leg pipe, and the nominal thickness of the clad is thicker than the typical thickness for a single weld layer used in the process. However, the focus of this analysis is on the as-welded residual stresses, while the interaction between the clad buildup and the base material during the many actual weld passes is not of interest. Therefore, the clad is assumed to be fully deposited in a single pass.

At this step, only the cold leg pipe base metal elements and clad material elements are active; all other components are deactivated during the analysis. At the end of the cladding application, the entire model is cooled to 70°F before the application of the boss weld.

4.2 Boss Weld

The boss weld connects the nozzle boss to the cold leg piping. As shown in Figure 3, the weld is composed of 40 nuggets deposited in 20 weld layers. In the absence of detailed weld fabrication information, a weld sequence is assumed based on standard welding practice at the time of fabrication. In particular, for every layer, the first nugget is deposited on the cold leg side, the second nugget on the nozzle side.

At this step, the nozzle elements and backing ring elements are reactivated, and the boss weld nuggets are reactivated sequentially to simulate the welding process. The preheat temperature of the boss weld is 250°F [4]. At the end of the boss weld, the entire model is cooled to 70°F before the application of the ID patch weld.

4.3 ID Patch Weld

The final weld step is to add the ID patch weld, which replaces the backing ring. As seen in Figure 4, the ID patch weld is composed of 6 nuggets deposited in 2 layers.

At this step, the backing ring is first deactivated to allow the residual stresses to redistribute, and the ID patch weld nuggets are reactivated sequentially to simulate the welding process. The preheat temperature of the ID patch weld is 250°F [4]. At the end of the ID patch weld, the entire model is cooled to 70°F before the application of the PWHT.

4.4 Post-weld Heat Treatment

PWHT is assumed to be performed as per the following procedure outlined in Article N-532 of the ASME Code, Section III [7] and the welding procedure [4] for welding on material group P-1:

1. Heat welded piping component to 1150°F at a heating rate of 400°F per hour divided by the maximum metal thickness (133° per hour for 3 inch thick cold leg) [7, Article N-532.3 (2)].
2. Hold at temperature for approximately 3 hours (1hr/in of weld thickness) [7, Table N-532.3].
3. Allow to cool to 600°F at a cooling rate of 500°F per hour divided by the maximum metal thickness (167° per hour for 3 inch thick cold leg) at temperatures above 600°F [7, Article N-532.3 (5)].
4. Air-cool from 600°F to ambient [7, Article N-532.3 (5)].
5. A steady state load step is imposed at the end of the PWHT process.

During the PWHT, creep behavior is activated for time steps with the maximum temperature above 800°F. At the end of the PWHT, the entire model is cooled 70°F before the application of the hydrostatic test.

4.5 Hydrostatic Test

A hydrostatic test pressure of 3110 psig (3125 psia) and a temperature of 400°F [8, page 9] are applied after the welding. The pressure is applied on the ID surfaces of the cold leg pipe and nozzle. An end-cap load, $P_{end\text{-}cap\text{-}cl}$, is applied at the free end of the cold leg piping. This is calculated based on the following expression:

$$P_{end\text{-}cap\text{-}cl} = \frac{P \cdot r_{inside\_cl}^{2}}{\left(r_{outside\_cl}^{2} - r_{inside\_cl}^{2}\right)} =$$

where,

P	= Hydrostatic test pressure (ksi)
$P_{end\text{-}cap\text{-}cl}$	= End cap pressure on cold leg pipe end (ksi)
r_{inside_cl}	= Inside radius of cold leg pipe (in)
$r_{outside\_cl}$	= Outside radius of cold leg pipe (in)

The applied pressure loads on the model are shown in Figure 5.

4.6 Five Normal Operating Cycles (NOC)

After the hydrostatic test, the assembled configuration is put into service and subjected to 5 cycles of shake down to stabilize the as-welded residual stresses. This step involves simultaneously ramping the model from zero-load to steady-state conditions at normal operating temperature and pressure then back to steady-state at 70°F and no pressure five times.

The applied operating pressure and temperature is 2085 psig (2100 psia) and 537°F [9]. The temperature is assumed to be uniform throughout the components and operating pressure is applied as an internal pressure on the ID surface, with corresponding end-cap pressure calculated using the equation in the previous section. The term "P" is replaced by the operating pressure in the expression.

5.0 RESULTS OF WELD RESIDUAL STRESS ANALYSIS

The ANSYS input files and computer output files for the analyses are listed in Appendix A.

5.1 Welding Temperature Contours

The maximum temperature prediction contours for each weld are created using macro **MapTemp.mac**. This type of contour plot is also called a "fusion boundary" plot because it provides an overview of the maximum temperature on each node throughout the thermal transient for each welding process. The plots are useful in visualizing the melting of weld metal and the extent of heat penetration.

The predicted fusion boundary contours for the cladding, boss weld, and ID patch weld are shown in Figure 6, Figure 7, and Figure 8, respectively. The purple color in the plots represents elements at melting temperature (>2500°F); the plots show complete melting of the weld metal for each weld and slight melting of the base metal along the weld interface.

5.2 PWHT Temperature Results

Figure 9 plots the inside surface temperature curve for the PWHT process. It shows the linear 133°F/hour heating rate, three hours (180 minutes) hold time at 1150°F, 167°F/hour cooling rate at temperature above 600°F, and the air cooling to room temperature of 70°F.

5.3 Residual Stress Results

Figure 10 plots the von Mises residual stresses after welding is complete, but before PWHT. It shows extensive residual stresses of greater than 66 ksi in the weld material. However, as shown in Figure 11, after the PWHT the residual stresses in the weld have relaxed significantly, to below 41 ksi, but the residual stresses in the cladding remain essentially unchanged.

To further investigate the effects of the PWHT, before and after PWHT residual stresses are extracted along the two through-wall paths shown in Figure 12. The through-wall residual stresses are compared in Figure 13, and it shows that there is little to no stress reduction in the clad material, while there is significant stress reduction in the pipe base metal.

The PWHT results from the FEA trend comparably well with the data in EPRI report TR-105697 [10], which contains a comparable through-wall clad residual stress distribution based on experimental measurements, as shown in Figure 14. The experimental measurements were for a low alloy steel vessel with a Type 304 stainless steel clad. The data shows tensile hoop stress through the clad thickness and the base metal near the clad interface, but the hoop stress drops rapidly to compressive values at farther distances from the clad.

Figure 15 depicts the predicted von Mises residual stresses after the hydrostatic test. It shows an insignificant reduction in maximum stress when compared to the post-PWHT step: 73.74 ksi (Figure 15) versus 73.75 ksi (Figure 11), while the overall stress contour remains essentially the same.

Figure 16 and Figure 17 depicts the combined weld residual plus operating radial and hoop stresses, respectively, at the fifth stabilization NOC cycle. The stress results at this step are used in the fracture mechanics evaluations.

6.0 CONCLUSIONS

Finite element residual stress analysis has been performed on the bounding cold leg nozzle boss weld at Palisades. Stresses at normal operating conditions combined with residual stresses have been obtained and saved for future use. The stress results will be used in a separate calculation to determine crack growth.

7.0 REFERENCES

1. SI Calculation No. 1400669.320, Rev. 0, "Finite Element Model Development for the Cold Leg Drain, Spray, and Charging Nozzles."
2. SI Calculation No. 0800777.307, Rev. 5, "Material Properties for Residual Stress Analyses, Including MISO Properties Up To Material Flow Stress."
3. ANSYS Mechanical APDL and PrepPost, Release 14.5 (w/ Service Pack 1), ANSYS, Inc., September 2012.
4. Combustion Engineering Welding Procedure No. MA-41, Rev.0, SI File No. 1400669.204.
5. "Steels for Elevated Temperature Service," United States Steel Co., 1949.
6. Publication SMC-027, "Inconel Alloy 600," Special Metals Corp., 2004, SI File 0800777.211.
7. ASME Boiler and Pressure Vessel Code, Section III, 1965 Edition with Addenda through Winter 1966.
8. Combustion Engineering Specification No. 0070P-006, Rev. 2, "Engineering Specification for Primary Coolant Pipe and Fittings," SI File No. 1300086.203.
9. Palisades Design Input Record, "Palisades Alloy 600 Flaw Eval DIR 3-4-15 Rev1.pdf," SI File No. 1400669.201.
10. EPRI Report No. TR-105697, "BWR Reactor Pressure Vessel Shell Weld Inspection Recommendations (BWRVIP-05)," September 1995.

Table 1: Elastic Properties for SA-516 Grade 70 (≤4" Thick)

Temperature (°F)	Young's Modulus ($x10^3$ ksi)	Mean Thermal Expansion ($x10^{-6}$ in/in/°F)	Thermal Conductivity (2) (Btu/min-in-°F)	Specific Heat (2) (Btu/lb-°F)
70	29.5	6.4	0.0488	0.103
500	27.3	7.3	0.0410	0.128
700	25.5	7.6	0.0369	0.138
1100	18.0	8.2	0.0290	0.171
1500	5.0	8.6	0.0218	0.198
2500	0.1	9.5	0.0014	0.204
2500.1	–	0.0	–	–

Notes:
1. All values per [2].
2. Density (ρ) = 0.283 lb/in^3 [2], assumed temperature independent.
3. Poisson's Ratio (υ) = 0.3 [2], assumed temperature independent.

Table 2: Elastic Properties for ER308L

Temperature (°F)	Young's Modulus ($x10^3$ ksi)	Mean Thermal Expansion ($x10^{-6}$ in/in/°F)	Thermal Conductivity (2) (Btu/min-in-°F)	Specific Heat (2) (Btu/lb-°F)
70	28.3	8.5	0.0119	0.116
500	25.8	9.7	0.0151	0.131
700	24.8	10.0	0.0164	0.135
1100	22.1	10.5	0.0189	0.140
1500	18.1	10.8	0.0213	0.145
2500	0.1	11.5	0.0292	0.159
2500.1	–	0.0	–	–

Notes:
1. All values per [2].
2. Density (ρ) = 0.283 lb/in^3 [2], assumed temperature independent.
3. Poisson's Ratio (υ) = 0.3 [2], assumed temperature independent.

Table 3: Elastic Properties for Alloy 600

Temperature (°F)	Young's Modulus ($x10^3$ ksi)	Mean Thermal Expansion ($x10^{-6}$ in/in/°F)	Thermal Conductivity (2) (Btu/min-in-°F)	Specific Heat (2) (Btu/lb-°F)
70	31.0	6.8	0.0119	0.108
500	29.0	7.6	0.0147	0.120
700	28.2	7.9	0.0161	0.125
1100	25.9	8.4	0.0192	0.139
1500	23.1	9.0	0.0222	0.148
2500	0.1	10.0	0.0306	0.177
2500.1	–	0.0	–	–

Notes:
1. All values per [2].
2. Density (ρ) = 0.300 lb/in^3 [2], assumed temperature independent.
3. Poisson's Ratio (υ) = 0.29 [2], assumed temperature independent.

Table 4: Elastic Properties for Alloy 82/182

Temperature (°F)	Young's Modulus ($x10^3$ ksi)	Mean Thermal Expansion ($x10^{-6}$ in/in/°F)	Thermal Conductivity (2) (Btu/min-in-°F)	Specific Heat (2) (Btu/lb-°F)
70	31.0	6.8	0.0119	0.108
500	29.0	7.6	0.0147	0.120
700	28.2	7.9	0.0161	0.125
1100	25.9	8.4	0.0192	0.139
1500	23.1	9.0	0.0222	0.148
2500	0.1	10.0	0.0306	0.177
2500.1	–	0.0	–	–

Notes:
1. All values per [2].
2. Density (ρ) = 0.300 lb/in^3 [2], assumed temperature independent.
3. Poisson's Ratio (υ) = 0.29 [2], assumed temperature independent.

Table 5: Stress-Strain Curves for SA-516 Grade 70 (≤4" Thick)

Temperature (°F)	Strain (in/in)	Stress (ksi)
70	0.00128814	38.000
	0.00187809	42.000
	0.00257329	46.000
	0.00381110	50.000
	0.00600383	54.000
500	0.00113553	31.000
	0.00142679	35.875
	0.00183954	40.750
	0.00261139	45.625
	0.00415246	50.500
700	0.00106667	27.200
	0.00132412	32.550
	0.00166876	37.900
	0.00228121	43.250
	0.00354341	48.600
1100	0.00116667	21.000
	0.05116163	22.125
	0.05915444	23.250
	0.06794123	24.375
	0.07755935	25.500
1500	0.00300000	15.000
	0.16717493	15.125
	0.16992011	15.250
	0.17268761	15.375
	0.17547742	15.500
2500[2]	0.01000000	1.000
	0.10961239	1.125
	0.12781277	1.250
	0.14689940	1.375
	0.16683167	1.500

Notes:
1. All values per [2].
2. Values at 2500°F assumed arbitrarily small values for convergence stability.

Table 6: Stress-Strain Curves for ER308L

Temperature (°F)	Strain (in/in)	Stress (ksi)
70	0.00203180	57.500
	0.02471351	61.563
	0.03107296	65.625
	0.03861377	69.688
	0.04747167	73.750
500	0.00140089	36.143
	0.00714793	40.250
	0.01065407	44.357
	0.01558289	48.464
	0.02233857	52.571
700	0.00132488	32.857
	0.00477547	37.125
	0.00743595	41.393
	0.01143777	45.661
	0.01727192	49.929
1100	0.00121913	26.943
	0.00264833	30.138
	0.00404100	33.332
	0.00634529	36.527
	0.01005286	39.721
1500	0.00117995	21.357
	0.05352064	21.563
	0.05610492	21.768
	0.05878975	21.973
	0.06157807	22.179
2500[(2)]	0.01000000	1.000
	0.10961239	1.125
	0.12781277	1.250
	0.14689940	1.375
	0.16683167	1.500

Notes:
1. All values per [2].
2. Values at 2500°F assumed arbitrarily small values for convergence stability.

Table 7: Stress-Strain Curves for Alloy 600

Temperature (°F)	Strain (in/in)	Stress (ksi)
70	0.00157419	48.800
	0.01658847	55.300
	0.02343324	61.800
	0.03212188	68.300
	0.04291703	74.800
500	0.00152069	44.100
	0.01539220	50.338
	0.02210610	56.575
	0.03072476	62.813
	0.04153277	69.050
700	0.00152128	42.900
	0.01634485	49.000
	0.02334760	55.100
	0.03227153	61.200
	0.04338643	67.300
1100	0.00155985	40.400
	0.02275193	44.475
	0.03004563	48.550
	0.03888203	52.625
	0.04943592	56.700
1500	0.00092641	21.400
	0.08827666	22.475
	0.09785101	23.550
	0.10796967	24.625
	0.11863796	25.700
2500[2]	0.01000000	1.000
	0.10961239	1.125
	0.12781277	1.250
	0.14689940	1.375
	0.16683167	1.500

Notes:
1. All values per [2].
2. Values at 2500°F assumed arbitrarily small values for convergence stability.

Table 8: Stress-Strain Curves for Alloy 82/182

Temperature (°F)	Strain (in/in)	Stress (ksi)
70	0.00179032	55.500
	0.03456710	60.113
	0.04292837	64.725
	0.05257245	69.338
	0.06359421	73.950
500	0.00164483	47.700
	0.02976152	52.313
	0.03809895	56.925
	0.04790379	61.538
	0.05929946	66.150
700	0.00159574	45.000
	0.02849157	49.538
	0.03680454	54.075
	0.04663682	58.613
	0.05812078	63.150
1100	0.00159073	41.200
	0.03568855	44.488
	0.04402702	47.775
	0.05360088	51.063
	0.06449835	54.350
1500	0.00106494	24.600
	0.11812735	25.325
	0.12540227	26.050
	0.13290814	26.775
	0.14064577	27.500
2500[2]	0.01000000	1.000
	0.10961239	1.125
	0.12781277	1.250
	0.14689940	1.375
	0.16683167	1.500

Notes:
1. All values per [2].
2. Values at 2500°F assumed arbitrarily small values for convergence stability.

Table 9: Creep Properties

Material	Temperature (°F)	Creep Strength (ksi)		*A* (ksi/hr)	*n*
		σ_1 (0.0001%/hr)	σ_2 (0.00001%/hr)		
SA-516 Gr. 70 (Based on carbon steel) Per [5]	800	19.0	12.4	1.26E-13	5.40
	900	9.0	6.7	3.59E-14	7.80
	1000	3.5	2.8	2.43E-12	10.32
	1100	1.4	0.8	2.50E-07	4.11
ER308L (Based on Type 304) Per [5]	800	33.4	25.0	7.73E-19	7.95
	900	24.0	17.6	5.67E-17	7.42
	1000	17.6	11.5	1.82E-13	5.41
	1100	11.5	7.1	8.62E-12	4.77
Alloy 600 Alloy 82/182 (Based on Alloy 600) Per [6]	800	40.0	30.0	1.50E-19	8.00
	900	28.0	18.0	2.87E-14	5.21
	1000	12.5	6.1	3.02E-10	3.21
	1100	6.8	3.4	1.72E-09	3.32

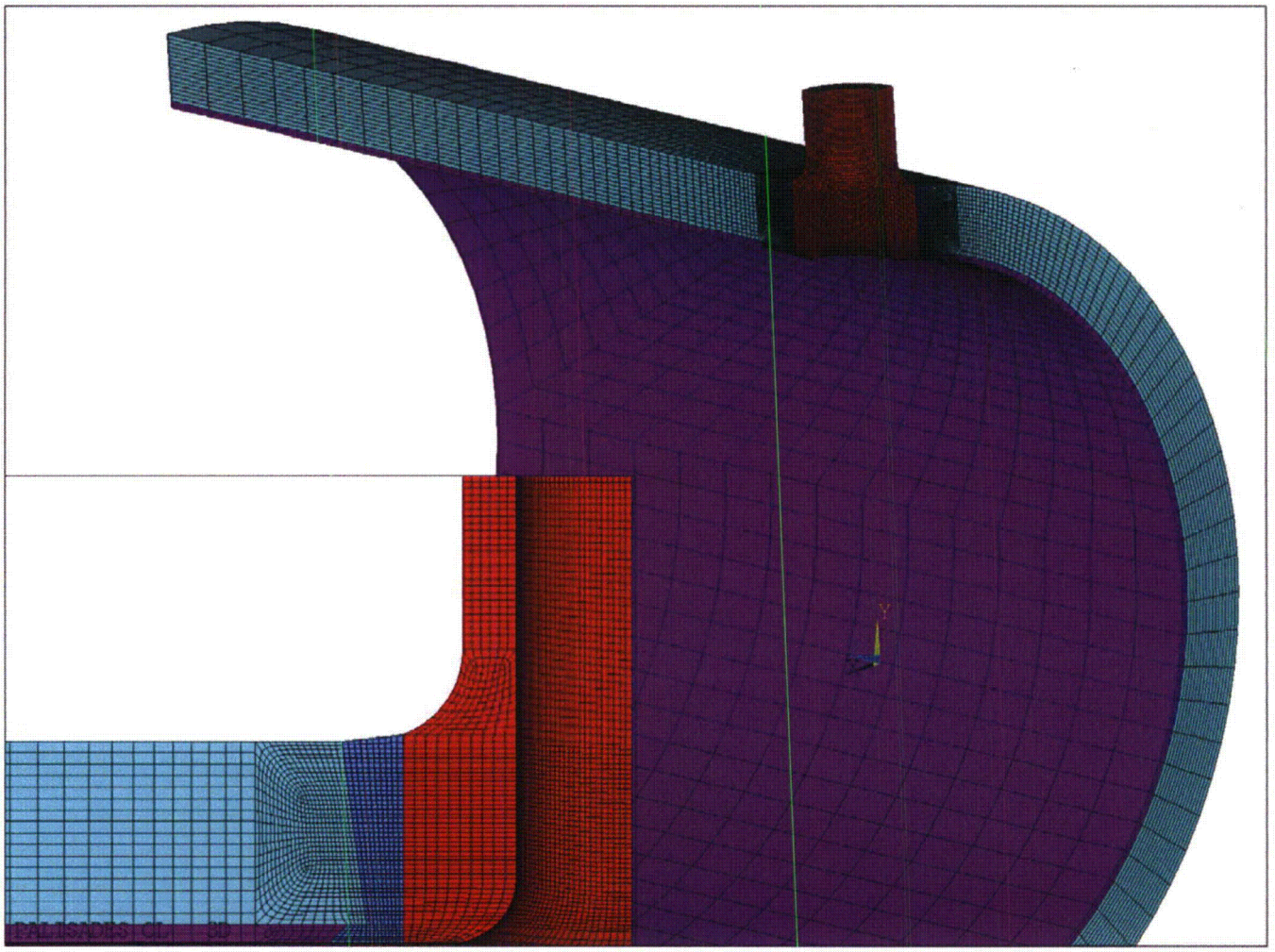

Figure 1: Finite Element Model for Residual Stress Analysis

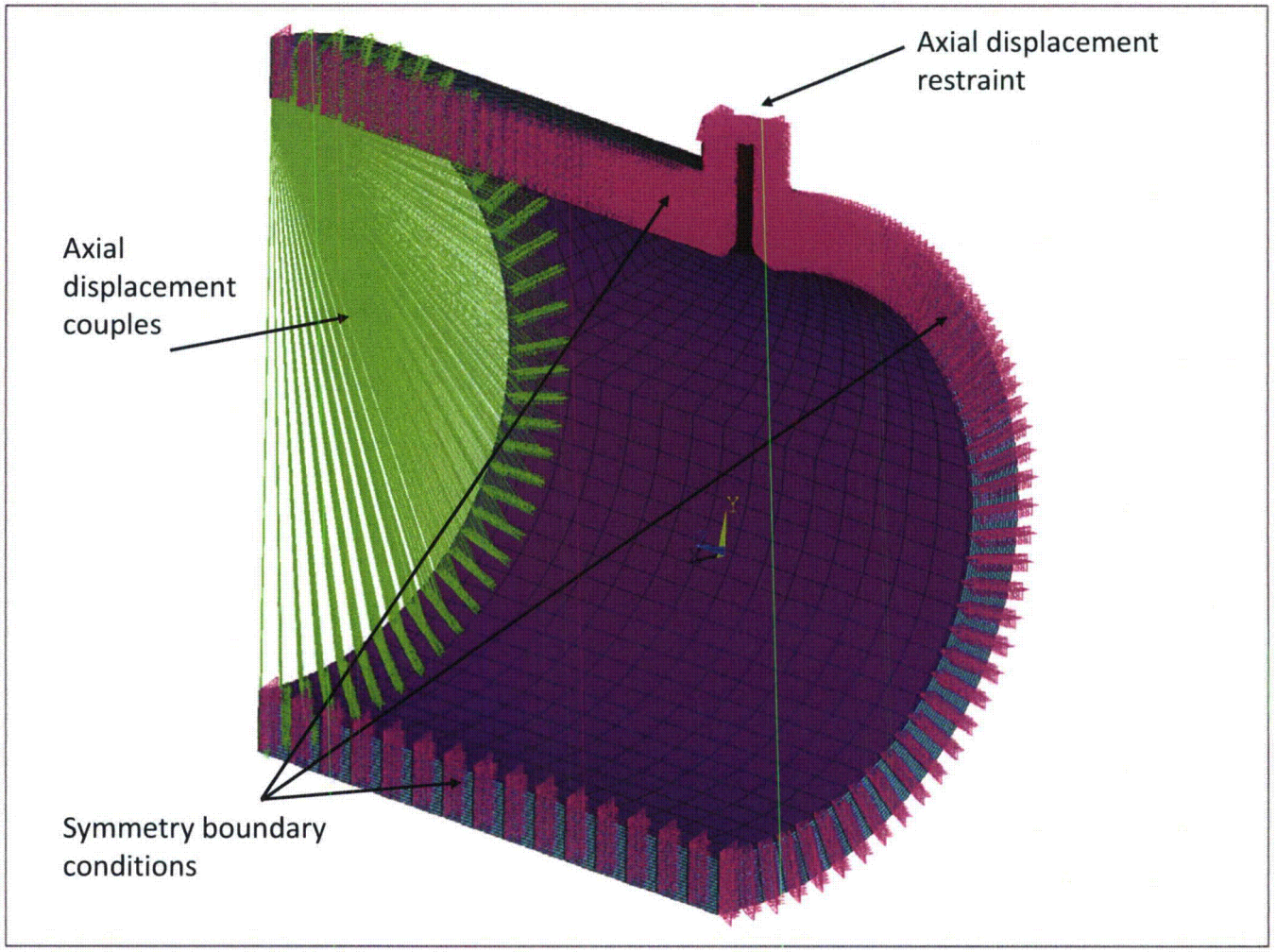

Figure 2: Applied Mechanical Boundary Conditions

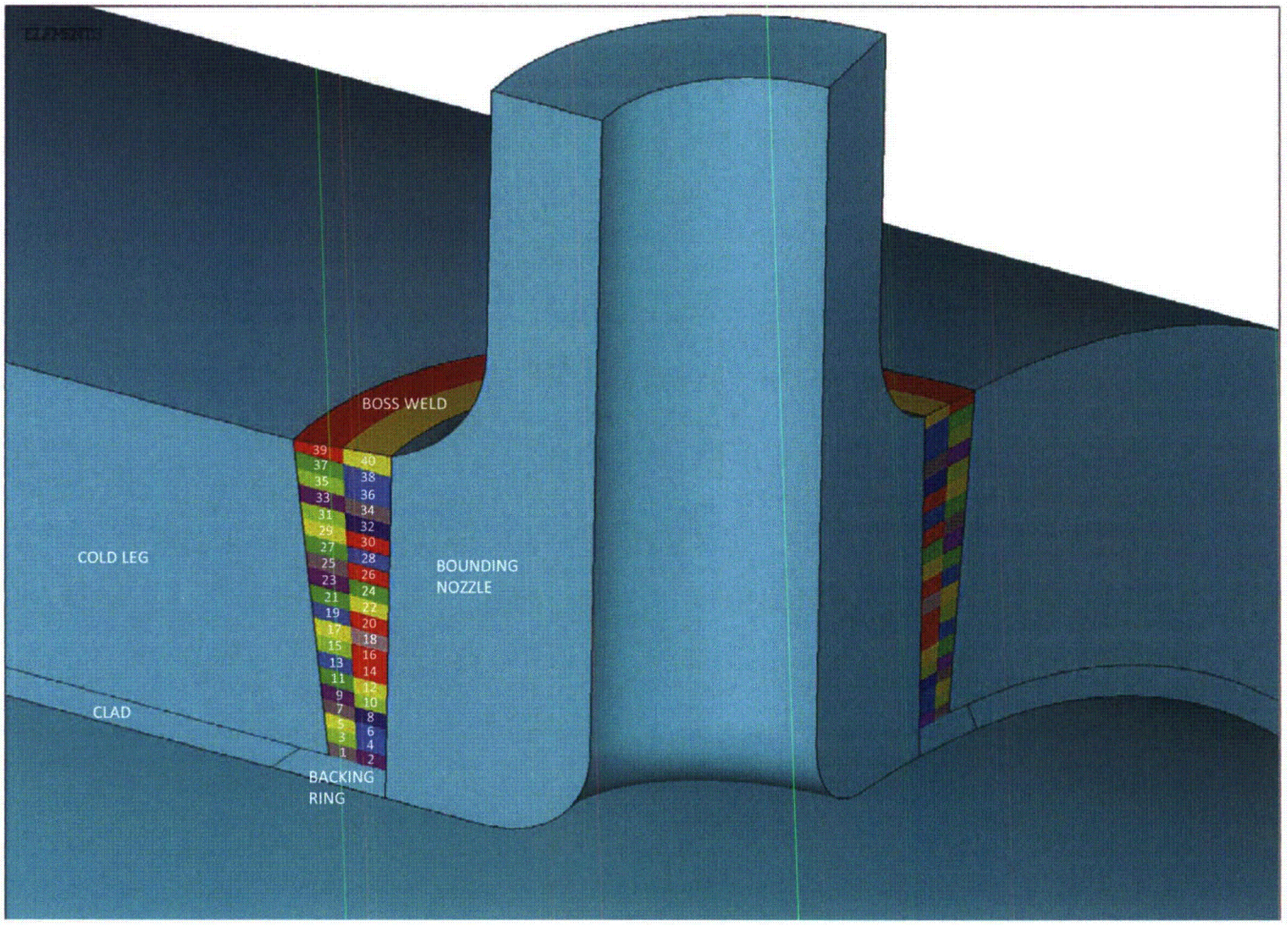

Figure 3: Weld Nugget Definitions for the Boss Weld

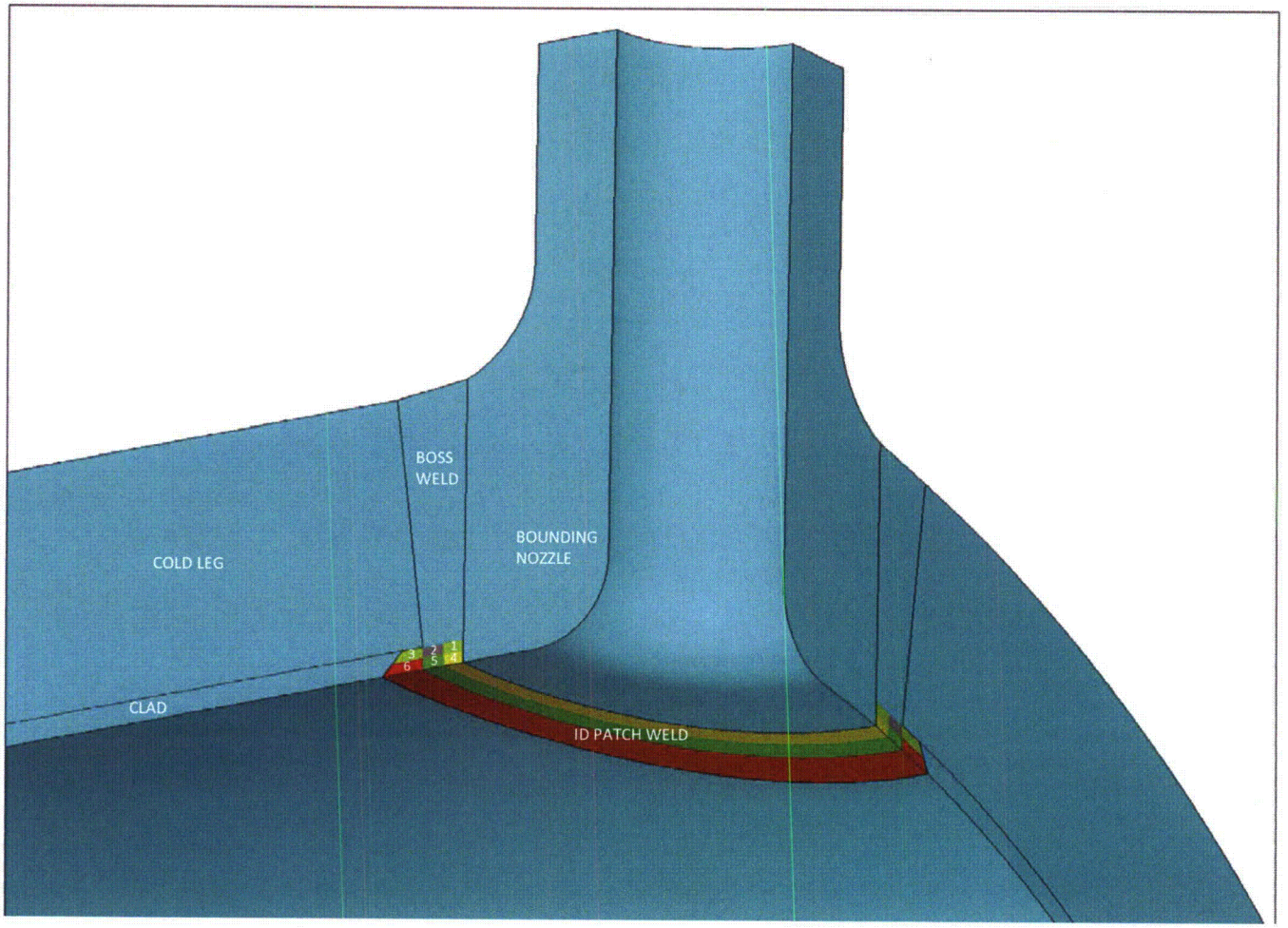

Figure 4: Weld Nugget Definitions for the ID Patch Weld

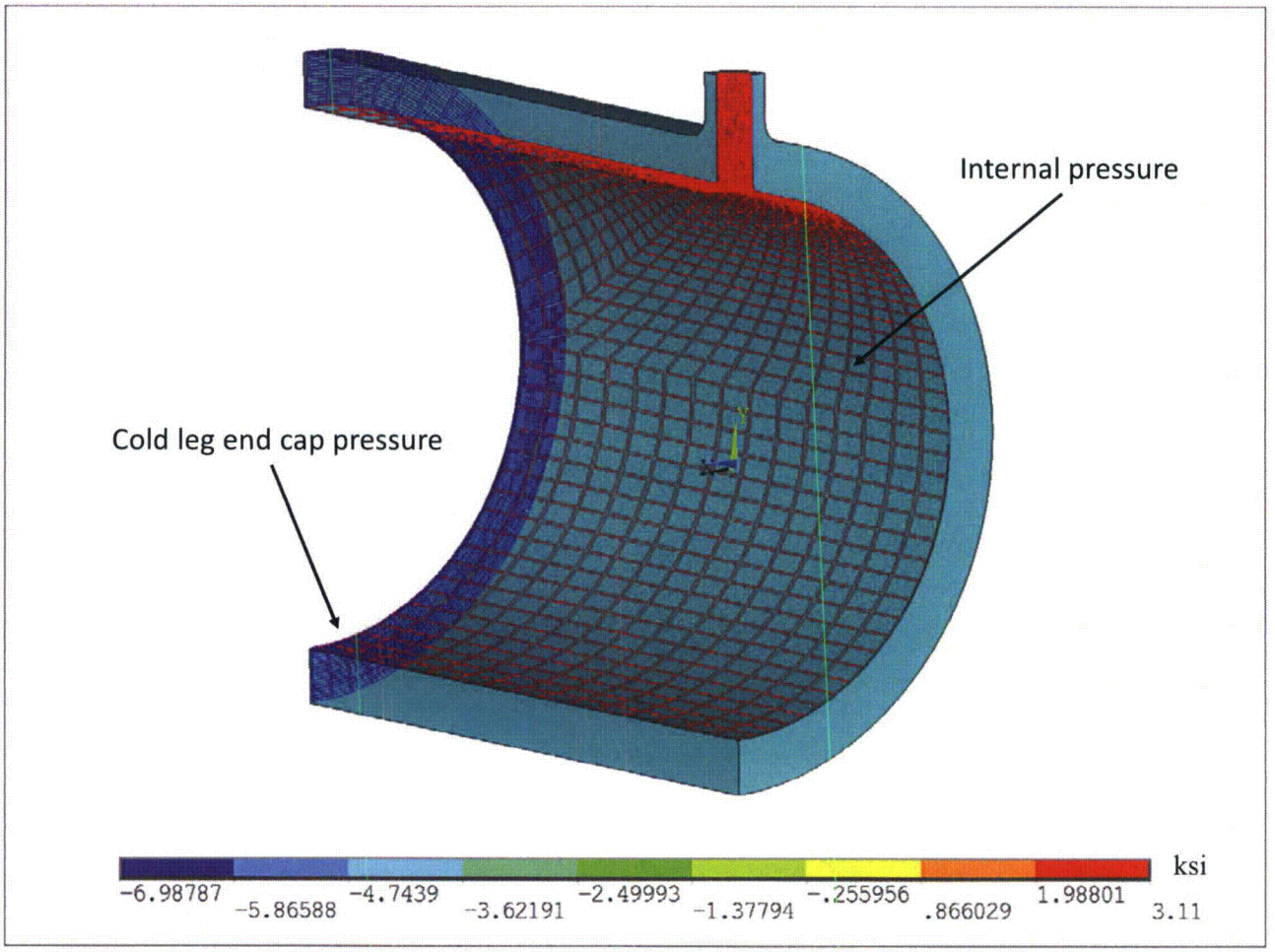

Figure 5: Applied Hydrostatic Test Pressure and Corresponding End Cap Pressure Loads

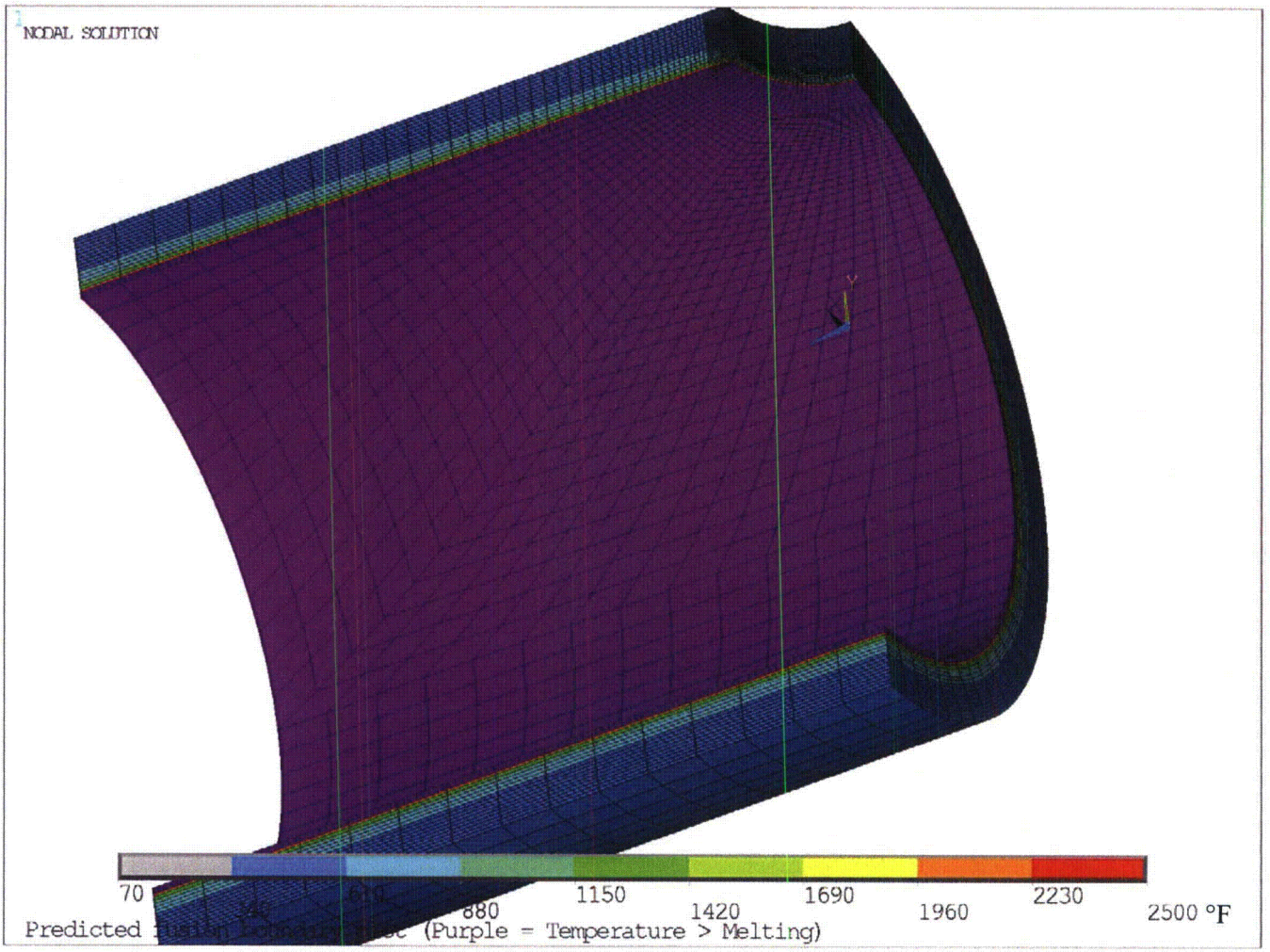

Figure 6: Predicted Fusion Boundary Plot for Cladding

(Note: Purple = Temperature > Melting Temperature of 2500°F)

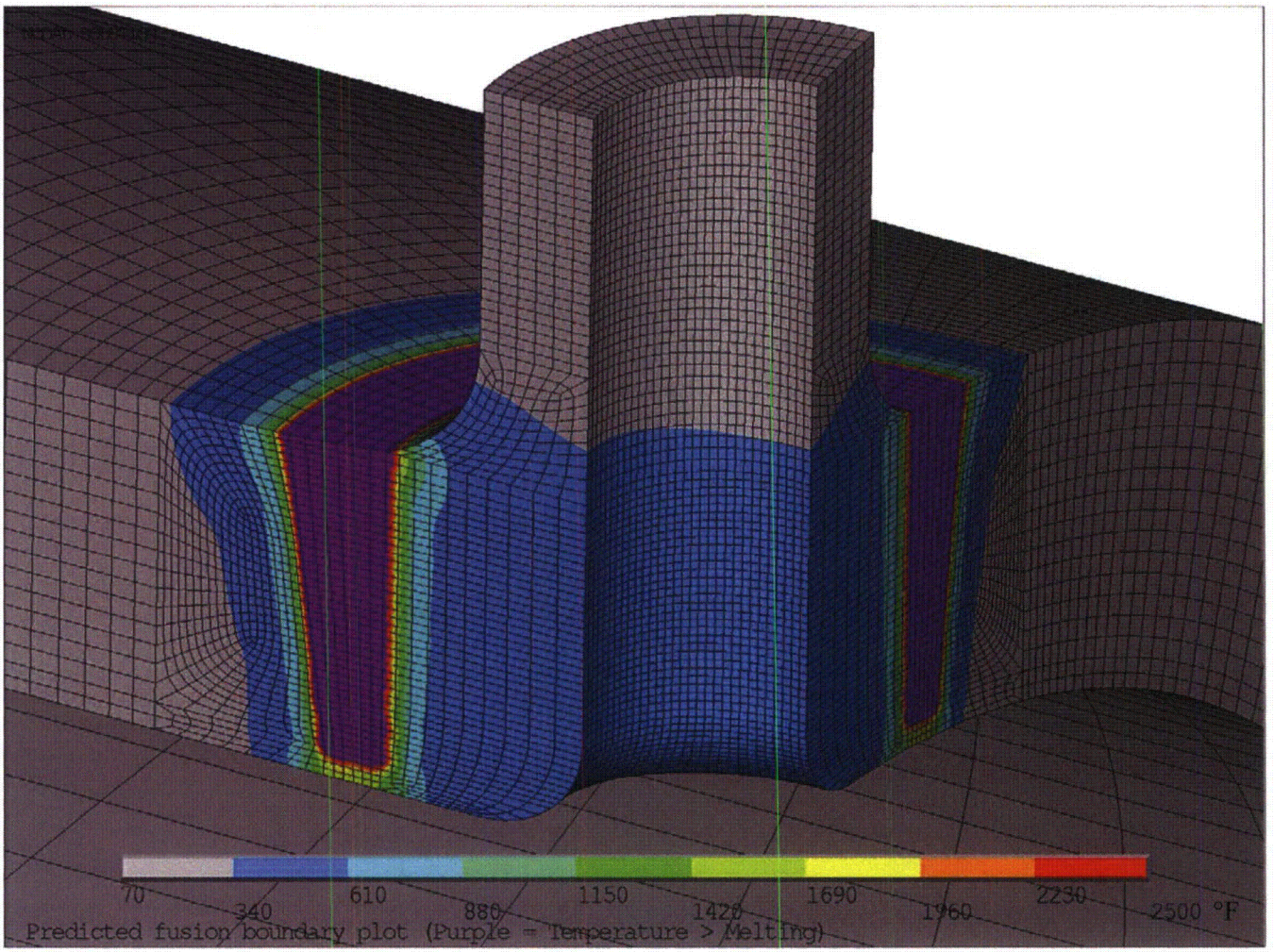

Figure 7: Predicted Fusion Boundary Plot for Boss Weld

(Note: Purple = Temperature > Melting Temperature of 2500°F)

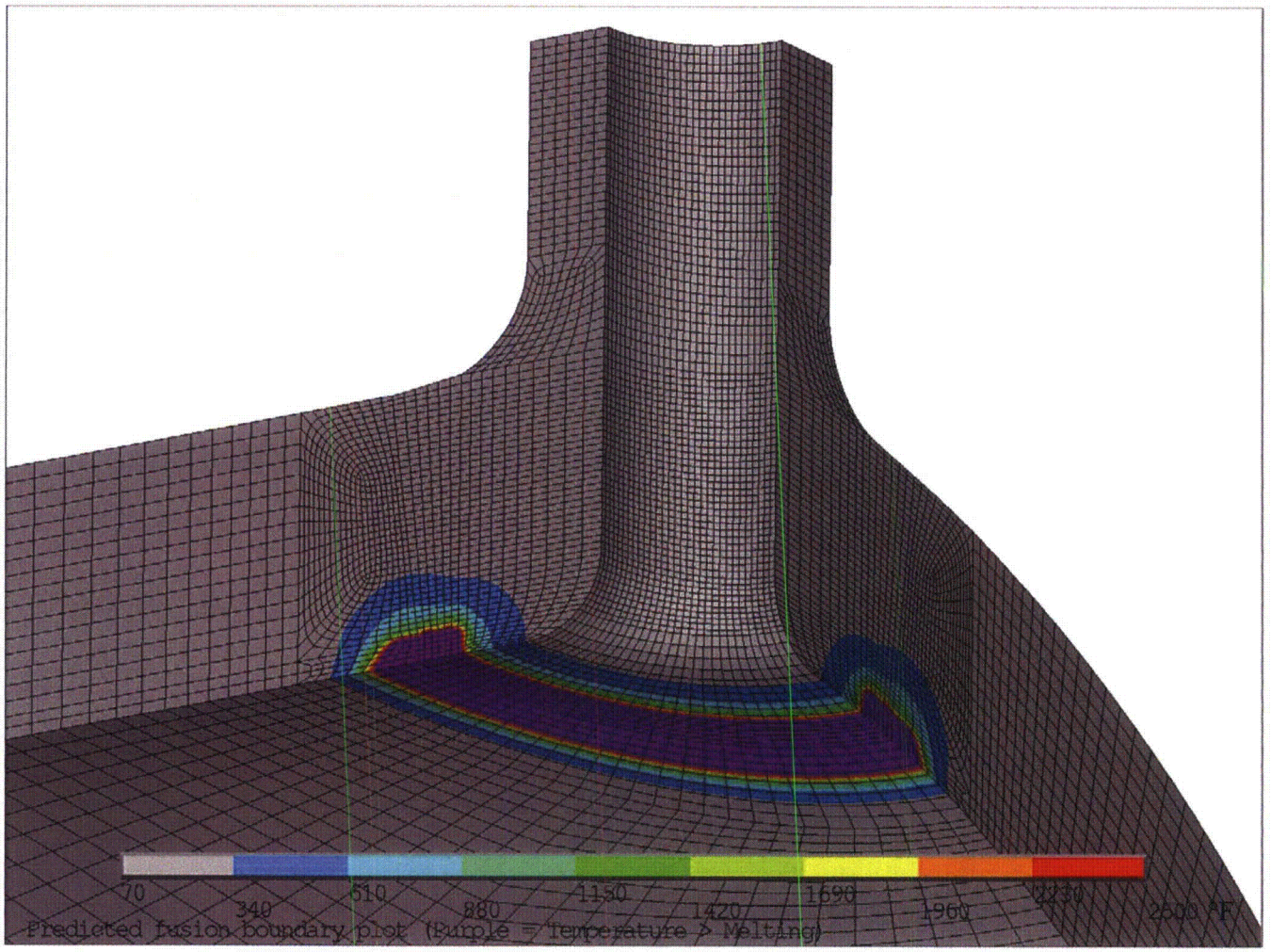

Figure 8: Predicted Fusion Boundary Plot for ID Patch Weld

(Note: Purple = Temperature > Melting Temperature of 2500°F)

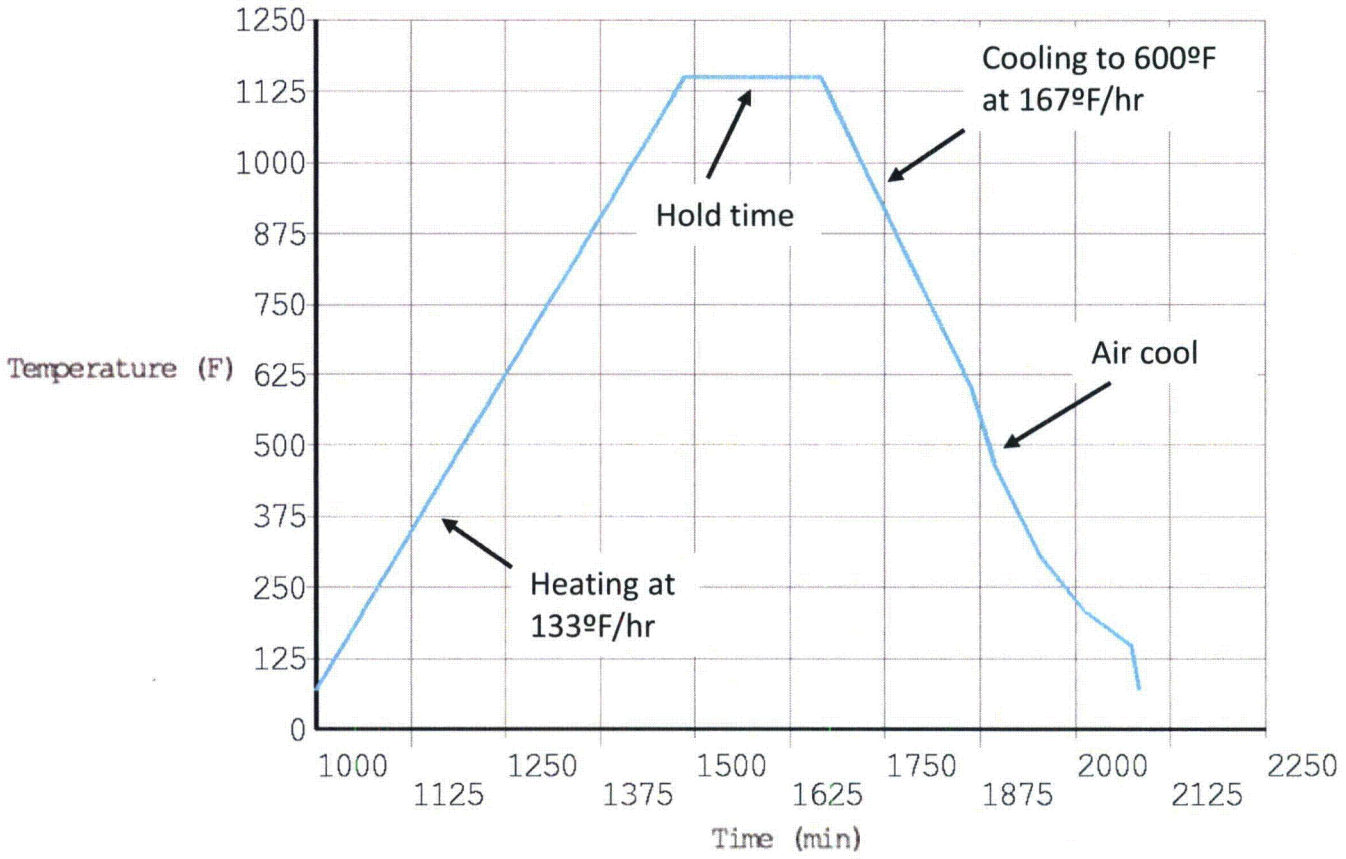

Figure 9: Time vs. Temperature Curve for PWHT

Note:
1. PWHT temperature history is for a typical ID node on the model.

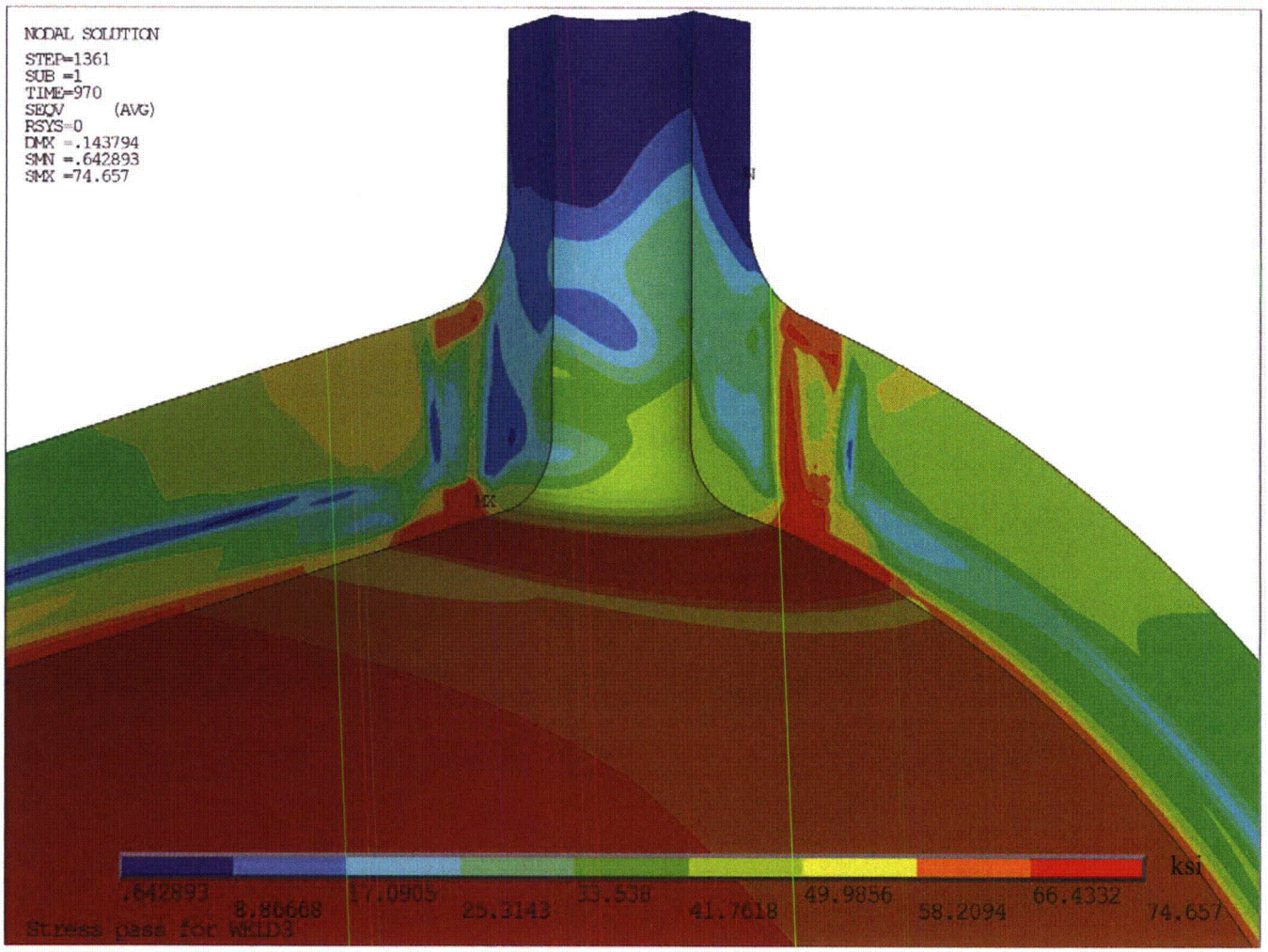

Figure 10: Predicted von Mises Residual Stress at 70°F after ID Patch Weld

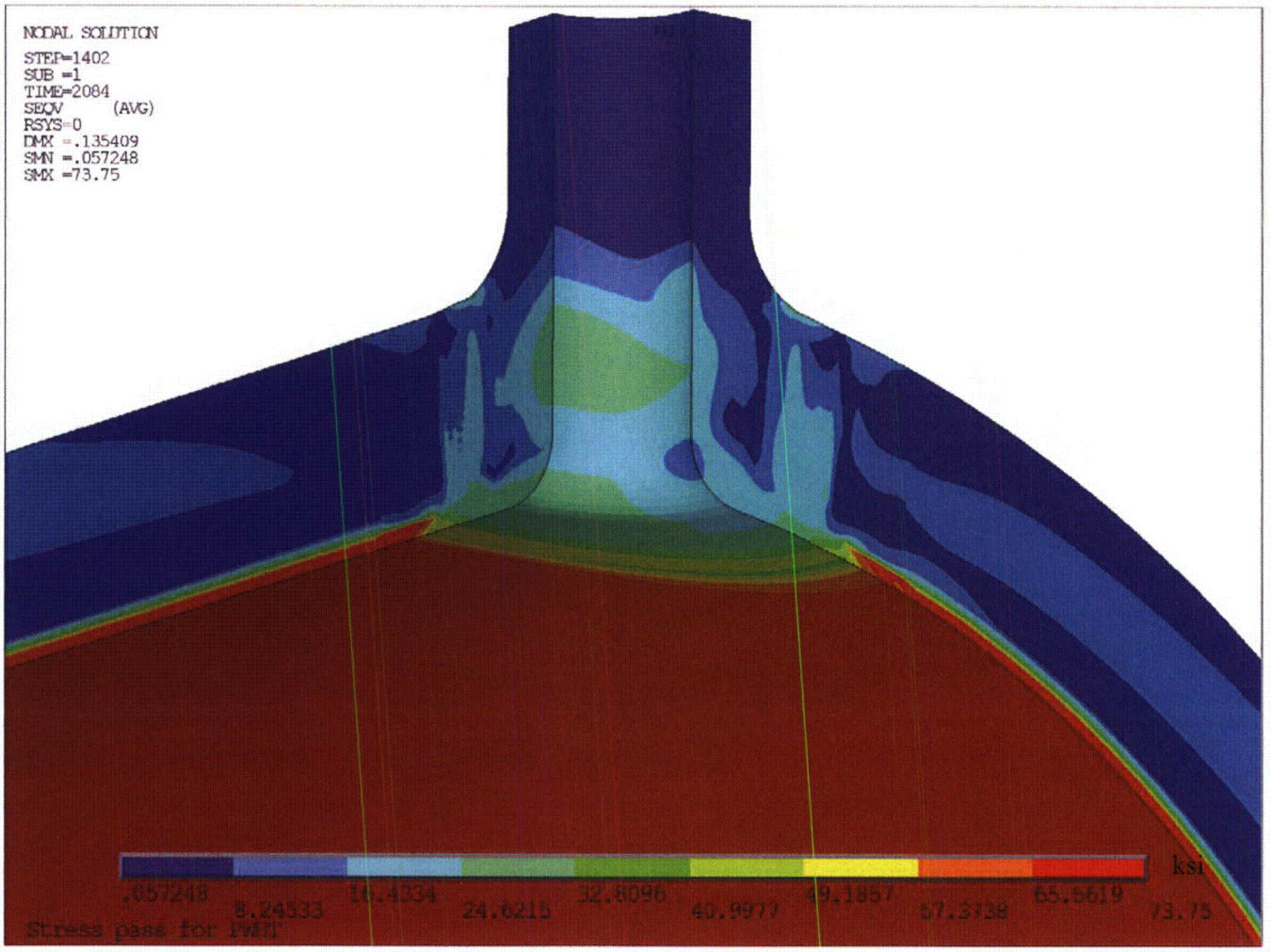

Figure 11: Predicted von Mises Residual Stress at 70°F after PWHT

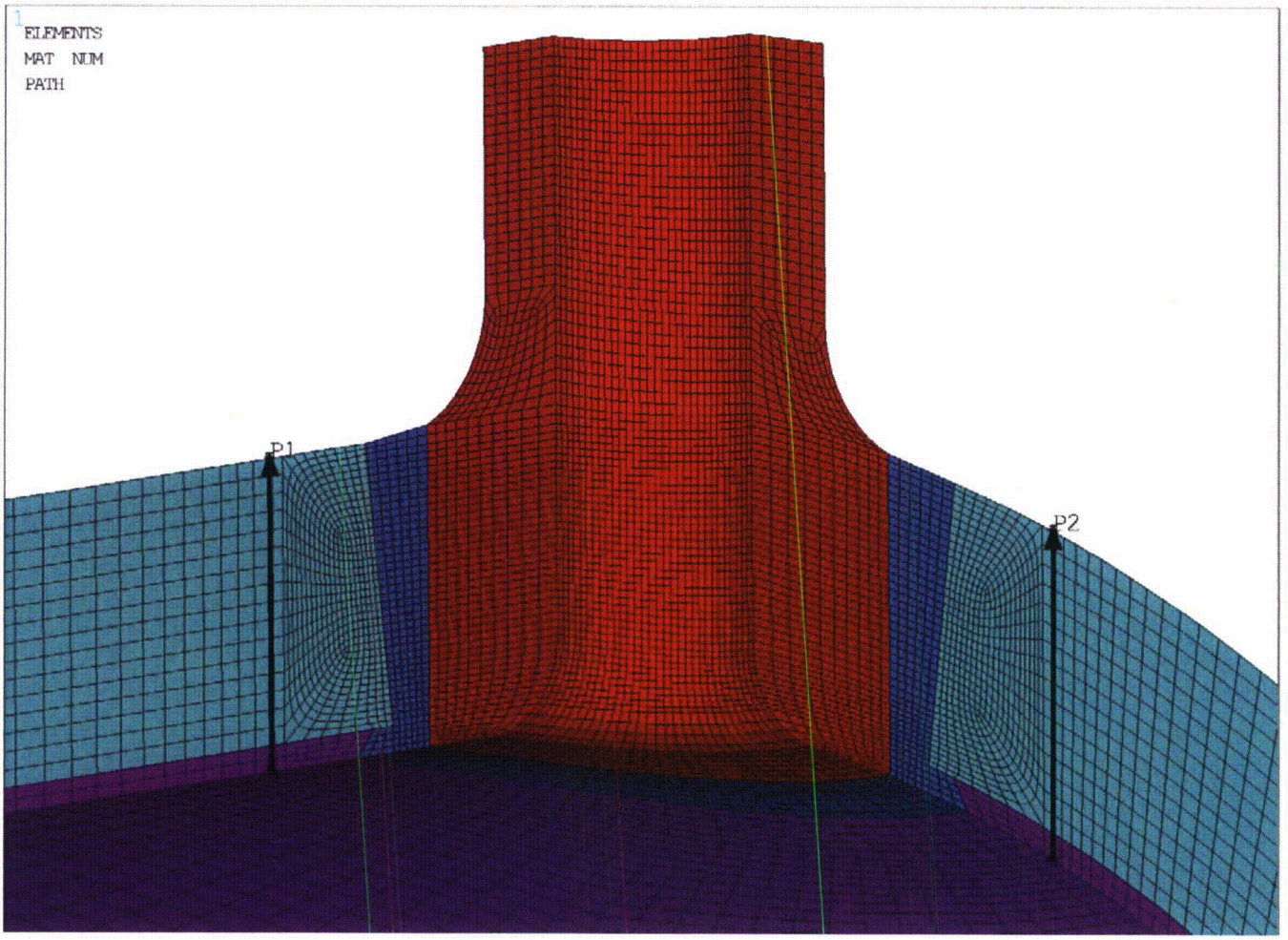

Figure 12: Paths for Stress Extraction

Notes:

1. In the cold leg coordinates, hoop residual stresses along path P1 and axial residual stresses along path P2 are extracted for comparison of before and after PWHT.
2. The before and after PWHT through-wall residual stresses are compared in Figure 13.

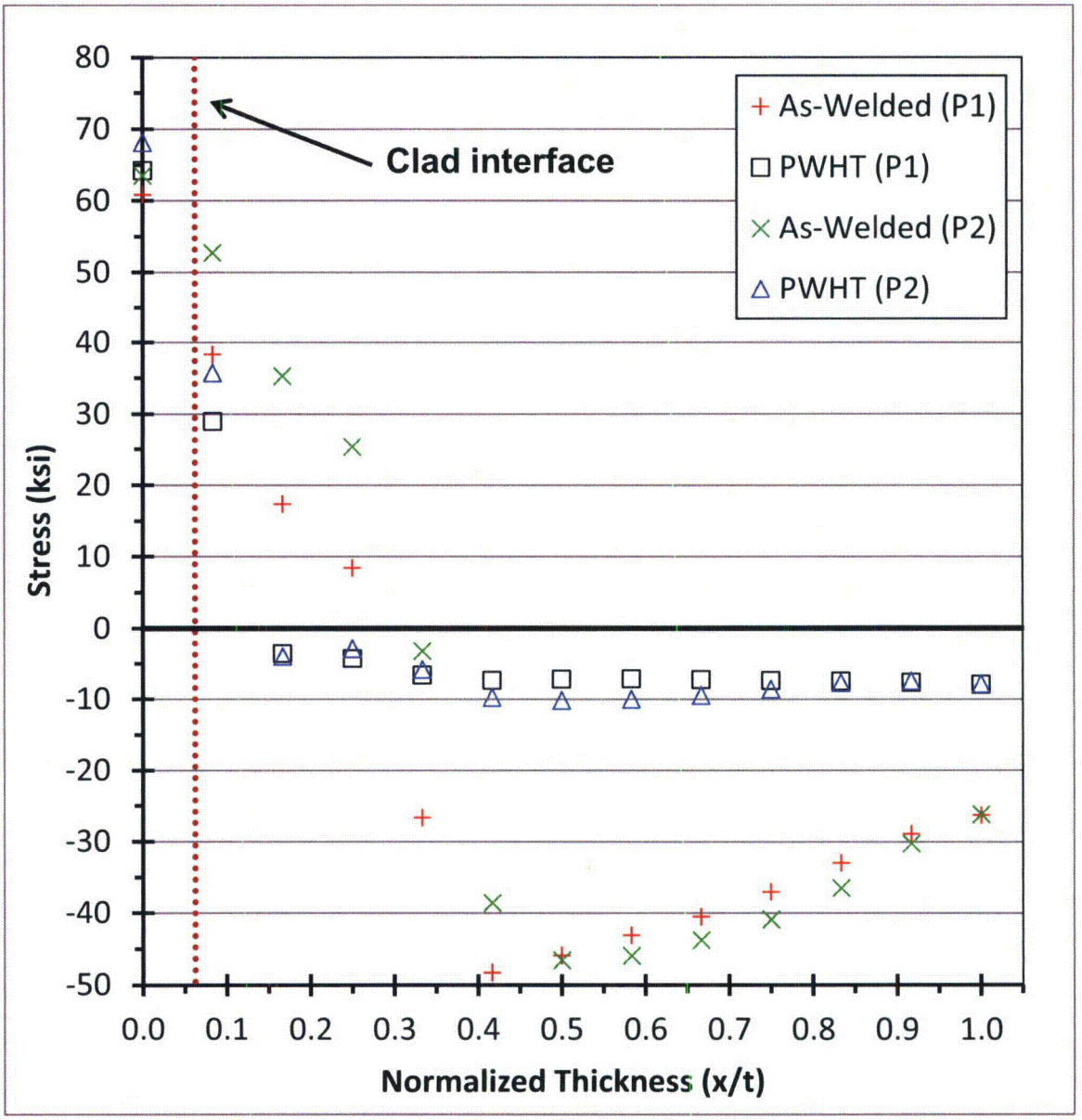

Figure 13: Residual Stress Comparison at 70°F Before and After PWHT

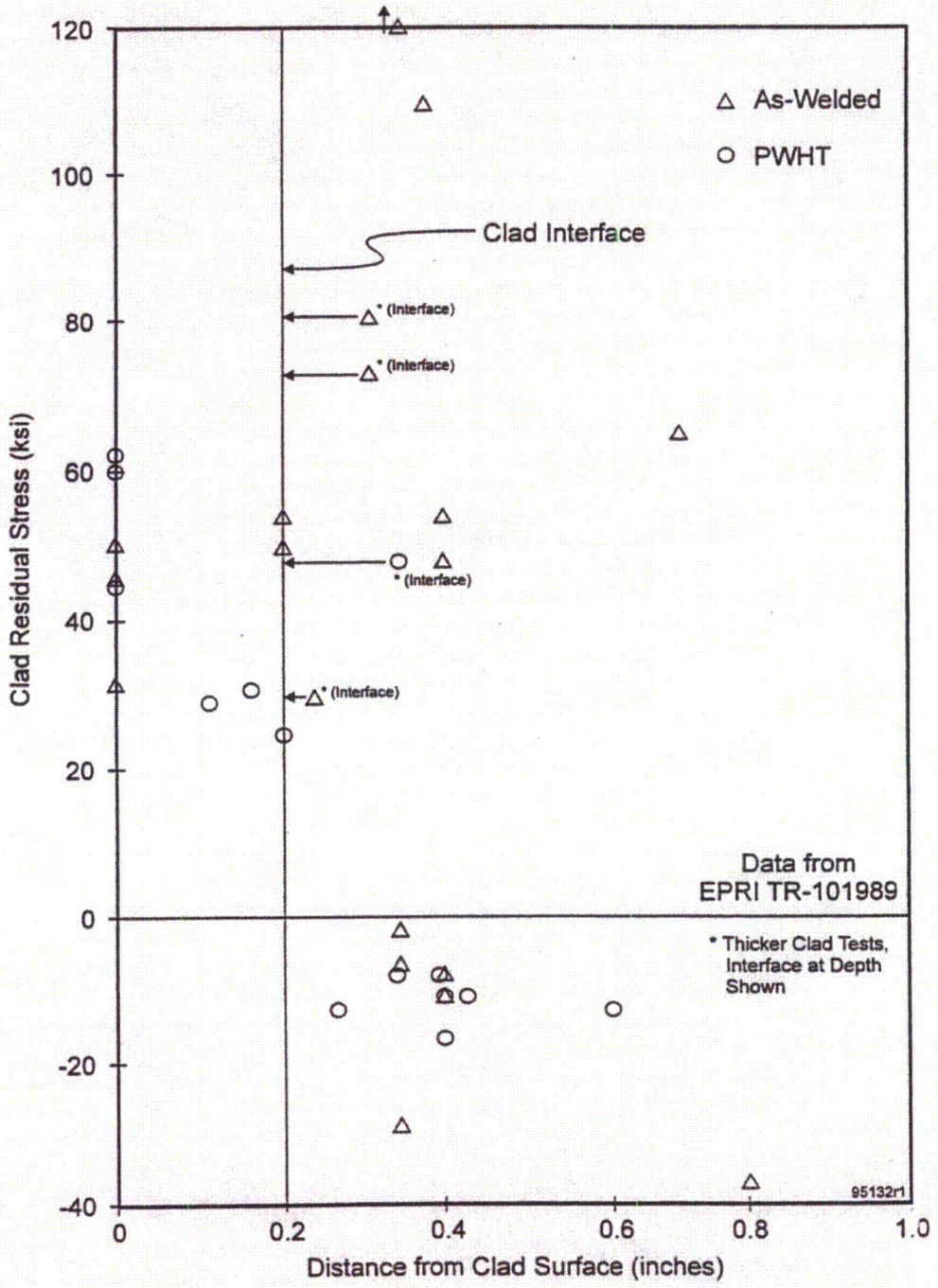

Figure 14: Measured Through-Wall Residual Stresses for PWHT

Notes:
1. Figure is obtained from EPRI report TR-105697 [10].
2. Measurements show little to no stress reduction in the cladding after PWHT.
3. Measurements show significant stress reduction in the base metal after PWHT.

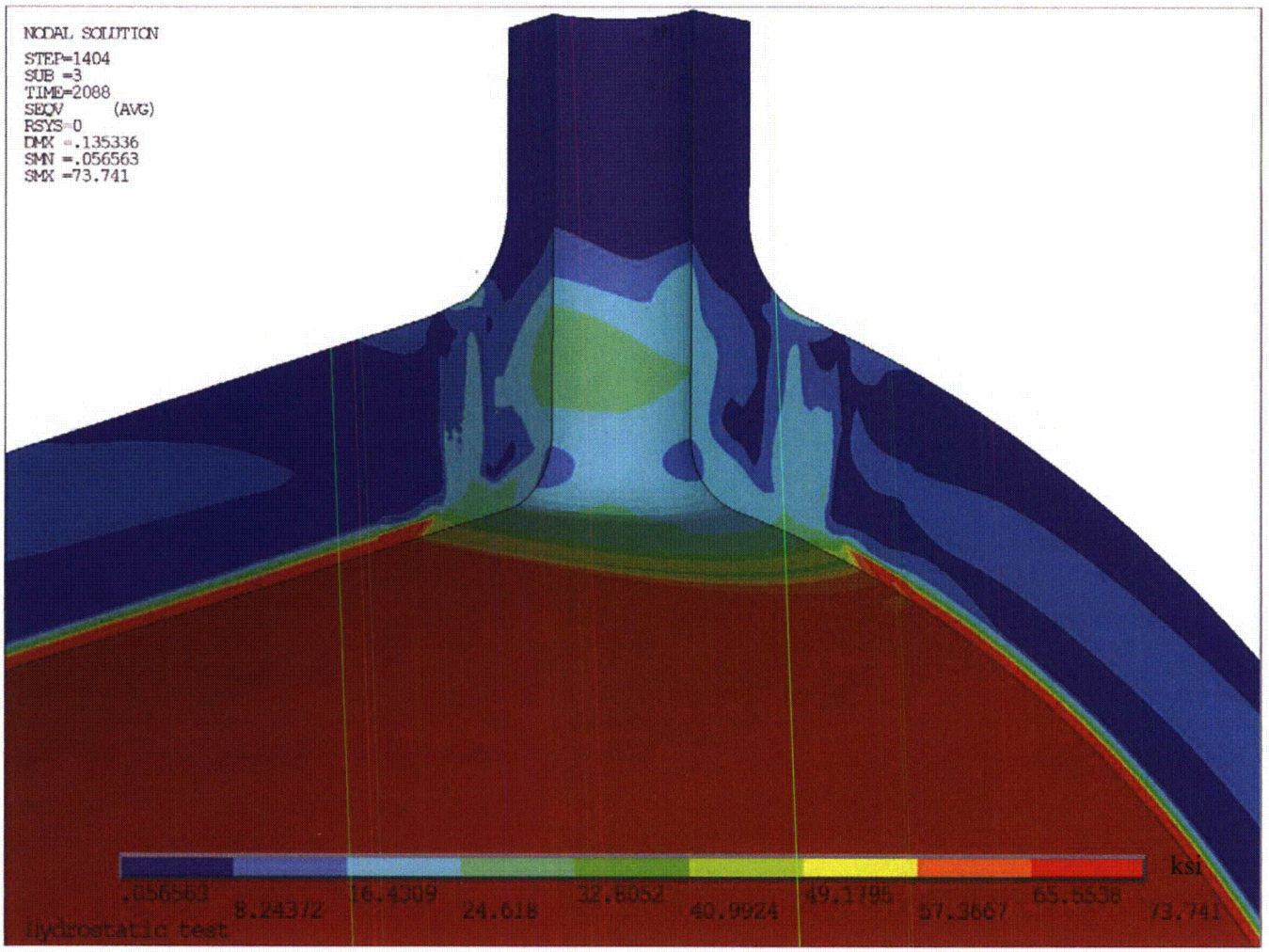

Figure 15: Predicted von Mises Residual Stress at 70°F after Hydrostatic Test

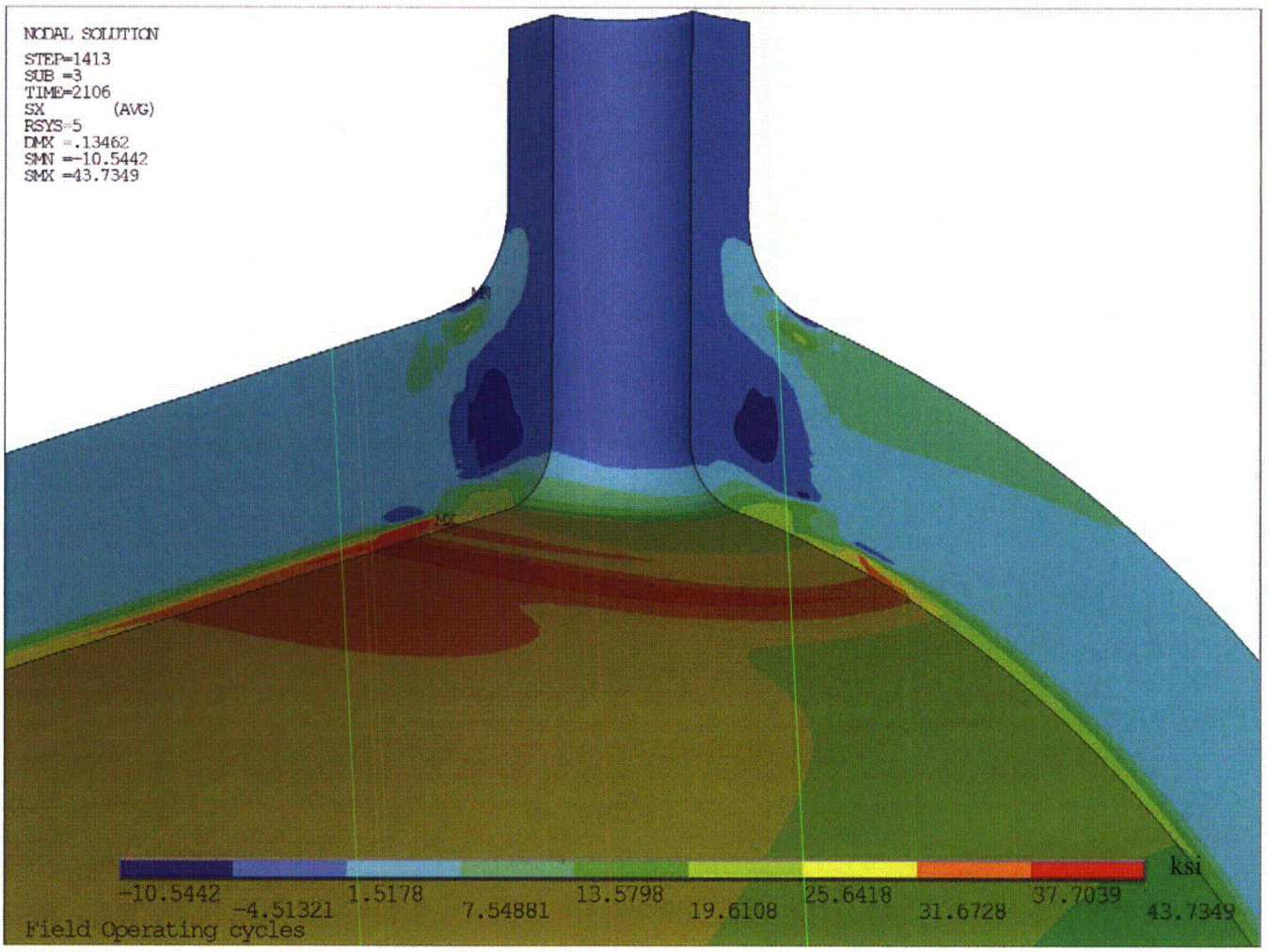

Figure 16: Predicted Radial Residual Stress + Operating Conditions (5th NOC Cycle)

Note:

1. Radial stresses shown in the nozzle axis radial direction.

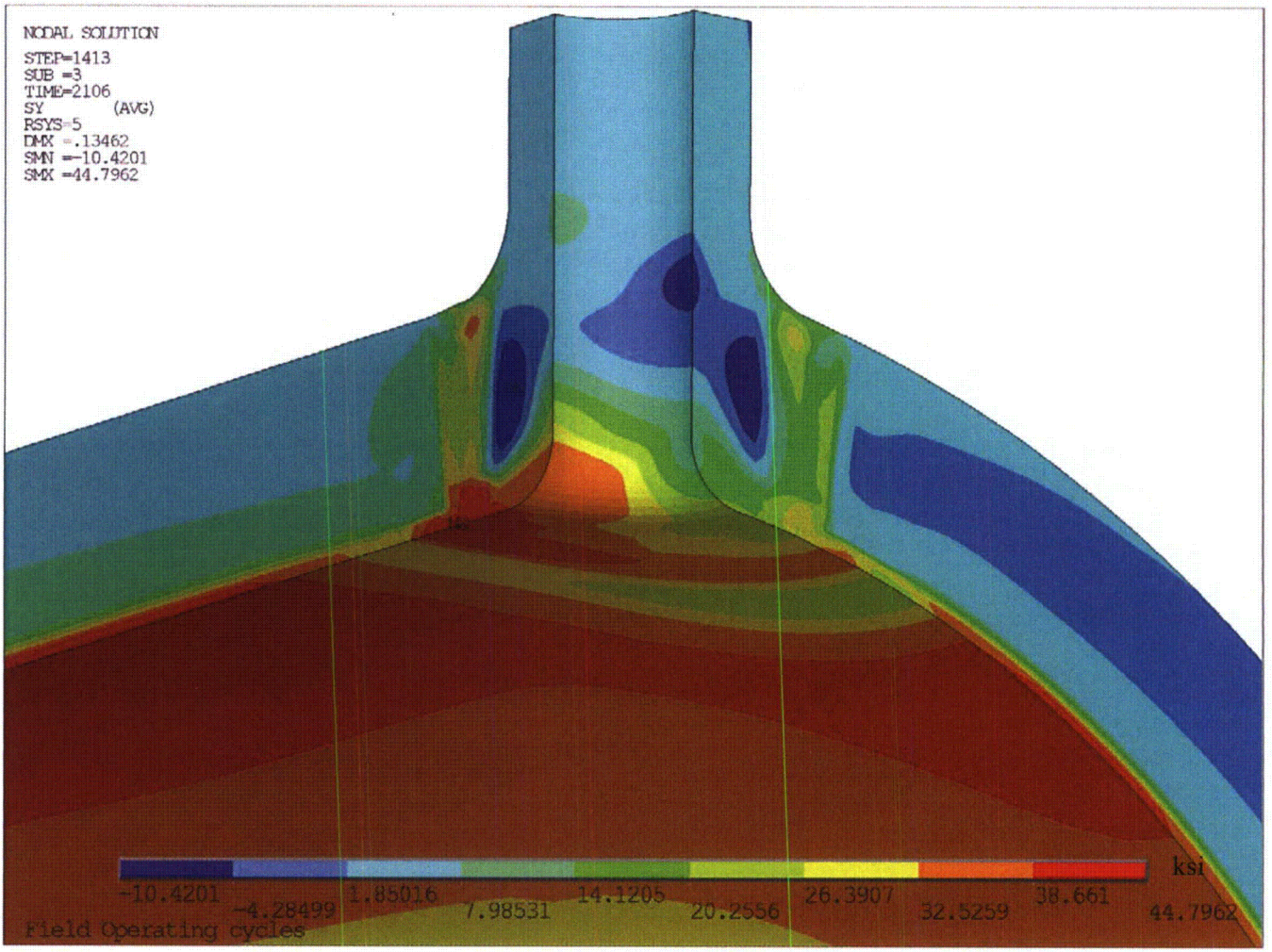

Figure 17: Predicted Hoop Residual Stress + Operating Conditions (5th NOC Cycle)

Note:

1. Hoop stresses shown in the nozzle axis circumferential direction.

APPENDIX A

COMPUTER FILES LISTING

File Name	Description
Palisades_CL.INP	Input file to create base geometry model [1]
MProp_MISO.INP	Elastic-plastic Material properties inputs [1]
Autonugsel.mac	Macro that groups elements into nuggets
BCNUGGET3D.INP	Weld pass and model boundary definition file
THERMAL3D.INP	Input file to perform the thermal pass of welding simulation
THM_PWHT.INP	Input file to perform the thermal pass of PWHT
STRESS3D.INP	Input file to perform the stress pass of welding simulation
CBC.INP	Input file to apply mechanical boundary conditions
THM_PWHT_mntr.inp	Processed thermal pass load steps for PWHT
WELD#_mntr.inp	Processed thermal pass load steps for stress pass # = 1-3
*.mac	WRS analysis macro files required for analysis
THERMAL3D.TXT	Parameter input file for thermal pass of welding simulation
STRESS3D.TXT	Parameter input file for stress pass
GenStress.mac	Macro to extract PWHT stress results
GETPATH.TXT	Through-wall stress path definition to extract PWHT stress results